

Dissertation Zur Erlangung Des Doktorgrades
Der Fakultät Für Biologie
Der Ludwig-Maximilians-Universität München

Identification and characterization of novel methyltransferases



Valentina V Ignatova

August 2019

Completed at the Helmholtz Center Munich
German Research Center for Environment and Health (GmbH)
Institute of Functional Epigenetics

Date of the thesis submission: 27.08.2019

The date of the oral defense: 30.04.2020

The first examiner Prof. Dr. Robert Schneider

The second examiner Prof. Dr. Heinrich Leonhardt

Most of the experiments described in this thesis are published or under revision as:

Ignatova VV., Jansen PWTC, Baltissen MP, Vermeulen M, Schneider R (2019) The interactome of a family of potential methyltransferases in HeLa cells, Scientific Reports. 9: 6584.

Ignatova VV., Kaiser S.[#], Ho JSY.[#], Bing X.[#], Stolz P., Ying Xim Tan, Gay FPH, Rico Lastres P., Valenta M., Gerlini R., Rathkolb B., Aguilar-Pimentel A., Sanz-Moreno A., Klein-Rodewald T., Calzada-Wack J., Ibragimov E., Lukauskas S., Marschall M., Fuchs H., Gailus-Durner V., Hrabe de Angelis M., Bultmann S., Rando OJ., Guccione E., Kellner SM. and Schneider R. METTL6 is a tRNA m³C methyltransferase that regulates translation and tumor cell proliferation (under revision in Science Advances).

Ignatova VV., Stolz P., Kaiser S, Gustafsson TH., Rico Lastres P., Sanz-Moreno A., Cho YL., Amarie OV., Aguilar-Pimentel A., Klein-Rodewald T., Calzada-Wack J., Becker L., Marschall M., Kraiger M., Garrett L., Seisenberger C., Hölter SM., Borland K., Van De Logt E., Jansen PWTC., Baltissen MP., Valenta M., Vermeulen M., Wurst W., Gailus-Durner V., Fuchs H., Hrabe de Angelis M., Rando OJ., Kellner SM., Bultmann S., and Schneider R. (2020) The rRNA m⁶A methyltransferase METTL5 is involved in pluripotency and developmental programmes (Gene&Dev, 34: 715-729).

Eidesstattliche Erklärung

Ich versichere hiermit an Eides statt, dass die vorliegende Dissertation von mir selbstständig und ohne unerlaubte Hilfe angefertigt ist.

München, 20th of August 2019

Valentina V Ignatova

Erklärung

Hiermit erkläre ich, dass die Dissertation nicht ganz oder in wesentlichen Teilen einer anderen Prüfungskommission vorgelegt worden ist.

Ich erkläre weiter, dass ich mich anderweitig einer Doktorprüfung ohne Erfolg nicht unterzogen habe.

München, 20th of August 2019

Valentina V Ignatova

In the results section of my thesis, I included experiments that were done by me and, in the cases then it is crucial for understanding logic and rationale of the next steps, experiments that were done in collaboration with other laboratories (I use “we” instead of “I” in these cases). In the discussion, since I am commenting on all results together, I use “we” everywhere for the simplicity of reading. All collaborators and experiments that were not performed by me are listed at page 111 of the thesis under title “Collaborators”.

Table of Contents

Summary	6
Zusammenfassung	8
1. Introduction	10
1.1. RNA modifications and the dawn of epitranscriptomics	10
1.2. 3-methylcytidine in RNA	11
1.3. N6-methyladenosine in RNA	13
RNA modification and translational control	16
m ⁶ A erasers	17
1.4. Mammalian methyltransferases	18
2. Results	19
2.1 Candidate based screen to identify novel methyltransferases	19
Expression and purification of potential methyltransferases	19
<i>In vitro</i> methyltransferase assay screen	21
2.2 Identification of METTL6 as a novel m ³ C tRNA methyltransferase	24
METTL6 methylates tRNA <i>in vitro</i>	24
METTL6 methylates specific tRNA ^{Ser} isoacceptors in human cells	27
Loss of METTL6 affects transcriptome and proteome of mouse cells	30
METTL6 regulates cell growth and pluripotency	32
METTL6 interacts with regulators of Hippo signaling pathway	32
2.3 Identification of METTL5 as a novel m ⁶ A RNA methyltransferase	36
METTL5 is an RNA methyltransferase	36
METTL5 catalyses N ⁶ -methyladenosine formation on 18S rRNA at A ₁₈₃₂	39
m ⁶ A-IP reveals METTL5-dependent methylation on mRNA	42
METTL5 is essential for mESC pluripotency and correct differentiation	45
2.4 Characterization of METTL-interacting proteins	47
Establishment of a setup to study METTL interactome	48
METTL interaction proteomics	49
METTL9 interacts with CANX	54
3. Discussion	57
3.1. Systematic identification of novel methyltransferases from METTL protein family	57
3.2. tRNA m ³ C methyltransferase METTL6 regulates translation	59
3.3. METTL5 is m ⁶ A RNA methyltransferase that controls pluripotency and differentiation	61
3.4. METTL proteins interactome	64
4. Materials and Methods	67
4.1 Materials	67
4.1.1 Chemicals and reagents	67
4.1.2 Consumables and kits	71
4.1.3 Technical instruments	73
4.1.4 Buffers and solutions	76
4.1.5 Antibodies	81
4.1.6 Oligo nucleotides	81
4.1.7 Bacteria	84
4.1.8 Expression plasmids	84
4.1.9 Cell lines	87
4.1.10 Software	88
4.2 Methods	89
4.2.1. Molecular biology methods	89
4.2.2. Bacterial cell culture	90
4.2.3. Mammalian cell culture	90

4.2.4. RNA methods.....	91
4.2.5. Biochemistry methods	92
4.2.6. Protein purification.....	93
4.2.7. Microscopy	94
4.2.8. <i>In vitro</i> assays	95
4.2.9. m ⁶ A-IP	96
4.2.10. Data analysis	97
4.2.11. Data availability	97
5. Bibliography	98
6. Appendix.....	110
Abbreviations	110
Collaborators.....	111
Acknowledgements	112

Summary

So far 172 different types of nucleic acid modifications had been identified. However, for many RNA and DNA modifications the function(s) and the modifying enzymes ("writers") are still not known. In my Ph.D. project, I focused on the identification of novel RNA and DNA methyltransferases. To identify novel enzymes, I systematically screened a collection of potential methyltransferases on the range of substrates in *in vitro* methyltransferase assay. I found four enzymes that exhibit robust methyltransferases activity towards RNA. Size exclusion chromatography in combination with labelling approaches and mass spectrometry allowed me to narrow down potential substrates and to identify the modified nucleosides for two candidate enzymes.

I characterized METTL6 as a tRNA methyltransferases that specifically catalyzes methylation of cytosines at position 3 (m³C). By performing methyltransferase assays as well as sequence-specific purification of individual tRNAs, I identified the specific tRNA isoacceptors that are METTL6 targets and the precise position of the methylated C. RNA-seq and Ribosome profiling of KO mES cell lines revealed global changes in the transcriptome and translome. In line with these changes, *Mettl6* KO cells showed slower proliferation rates. Interestingly, METTL6 depletion resulted in slower hepatocellular tumor growth in *in vitro* models. In agreement with this, patients with high METTL6 expression levels have a reduced survival rate.

I identified, METTL5 as a novel m⁶A RNA methyltransferase. Mass spectrometry analysis of RNA from *Mettl5* KO mES cells revealed a decrease in m⁶A levels in 18S rRNA. By performing m⁶A-immunoprecipitation followed by sequencing in wt and *Mettl5* KO cells, I mapped the transcript wide distribution of m⁶A in non-ribosomal RNAs. In addition to this, *Mettl5* KO mES cells are less pluripotent and compromised in their ability to differentiate into neuronal precursors cells.

In a complementary approach, I wanted to identify the interactome of METTL proteins. For this, I generated stable cells lines expressing tagged METTL family members, purified the complexes, and analysed interaction partners by mass spectrometry. The systematic identification of the complexes in which these potential enzymes act provides a useful resource for the epitranscriptomics community as it helps to understand METTL proteins function(s) and substrate specificities.

Overall, in my Ph.D. project, I profiled the enzymatic activities and the interactome of 13 proteins of the METTL family. For two novel RNA methyltransferases, I characterized the substrates and the type of methylation they catalyse, profiled changes in the transcriptome and translome, and characterized the phenotypes of mES cells upon KO of these two enzymes.

Zusammenfassung

Bisher wurden 172 verschiedene Arten von Nukleinsäuremodifikationen identifiziert. Für viele dieser RNA- und DNA-Modifikationen sind die Funktion (en) und die modifizierenden Enzyme ("Writer") jedoch noch nicht bekannt. In meinem Promotionsprojekt beschäftigte ich mich mit der Identifizierung neuartiger RNA- und DNA-Methyltransferasen. Um neue Enzyme zu identifizieren, habe ich systematisch eine Sammlung potenzieller Methyltransferasen in in-vitro-Methyltransferase-Assays auf verschiedenen Substraten untersucht. Ich habe vier Enzyme identifiziert, die robuste Methyltransferaseaktivität gegenüber RNA aufweisen. Größenausschlusschromatographie in Kombination mit Markierungsansätzen und Massenspektrometrie ermöglichten es mir, potenzielle Substrate einzugrenzen und die modifizierten Nukleoside für zwei positive Kandidaten zu identifizieren.

Ich charakterisierte METTL6 als tRNA-Methyltransferase, die spezifisch m³C katalysiert. Durch Methyltransferase-Assays sowie sequenzspezifische Aufreinigung einzelner tRNAs identifizierte ich spezifische tRNA-Isoakzeptoren als METTL6-Tagets und die genaue Position des methylierten Cytosins. RNA-seq- und Ribosomen-Profiling von KO-mES-Zelllinien ergab globale Veränderungen im Transkriptom und Translatom. In Übereinstimmung mit diesen Änderungen zeigten *Mettl6*-KO-Zellen geringere Proliferationsraten. Interessanterweise führte METTL6-Depletion in in vitro-Modellen zu einem langsameren Wachstum hepatozellulärer Tumore. In Übereinstimmung damit haben Patienten mit hoher METTL6 Exoression eine verringerte Überlebensrate.

Ich identifizierte METTL5 als eine neue m⁶A-RNA-Methyltransferase. Die massenspektrometrische Analyse von RNA aus *Mettl5* KO mES-Zellen ergab eine Abnahme der Menge an m⁶A in 18S-rRNA. Durch das Durchführen von m⁶A-Immunpräzipitationen, gefolgt von Sequenzierung in wt- und *Mettl5* KO-Zellen, kartierte ich

die transkriptweite Verteilung von m⁶A in nicht-ribosomalen RNAs. Diese METTL5-KO mES-Zellen verlieren Pluripotency und ihre Fähigkeit sich korrekt in neuronale Vorläuferzellen zu differenzieren.

In einem komplementären Ansatz wollte ich das „Interaktom“ von METTL-Proteinen identifizieren. Zu diesem Zweck erzeugte ich stabile Zelllinien, die getagte METTL Protein exprimieren, reinigte die Komplexe und analysierte die Interaktionspartner durch Massenspektrometrie. Die systematische Identifizierung von Komplexen, in denen diese potenziellen Enzyme wirken, ist eine nützliche Ressource für das Epitranscriptomics Field, da sie zum Verständnis der Funktionen und Substratspezifitäten von METTL-Proteinen beitragen kann.

Insgesamt habe ich in meiner Doktorarbeit die enzymatische Aktivität und das Interaktom von 13 Proteinen der METTL-Familie analysiert. Für zwei neue RNA-Methyltransferasen charakterisierte ich die Substrate und die Art der Methylierung, die sie katalysieren, profilierte Veränderungen im Transkriptom und Translatom und identifizierte die Phänotypen von mES-Zellen auf KO dieser beiden Enzyme.

1. Introduction

1.1. RNA modifications and the dawn of epitranscriptomics

Modifications of DNA and histones have the potential to encode information in addition to the information encoded in the genome. Recently RNA modifications and with it epitranscriptomics emerged as a novel, additional layer in the regulation of gene expression programs^{1,2,3}. Interestingly, methylation, the most widespread modification of RNA and DNA can be removed by demethylases^{4,5}. Thus, nucleoside methylation could carry more stable “epigenetic” information or could be dynamic with high regulatory potential.

It is of interest to note that of 34 naturally occurring DNA modifications in Eukaryotes (46 in all kingdoms of life), only 6 have so far been shown as functional and implicated into the regulation of gene expression: m⁵C with its intermediates and m⁶A. To the best of our knowledge, other modifications that have been found in DNA are various forms of DNA lesions resulting from non-enzymatic chemical reactions.

Since RNA appeared early than DNA in molecular evolution and many different types, structures and functions of RNA molecules exist, it is not surprising that the repertoire of RNA modifications exceeds what can be found in DNA. To date, there are 172 naturally occurring RNA modifications described with all classes of RNA are known to be enzymatically modified⁶. 72 of these modifications are different forms of methylations. Methylation is the most common modification in nucleic acids. It is relatively small in size, has a neutral charge and low chemical reactivity⁷. However, the functions of many methylations marks as well as the modifying enzymes are still unknown. The resurgent interest in RNA modifications has been triggered by a wave of discoveries of novel sites of RNA modifications, of specific “writer” and “eraser” enzymes that can add or remove these modifications as well as of “binders” that can read out the modifications^{8,9}. Ongoing

development of new methods for detection and analysis of RNA modification as well as genome engineering methods like CRISPR/Cas9, that allows easy generation of cell lines with KO of writers, readers, and erasers, assures many exciting discoveries in the field of Epitranscriptomics in the nearest future.

1.2. 3-methylcytidine in RNA

Despite high overlap between RNA and DNA modification, some of the modifications that are functional in RNA lead to damage if occur in DNA. One of such examples is m³C. First, this modification was identified in DNA (in 1970)¹⁰ and, at the moment, is considered to be cytotoxic. m³C has a very strong impact on Watson-Crick base pairing and is preferentially found in ssDNA. Supposedly it occurs during transcription and replication - the stages at that DNA is transiently single-stranded. Polymerases are not able to insert the correct nucleotide opposite to m³C (contrary to m⁵C), thus such lesion has to be repaired by the cell. Interestingly one enzyme - hABH3, can remove m³C from both ssDNA and ssRNA.

If catalyzes enzymatically, the establishment of m³C modification in RNA is an essential step in RNA biogenesis. This modification was discovered in tRNA^{Ser} from rat liver in 1971¹¹ and so far tRNAs remain the most characterized substrate of m³C methyltransferases (Figure 1.2.1). Recently, it was proposed that m³C can be catalyzed enzymatically not only in tRNA but in mRNA by a homolog of m³C tRNA methyltransferases¹².

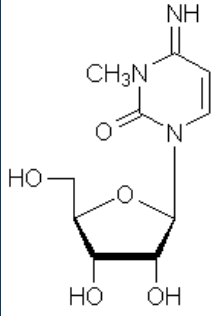
3-methylcytidine		Phylogenetic source		
		Archaea	Bacteria	Eukarya
 <p>Common name: 3-methylcytidine</p> <p>Symbol: m³C</p> <p>CA index name: Cytidine, 3-methyl-</p> <p>CA registry numbers: ribonucleoside 2140-64-9 base 4776-08-3</p> <p>elemental composition: C₁₀H₁₅N₃O₅</p> <p>nucleoside mass: 257.25</p>	Source type			
	tRNA		+	+
	rRNA			unclear

Figure 1.2.1. m³C chemical structure and distribution among RNA species.

Adapted from <https://mods.rna.albany.edu/mods/modifications/>

tRNAs are known for its peculiar cleave-leaf shape with the most of the molecule being double-stranded. Maintenance of the correct structure of tRNA is crucial for the base pairing of tRNA with mRNA during the translation process. By analogy with DNA, m³C in tRNA is found in the ssRNA regions: in the anticodon and variable loops. Yet the exact function of m³C in tRNA is not clear. In general, tRNA modifications were found to be implicated in the control of tRNA stability, folding, decoding properties or interactions with the translation machinery¹³. tRNA modifications are critical to regulating protein synthesis rate, especially during animals development¹⁴. Alterations in the translation are found in many types of cancers too. Additionally, an increasing number of disease-causing mutations have been mapped to human genes that encode tRNA modifying enzymes making these enzymes promising targets for drug discovery¹⁵. The enzymes that are implicated in tRNAs modification are well characterized in yeast however much less is known about their homologs in animals. Taking into account the potential implication of m³C in cancer development and that we currently do not know the enzymatic complex responsible for its establishment in higher eukaryotes, the discovery of potential m³C methyltransferases arises as an important question in biomedical research.

1.3. N6-methyladenosine in RNA

One of the most abundant and studied RNA modifications is N6-methyladenosine (m⁶A) (Figure 1.3.1). m⁶A was estimated to occur in 0.1–0.4% of all adenosines in global cellular RNAs and accounts for approximately 50% of all methylated cellular ribonucleotides¹⁶. This modification was discovered in 1974¹⁷ and gained new attention recently due to the development of the method that allowed to map m⁶A in the RNA for the first time – m⁶A-immunoprecipitation (IP) followed by NGS^{18,19}.

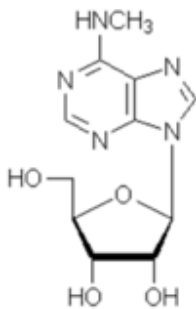
N⁶-methyladenosine  Common name: N ⁶ -methyladenosine Symbol: m ⁶ A CA index name: Adenosine, N-methyl- CA registry numbers: ribonucleoside 1867-73- base 443-72-1 elemental composition: C ₁₁ H ₁₅ N ₅ O ₄ nucleoside mass: 281.27	Source type	Phylogenetic source		
		Archaea	Bacteria	Eukarya
	tRNA	+	+	
	rRNA	16S	16S+23S, 23S	17S, 18S, 28S
	mRNA			+
	snRNA			+

Figure 1.3.1. m⁶A chemical structure and distribution among RNA species.

Adapted from <https://mods.rna.albany.edu/mods/modifications/>

So far, three enzymatic complexes have been described in mammals that can deposit m⁶A on RNA (Table 1.3.1). METTL3 catalyzes the formation of m⁶A in mRNA^{20,21} as well as non-coding RNA like primary-microRNAs²², Xist (X-inactive specific transcript) RNA²³ and U2, U4 and U6 spliceosomal RNA²⁴. Interestingly, to be active METTL3 has to be in a well-defined complex together with METTL14²⁵. Another newly identified m⁶A RNA methyltransferase – METTL16, seems not to require additional proteins for its methyltransferases activity²⁶. In addition to this, ZCCHC4 was recently described as a 28S

rRNA methyltransferase². Those three enzymes have various substrates preferences and RNA recognition modes as summarized in Table 1.3.1.

m⁶A methyltransferase	Type of RNA substrate	Recognition of substrate via
Mettl3	mRNA, pri-miRNA, Xist RNA	specific binding motif
Mettl16	U6 small nuclear RNA, Mat2a mRNA	secondary structure
ZCCHC4	28S rRNA	? / specific binding motif

Table 1.3.1. Characteristics of m⁶A RNA methyltransferases identified to date.

All three m⁶A catalyzing enzymes have different substrate recognition modes. The METTL3/METTL14 complex preferentially methylates adenosines within a sequence RRACH (R = A or G; H = A, C, or U)²⁷. METTL16 recognizes its motif preferentially in a bulge of a stem-loop structure of RNA²⁶. For the rRNA methyltransferase ZCCHC4 a specific binding motif was identified, yet the highly structured nature of ribosomal RNAs allows one to speculate that RNA secondary structure could impact ZCCHC4 binding²⁸.

m⁶A in RNA has been implicated in regulating RNA structure, stability, splicing, translation efficiency, localization and altering secondary structure of RNA (m⁶A-RNA switches)^{29,9,30} (Figure 1.3.2).

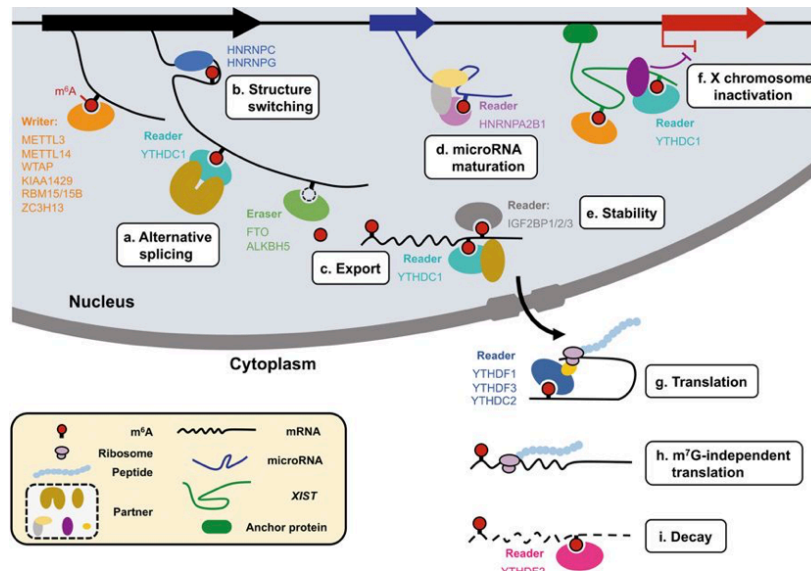


Figure 1.3.2. m⁶A impacts all steps of RNA biogenesis. Adapted from Yang et al³⁰.

After several years of an extensive investigation of m⁶A function in various cells and RNAs, it appears that m⁶A affects RNAs in a context-dependent manner. Even the same mRNA can be affected by the presence of m⁶A in different ways in different cell types or cell states (personal communications from Functions of Epitranscriptoms meeting in Chicago, 2019). Additionally, location of m⁶A within transcripts can lead to various consequences: m⁶A in 3'UTR preferentially impacts translation and interaction with miRNA, m⁶A in 5'UTR - Cap-independent translation, m⁶A in the RNA body was shown to affect RNA stability and decay and m⁶A within introns and near splice-junction sites was proposed to be involved in regulation of splicing⁹. On the whole-transcriptome level, m⁶A effects vary too. In the original paper from Howard Y Chang lab³¹ m⁶A was shown to promote RNA degradation as mRNAs, in general, were more stable upon *Mettl3* KO in mESC. Contrary to this, upon conditional KO of *Mettl14* in neuronal precursor stem cells mRNA was less stable than in the presence of m⁶A³².

The impact of m⁶A on other than mRNA RNA types is not fully understood to date. In pri-miRNAs m⁶A affects biogenesis of mature miRNAs via modulating of pri-miRNAs

processing²². m⁶A effects on long non-coding RNAs remain to be discovered. In the Xist lncRNA m⁶A was shown to be important for Xist function in X chromosome inactivation²³.

RNA modification and translational control

Interestingly, there are two m⁶A sites in human rRNA: one in 18S rRNA at positions A1832 and one in 28S rRNA at position A4220³³. For 18S rRNA, functions of this m⁶A site and a methyltransferase that catalyzes it are still not known. m⁶A at A4220 in 28S rRNA was linked to translation efficiency. HepG2 cells with a KO of the corresponding writer, ZCCHC4, had ~ 25% reduction in global translation rate. Although the level of the mature rRNAs was not affected upon ZCCHC4 KO, level of the 60S ribosome subunits was reduced in KO cells². Additionally, the proliferation of ZCCHC4 KO cells was reduced in comparison to wt cells². It is important to note that those experiments were performed in human HepG2 cells as translation rate can vary greatly in different cell types.

Differentiated cells are characterized by high translation rate. It was estimated that HeLa cells growing in the logarithmic phase synthesize ~ 7,500 new ribosomal subunits per minute³⁴. Therefore, any defects in ribosomes biogenesis and assembly can have dramatic effects on cell viability. Mutations in ribosomal proteins and components of ribosome biogenesis machinery lead to numerous diseases under common name ribosomopathies³³. In contrary to that, the low translation rate is a hallmark of embryonic and somatic stem cells. In recent years it has been shown that the regulation of ribosome biogenesis and protein synthesis is the key for the transition from pluripotency to differentiation³⁵. During ESC differentiation protein synthesis rate is increasing ~2-fold with 78% of transcripts exhibit increased ribosome loading thus resulting in ~30% more steady-state level of proteins per cell^{36,37}. Ribosome heterogeneity was proposed to explain differences in translation between various cell lines, upon reaction to environmental stimuli, and during development and disease³⁷. According to this hypothesis, not all

ribosomes are identical due to variations in ribosome proteins composition. It is plausible to speculate that rRNA modifications can contribute to ribosome heterogeneity and cell-specific translation.

m⁶A erasers

Similarly to methylation on DNA and histones, “eraser” proteins can actively remove m⁶A methylation from RNA, allowing dynamic regulation and fine-tuning at each step of RNA biogenesis. FTO and ALKBH5 are two m⁶A erasers identified to date. ALKBH5 preferentially removes m⁶A from mRNA in the nucleus thus affecting mRNA export to the cytoplasm³⁸. FTO was shown to demethylate RNA in both nucleus and cytoplasm³⁹. These two demethylases have different expression profiles that can contribute to differences in m⁶A levels between various tissues and cell lines. So far, rRNA is the only RNA type for that m⁶A erasers are not identified. Due to rRNA 3D structure and locations of m⁶A marks, they might simply be not accessible for potential erasers. If such eraser(s) exist, one can speculate that changes in m⁶A level in rRNA can be one of the ways for dynamic regulation of translation.

The KO of METTL3, the catalytic subunit of the METTL3/METTL14 complex, does not abolish m⁶A in mRNA⁴⁰. This could be explained by the presence of other methyltransferases including METTL16⁴¹. Since there is no data available about m⁶A levels in METTL3 and METTL16 double KOs, it is unclear if these are the only m⁶A methyltransferases. With the fact that there has been no enzyme identified that catalyzes m⁶A in human 18S rRNA, this opens up the question about further uncharacterized m⁶A methyltransferase(s) in mammalian cells.

1.4. Mammalian methyltransferases

Methyltransferases (MTase), including Nucleic Acids methyltransferases, are a diverse family of proteins, characterized by the presence of methyltransferase like domains and a structurally conserved S-adenosylmethionine (SAM) binding domain that is formed by a central seven-stranded beta-sheet structure⁴⁰. Some nucleic acids methyltransferases pose RNA or DNA binding domains, but some require additional proteins to bind specific substrates⁴¹. Interestingly some methyltransferases can modify both: RNA and DNA. Also, many of the nucleic acid modifications are modifications of the nitrogenous base rather than sugar⁴². Having this in mind it looks plausible that DNA methyltransferases evolved from RNA methyltransferases⁴³. Thus, one could expect the existence of the methyltransferases families that comprise enzymes with diverse substrates specificities.

The DNA (cytosine-5)-methyltransferase (DNMT) protein family is the best studied and identified as DNA (Dnmt1, 3a, and 3b)^{44,45} and RNA (Dnmt2)⁴⁶ methyltransferases. Recently members of the methyltransferase like protein family (METTL) have been shown to methylate RNA in mammals: complex of METTL3 and METTL14 catalyze the formation of m⁶A in mRNA, non-coding RNA^{20,21} and primary-microRNAs²²; METTL1 is shown to catalyze m⁷G (7-methylguanosine) formation in mRNA and tRNA in a complex with its non-catalytic subunit - the tRNA (guanine-N(7)-)-methyltransferase WDR4⁴⁷. Contrary to that, another newly identified m⁶A RNA methyltransferase – METTL16, does not require additional proteins for its methyltransferases activity²⁶. During my work on this project, three members of the METTL family were shown to catalyse m³C in RNA¹². METTLs can also methylate proteins as shown for METTL10⁴⁸ and METTL11A⁴⁹. Additionally, METTL4 was suggested to methylate DNA⁵⁰. These recent findings, along with missing enzymes for some modifications and the possible existence of additional m⁶A methyltransferases, suggest existence of novel nucleoside methyltransferases among METTL proteins.

2. Results

2.1 Candidate based screen to identify novel methyltransferases

Expression and purification of potential methyltransferases

Human methyltransferase like proteins (METTL) are part of a large protein family characterized by the presence of binding domains for S-adenosyl methionine, a co-substrate for methylation reactions. Despite the fact that members of this protein family were shown or predicted to be DNA, RNA or protein methyltransferases^{9,48,41} most METTL proteins are still poorly characterized.

To identify novel methyltransferases, I used a candidate-based screening approach. For this, I choose METTL proteins that (at the time of candidates selection) were poorly characterized and, preferentially, have nuclear localization. As a positive control, I chose METTL3 and METTL14 that form a methyltransferase complex catalysing m⁶A in RNA and that were extensively characterized *in vitro*²⁰.

I acquired from Origene plasmids containing cDNAs of chosen METTL proteins (13 potential and 2 known methyltransferases) tagged with GST at the N-terminus for recombinant expression in *E.coli* (Table 2.1.1 and section 4.1.8 of Materials and Methods).

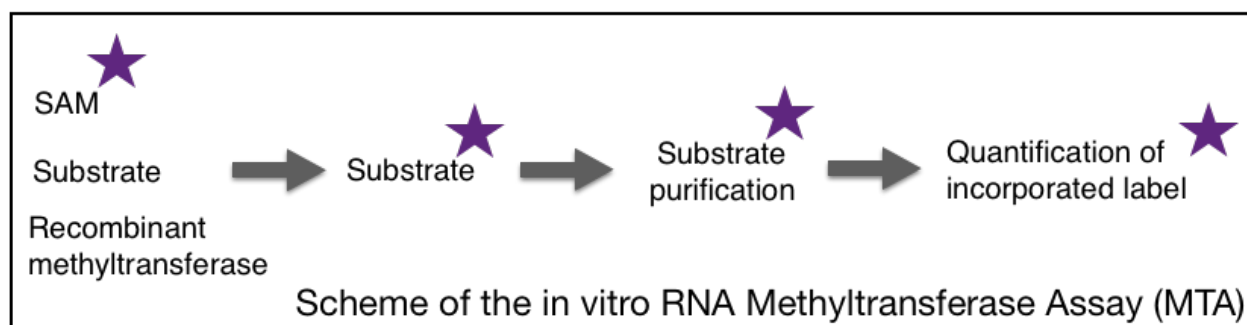
Uniprot ID	Q6P1Q9	Q86U44	Q9NRN9	Q8TCB7	Q6UX53	Q9H825	Q9H1A3
Protein	METTL2B	METTL3	METTL5	METTL6	METTL7B	METTL8	METTL9

Q5JPI9	Q8N6R0	Q9HCE5	A6NJ78	Q86W50	Q5VZV1	Q5JXM2	Q8N6Q8
METTL10	METTL13	METTL14	METTL15	METTL16	METTL21C	METTL24	METTL25

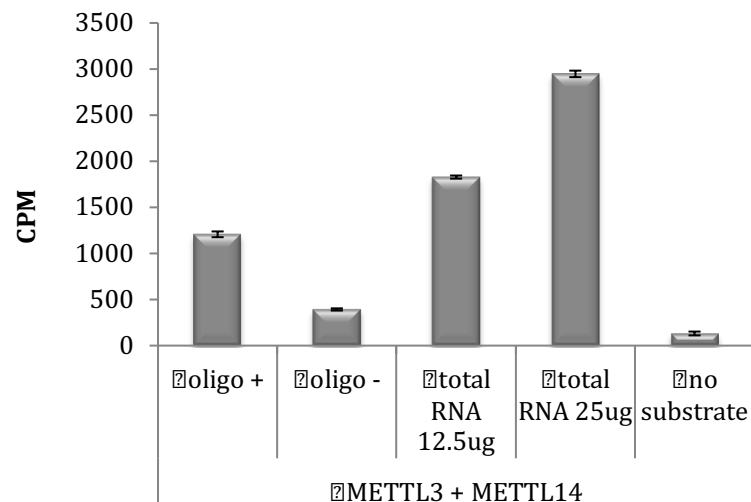
Table 2.1.1. METTL family members studied.

For expression, I tested two bacterial strains: BL21 Gold (DE3) and Rosetta Blue and the following conditions: induction with IPTG at concentrations in the range from 0.1 M to 1 M, temperature for induction from 16°C o/n to 37°C for 3 hours. BL21 Golds (DE3) and induction with 0.5M IPTG at 18°C o/n were the best conditions, since using these conditions I was able to purify amounts of soluble proteins of interest that were detectable by Coomassie Brilliant Blue (data not shown). I performed GST purification of 15 proteins followed by competitive elution. To optimise conditions of the methyltransferase assay (MTA) I used METTL3 and METTL14 with RNA oligos (as described earlier⁵¹) and with total RNA from HeLa cells as substrates (see section 4.2.7 of Materials and methods for full description of the experimental conditions) and tritium labeled SAM (S-adenosylmethionine) as a methyl group donor. This allows me to quantify the incorporation of tritium-labelled methyl groups into the substrate by liquid scintillation counting (LSC) (Figure 2.1.1a). The results of the MTA with METTL3 and METTL4 on oligos were comparable to published data⁵¹: Activity on an RNA oligo that harbours METTL3/METTL14 methylation motif (“oligo +” in the Figure 2.2.1b) drops upon mutation of one nucleotide in this motif (“oligo -” in the Figure 2.2.1b). Performing MTA with METTL3/METTL14 and different amounts of total RNA as substrates allowed me to choose conditions for screening for potential novel enzymes.

a



b



2.1.1. MTA screen conditions were optimized with METTL3/METTL14. (a) Scheme of the *in vitro* methyltransferase assay with recombinant proteins. (b) *In vitro* RNA methyltransferases assay (MTA) on total HeLa RNA with recombinant GST-METTL3 and GST-METTL14 and tritium labeled SAM (S-adenosylmethionine) as a methyl group donor. RNA was purified and tritium signal quantified by liquid scintillation counting (LSC). Counts per minutes are shown. Data displayed as an average of 3 technical replicates with a standard deviation plotted.

***In vitro* methyltransferase assay screen**

For the *in vitro* MTA screen I prepared the following set of substrates: (1) total RNA isolated from HeLa cells; (2) RNA longer then 200 nt that was obtained by size selection of total RNA with RNA mini-prep purification kit from ZymoResearch (3) dsRNA from HeLa cells that was obtained by digestion of total RNA with RNaseA; (4) gDNA isolated from HeLa cells. To check for activity towards small RNAs I perform additional *in vitro* assays on total RNA and resolved the reactions with RNA polyacrylamide gel electrophoresis (PAGE), followed by gel drying and tritium detection with high sensitivity films.

	total RNA	total RNA >200nt	dsRNA	small RNAs	HeLa gDNA
METTL2B	-		-		-
METTL5	++	+	+++	100 - 1000 nt	-
METTL6	+++	-	-	< 100 nt	+
METTL7B	+	+	-	unclear / < 100 nt	-
METTL8	++	++	+++		+
METTL9	-	-			
METTL10	+	-	-	unclear	-
METTL13	-		-		+++
METTL15	-		-		unclear
METTL16	-		+++		+++
METTL21C	-		-		
METTL24	-		-		+++ / unclear
METTL25	+		-		+++ / unclear

Table 2.1.2. Results of the *in vitro* MTA screen. Activity is assigned based on CMP of the *in vitro* reaction normalized to the corresponding non-substrate control: “-” – less than 3 fold activity compared to a control, “+” - 3-7 fold activity compared to a control, “+++” – 7-15 fold activity compared to a control, “+++” – more than 15 fold activity compared to a control, “unclear” indicate that an enzyme was active in the range 0 to 10 fold compared to a control in various purifications. For small RNAs analysis, *in vitro* MTAs were resolved by PAGE with subsequent autoradiography. Size distributions of radiolabelled RNAs are indicated in the table. Empty cells correspond to substrate–protein pairs that were not tested.

The results of the MTA screen are summarized in Table 2.1.2. Based on the results of this screen, I found 5 METTL proteins that have methyltransferase activity under the tested experimental conditions: (1) METTL5 could be a potential m⁶A RNA methyltransferase since it has a DNA methylase m⁶A adenosine specific conserved site⁵² and is active on RNA in my assays; (2) METTL6 is a potential small RNA methyltransferase; (3) METTL8, potentially, is a dsRNA or DNA methyltransferase; (4) METTL13 is a potential DNA methyltransferase; (5) METTL16, potentially, is a dsRNA or DNA methyltransferase. Despite the positive outcome of the MTA screen, METTL13 and METTL8 were extremely difficult to purify with significant batch-to-batch variability in terms of activity. Additionally, enzymes that catalyse modifications on a nitrogenous base, like m⁶A, have the ability under *in vitro* conditions to use both DNA and RNA as substrates. Having this in mind, I did not consider enzymes that were active on DNA *in vitro* as bona fide DNA methyltransferases. While I was doing experiments to narrow down substrate specificity for METTL16, several publications described this enzyme as m⁶A methyltransferase and identified its substrate RNAs^{3,53,54}. As a result, the main focus of my Ph.D. thesis was on METTL5 and METTL6.

2.2 Identification of METTL6 as a novel m³C tRNA methyltransferase.

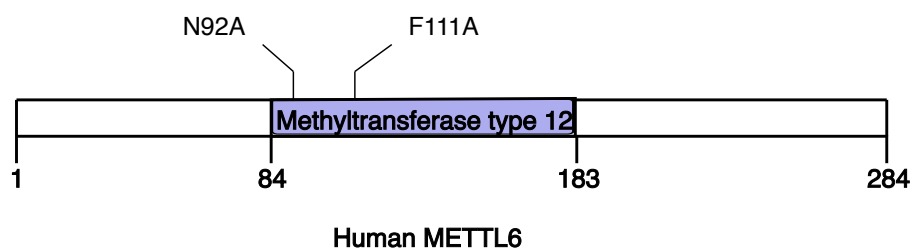
The majority of this work is currently submitted for publication as:

Ignatova VV., Kaiser S.[#], Ho JSY.[#], Bing X.[#], Stolz P., Ying Xim Tan, Gay FPH, Rico Lastres P., Valenta M., Gerlini R., Rathkolb B., Aguilar-Pimentel A., Sanz-Moreno A., Klein-Rodewald T., Calzada-Wack J., Ibragimov E., Lukauskas S., Marschall M., Fuchs H., Gailus-Durner V., Hrabe de Angelis M., Bultmann S., Rando OJ., Guccione E., Kellner SM. and Schneider R. METTL6 is a tRNA m³C methyltransferase that regulates translation and tumor cell proliferation (under revision in Science Advances)⁵⁵.

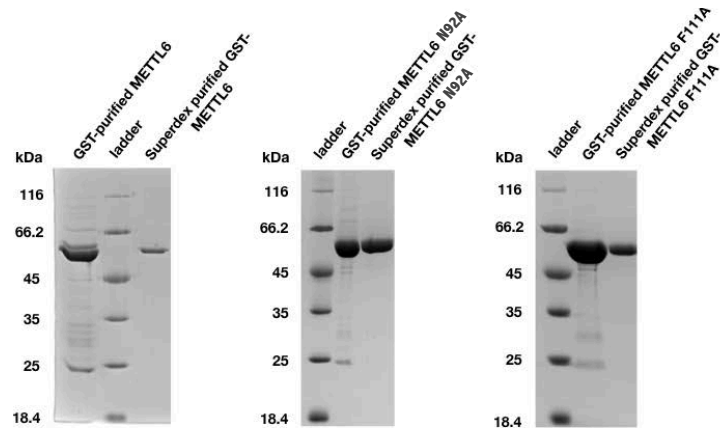
METTL6 methylates tRNA *in vitro*

To demonstrate that METTL6 by itself is an active enzyme, I expressed recombinant wt GST-METTL6 and GST-METTL6 harboring two point mutations: N92A and F111A. These mutations are located within the S-adenosyl methionine (SAM) binding region of METTL6 and thus should be essential for the enzymatic activity of the protein (Figure 2.2.1a and b). As shown in the Figure 2.2.1c, GST-METTL6 can methylate total RNA, in *in vitro* methyltransferase assays with radiolabelled SAM as methyl group donor, whereas the N92A and F111A mutations of METTL6 both abolish the activity on RNA.

a



b



c

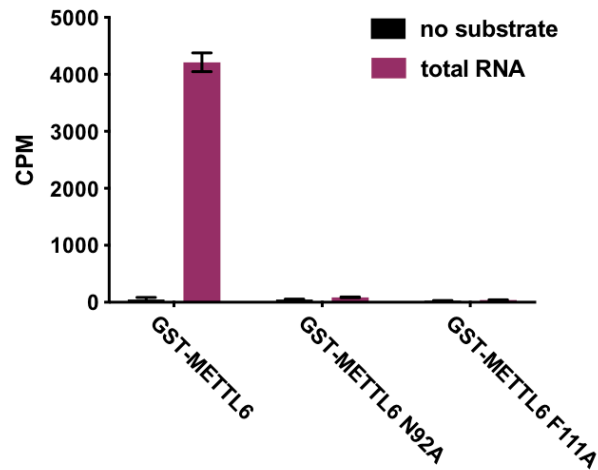


Figure 2.2.1. METTL6 is an RNA methyltransferase. (a) Domain structure of METTL6. Point mutations used in this study that disrupt the catalytic activity are indicated. (b) Coomassie staining of PAGE showing step-wise purification of recombinant wt GST-METTL6 (left), GST-METTL6 N92A (middle) and F111A (right) mutants with Glutathione-Sepharose beads followed by Superdex column purification. **c.** *In vitro* RNA methyltransferases assay (MTA) on total HeLa RNA with recombinant wildtype (wt) GST-METTL6, GST-METTL6 N92A and F111A mutants and tritium labeled SAM (S-adenosylmethionine) as a methyl group donor. RNA was purified and tritium signal quantified by liquid scintillation counting (LSC). Counts per minutes are shown. Data displayed as an average of 3 technical replicates with a standard deviation plotted.

To identify the type of methylation catalyzed by METTL6 I applied (in a collaboration with Stefanie Kellner lab) Methyl-NAIL (Nucleic acid isotope labeling)⁵⁶. For this, I grew cells in medium containing D3-methionine for 7 days to ensure that all methyl groups in the cells contain deuterium. I extracted RNA from these cells and used it as a substrate in *in vitro* RNA MTAs with recombinant GST-METTL6 and unlabeled SAM as a methyl group donor. By LC-MS/MS of RNA, purified after the *in vitro* methylation reaction, we identified the *de novo* methylated nucleoside as 3-methylcytidine (m^3C). There was no detectable incorporation of m^5C or m^3U into the RNA (data not shown). To identify which RNA species are methylated by METTL6 we applied size fractionation followed by LC-MS/MS of the *in vitro* methylated RNA from the previous experiment. This experiment revealed tRNA and tRNA fragment (tRF) containing fractions as the main METTL6 substrates based on the increase in m^3C level in these RNA fractions after MTA (Fig. 2.2.2.).

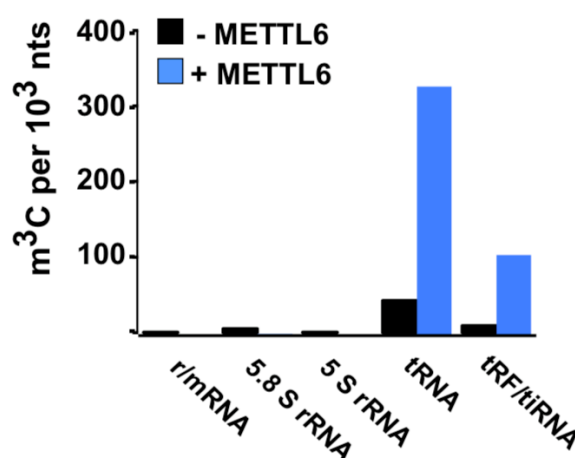


Figure 2.2.2. METTL6 catalyzes m^3C in tRNAs and tRNA fragments *in vitro*.

Fractionation of total RNA from Methyl-NAIL experiments using size exclusion chromatography and analysis of m^3C abundance in different fractions. Fraction 1 contains mainly rRNA and mRNA, fraction 2: 5.8 S rRNA, fraction 3: 5 S rRNA, fraction 4: tRNAs and fraction: 5 tRF and tiRNAs. The number of m^3C per 1000 nucleotides (nts) was determined from samples incubated with SAM and GST-METTL6 (blue) or SAM only (black).⁵⁵

METTL6 methylates specific tRNA^{Ser} isoacceptors in human cells

Next, I aimed to confirm the activity and specificity of METTL6 in human cells. For this, I used wt and METTL6 KO HAP1 cell line obtained from Horizon discovery (section 4.1.9 of Materials and Methods). As the chromatogram in Figure 2.2.3 shows RNA isolated from these KO cells has indeed significantly lower m³C levels compare to wt (Fig 2.2.3, collaboration with S. Kellner).

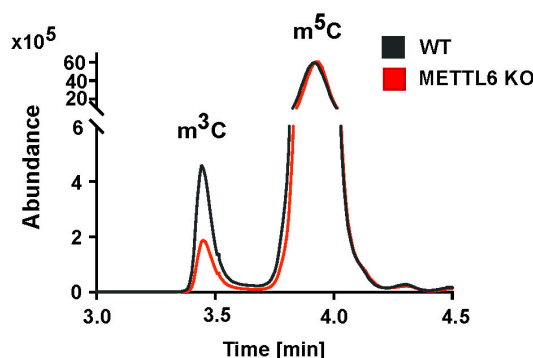
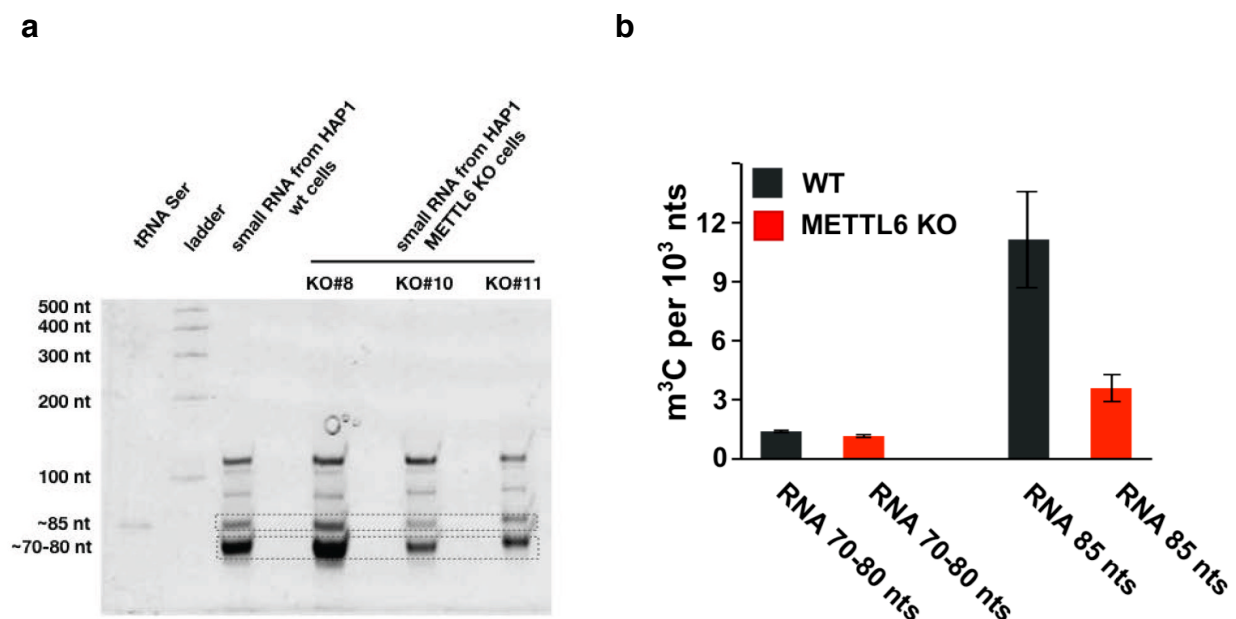


Figure 2.2.3. METTL6 catalyzes m³C in cells. LC-MS/MS chromatogram of total RNA from wildtype (black) and METTL6 KO (red) HAP1 cells. Chromatogram of the mass transition from 258 to 126 is shown. The first peak is identified as 3-methylcytidine (m³C) and the second as 5-methylcytidine (m⁵C) using synthetic standards.⁵⁵

Next, I analysed m³C levels in different tRNA fractions isolated from the METTL6 KO and wt HAP1 cells. For that, I perform gel purification of two tRNA fractions: ~ 70-80 nucleotides and ~ 85 nucleotides (Fig 2.2.4a). The 85 nucleotides fractions contain Serine tRNA (tRNA^{Ser}) and Leucine tRNA (tRNA^{Leu}) that have a long variable loop⁵⁷ whereas 70-80 nucleotides fractions contain all other tRNAs. In the tRNA fraction of 70-80 nucleotides length were no significant alterations in the m³C levels upon loss of METTL6, however in tRNA fractions of 85 nucleotides m³C levels were strongly reduced (Fig 2.2.4b, collaboration with S Kellner lab).

Human tRNA modifications were recently mapped by sequencing upon *in vitro* demethylation to ensure efficient cDNA generation step⁵⁸. These study showed that m³C occurs at positions 32 and/or 47d of several Serine and Threonine isoacceptor tRNAs (tRNA^{Ser} and tRNA^{Thr}), two arginine isoacceptor tRNAs (tRNA^{Arg}) and the tRNA^{Leu}CUG isoacceptor⁵⁸. To investigate which tRNA isoacceptors are methylated by METTL6 I performed nucleic acid isotope labeling of METTL6 wildtype and KO HAP1 cells. After 7 days of labeling, cells were mixed, tRNA fraction was isolated and used for sequence-specific purification of tRNA isoacceptors followed by mass spectrometry (collaboration with Stefanie Kellner lab). LC/MS-MS detected an approximately 2-fold decrease of m³C in the tRNA^{Ser}CGA, tRNA^{Ser}GCU and tRNA^{Ser}UGA/AGA isoacceptors (Fig 2.2.4c). This experiment indicates that METTL6 methylates specific tRNA^{Ser} isoacceptors in human cells. In order to map the methylated cytosine within the tRNA^{Ser} isoacceptors, I used *in vitro* transcribed tRNA^{Ser} with C32 to G and C47d to U mutations as substrates in *in vitro* RNA MTA with recombinant GST-METTL6 and tritium labeled SAM as a methyl group donor. As shown in Figure 2.2.4d, the mutation of C32 but not C47 in tRNA^{Ser} abolishes the methylation by METTL6. Thus, METTL6 specifically methylates C32 in a subset of tRNA^{Ser} isoacceptors.



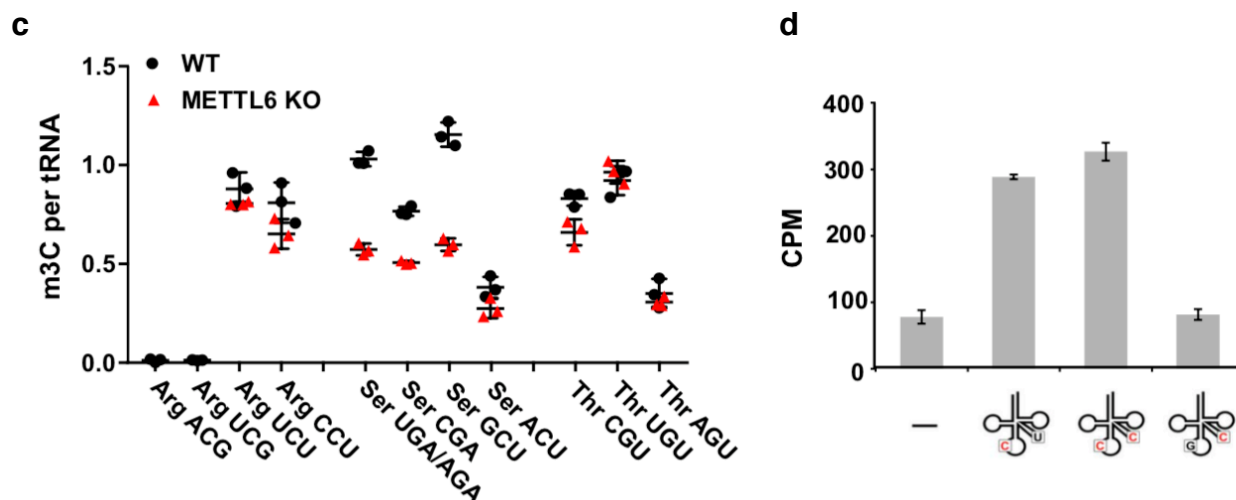


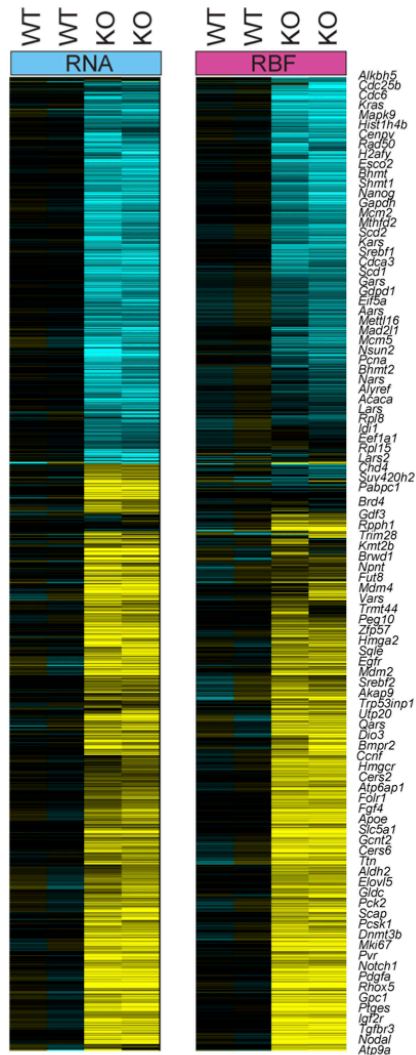
Figure 2.2.4. METTL6 methylates specific Serine tRNAs *in vivo*. (a) EtBr staining of the UREA-PAGE resolving tRNAs of 70-80 and 85 nucleotides length. RNAs of 85 and 70-80 nucleotides were isolated from the gel and RNA modifications analysed by LC-MS/MS. (b) LC-MS/MS analysis of PAGE-purified tRNA of 70-80 nucleotides length and 85 nucleotides length from wt (black) and METTL6 KO (red) HAP1 cells. Note the drop in m³C level in tRNA fraction of 85 nucleotides, but not in 70-80 nucleotides fraction from KO cells. The 85 nucleotides fraction contains mainly tRNA Serine. (c) NAIL-MS (nucleic acid isotope labeling coupled mass spectrometry) results demonstrating m³C abundance in tRNA isoacceptors purified from wt (black) and METTL6 KO HAP1 cells (red). Only specific tRNA Serine isoacceptors (tRNA^{SerCGA}, tRNA^{SerGCU}, and tRNA^{SerUGA/AGA}) show a decrease in m³C abundance upon loss of METTL6, while tRNA Threonine and Arginine isoacceptors are not affected. Note that KO of METTL6 does not affect the m³C abundance in the tRNA^{SerACU}. (d) *In vitro* RNA MTA on *in vitro* transcribed wild type tRNA^{Ser} and C47d to U and C32 to G mutants with recombinant wt GST-METTL6. Note that C32 is a target of METTL6. RNA was purified and tritium signal quantified by liquid scintillation counting (LSC). Counts per minutes are shown. Data displayed as an average of 3 technical replicates with a standard deviation plotted.⁵⁵

Loss of METTL6 affects transcriptome and proteome of mouse cells

Next, I sought to identify potential effects of loss of METT6 on genome-wide gene regulation and translation. As HAP1 cells are an unstable haploid cell line that spontaneously diploidise⁵⁹ I used *Mettl6* knock out mES cells (generated by Sebastian Bultmann laboratory⁵⁵) as a more suitable model for further analysis. In a collaboration with Oliver Rando laboratory, we performed ribosome profiling in the *Mettl6* KO and wt mES cells with matching RNA abundance profiling^{60,61} to identify effects of METT6 loss on transcription or mRNA stability and to be able to calculate translation efficiency per gene.

Focusing first on gene-level changes in transcript abundance and ribosome occupancy, we identified several hundred genes significantly (p-value adjusted for multiple hypothesis testing < 0.05) misregulated in the *Mettl6* KO mESC line relative to WT control (see Figure 2.2.5a and Ignatova et al.⁵⁵ for the whole data set). As expected and consistent with prior ribosome footprinting analyses of tRNA modification mutants in budding yeast^{61–63}, the majority of changes in ribosome occupancy resulted from altered mRNA abundance, presumably reflecting widespread regulatory derangements caused by upstream changes in translation. GO analysis revealed a number of biological processes affected in the *Mettl6* KO mESCs (Figure 2.2.5b), including widespread changes of proliferation-related genes. This reflected in downregulation of cell cycle genes as *Cdc6*, *Cdc25b*, *Kras*, *Mapk9*, *Mcm2*, *Rpa3*, *Mcm5* and others⁵⁵ and, on the other side, upregulation of genes involved in signaling and growth control like *Notch1*, *Notch2*, *Fgf4*, *Egfr*, *Pdgfa*, *Nodal*, *Fgfr2* and others⁵⁵. Translation and proteostasis are also broadly affected in the *Mettl6* KO cells as evinced by the broad downregulation of genes involved in ribosome biogenesis: *Rpl27*, *Rpl26*, *Rpl23*, *Rpl32*, *Rpl22l1*, *Rpl4*, *Rpl8*, *Rpl19*, *Rpl14*, *Rpl34*, *Rps27a*, *Nop2*; translation: *Gtf2e2*, *Eif5a*, *Eif4a1*, *Eif2a1/2*, *Eif3m*, *Rps6ka6*; tRNA aminoacylation: *Kars*, *Gars*, *Aars*, *Lars*, *Nars*; proteasome assembly: *Psmd12*, *Pasma4*, *Psmd11*, *Psmb6*, *Psmb3*, *Psmd13*, *Psmd1*.

a



b

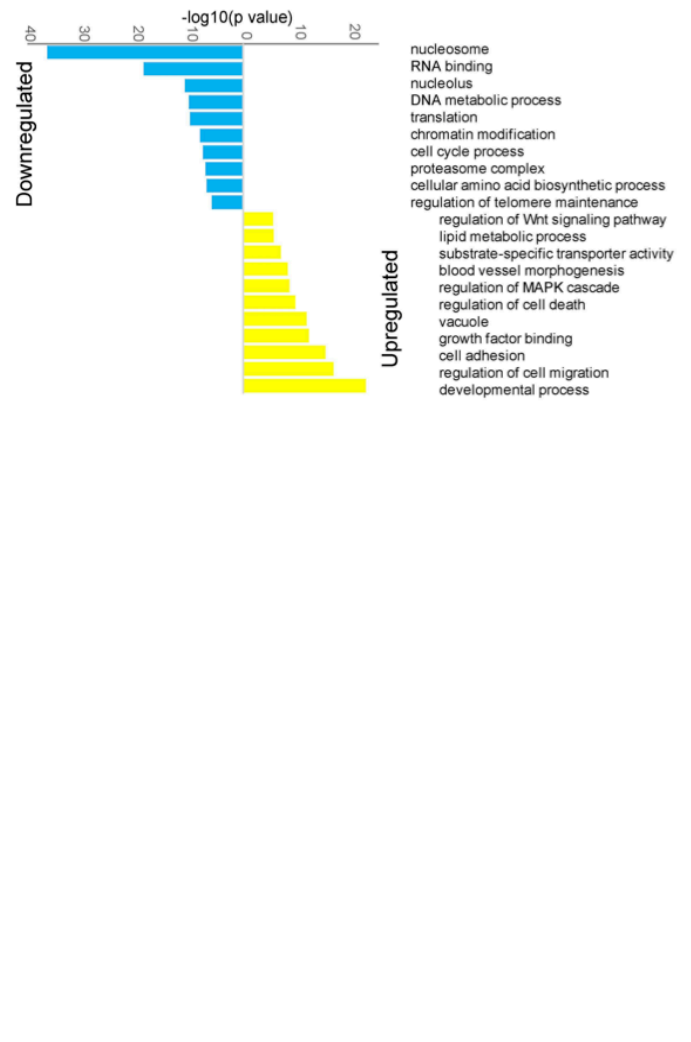


Figure 2.2.5. Loss of m³C in tRNA^{Ser} affects mRNA translation. (a) Translation efficiency of mRNAs in wild type and *Mettl6* KO mESCs clones G6. The heat map shows mRNA translation efficiency in log2 value for two replicates relative to wt is shown. (b) GO analysis of misregulated and mistranslated genes.

METTL6 regulates cell growth and pluripotency

In line with the global misregulation of transcriptome and changes in the translation of a subset of proliferation reflected genes, I observed alterations in the phenotype of *Mettl6* knock out mESCs. As displayed in Figure 2.2.6, *Mettl6* KO mES cells spontaneously lose pluripotency and have a reduced proliferation rate.

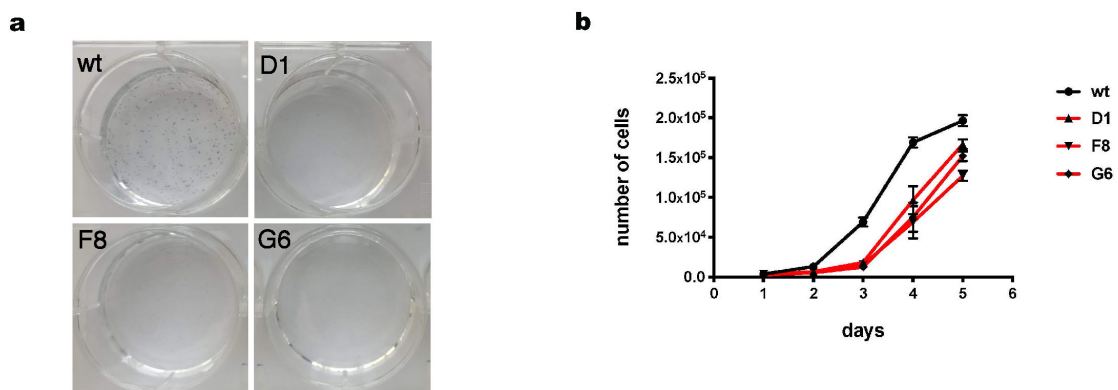


Figure 2.2.6. Loss of METTL6 in mESC impairs pluripotency and proliferation.

(a) Alkaline phosphatase staining of wt and *Mettl6* KO mES cells (clones D1, F8, G6) four days after seeding in Serum-Lif media. A representative experiment of three independent experiments is shown. Wt mES cells maintain pluripotent state whereas three independent *Mettl6* KO mES cell clones starting to differentiate (collaboration with Sebastian Bultmann lab) (b) *In vitro* growth curves of wt and *Mettl6* KO mES cells (clones D1, F8, G6). A representative experiment of two independent experiments is shown.

METTL6 interacts with regulators of Hippo signaling pathway

To identify interaction partners of METTL6, I generated a HeLa-FRT cell line for inducible expression of GFP-METTL6 (described in van Nuland et al.⁶⁴ and Ignatova et al.⁴¹ and section 4.2.1 of Material and Methods). I identified interaction partners of METTL6 using GFP-METL6 purification from HeLa whole-cell extract followed by label-free

quantitative mass spectrometry in collaboration with the Michiel Vermeulen lab. We found that METTL6 interacts specifically (\log_2 fold change (FC) > 8 compared to the GFP-alone expressing control) with the Protein salvador homolog 1 (Sav1)⁶⁵ and Serine/threonine-protein kinase 4 (STK4)⁶⁶ that are the key components of the Hippo signaling pathway (Figure 2.2.7).

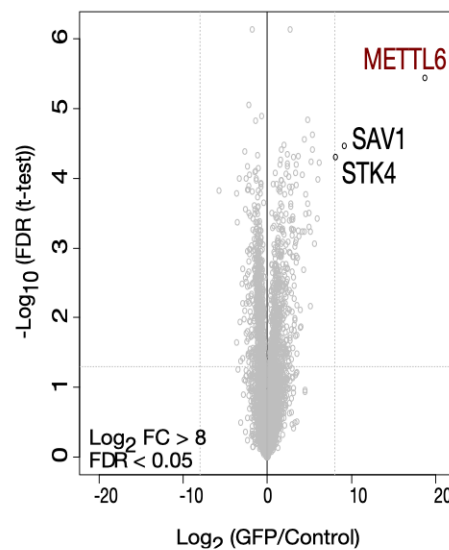


Figure 2.2.7. Sav1 and STK4 interact with METTL6. Volcano plot visualization of interaction partners of METTL6 identified by mass spectrometry of GFP-METTL6 purification. The \log_2 Fold Change (FC) of protein abundances in GFP-METTL6 IP compared to a control IP (GFP alone expressing cell line) in label-free quantification are plotted against the $-\log_{10}$ of the FDR calculated by a permutation-based FDR adapted t-test.

Next, I wanted to verify the interaction between METTL6 and Sav1 and STK4. To do so, I performed GFP-METTL6 immunoprecipitation and detected, as expected, Sav1 (Figure 2.2.8a) and STK4 (Figure 2.2.8b) as interactors by western blotting. The complex of Sav1/STK3/STK4 was shown to phosphorylate other components of Hippo signaling pathway including Sav1⁶⁷ and poses *in vitro* phosphorylation activity towards core

histones. To check whether the GFP-METTL6 co-purified protein fraction has indeed kinase activity I performed *in vitro* phosphorylation assay with GFP- and GFP-METTL6 purifications on core histones (Sigma - Aldrich) with P^{32} as a phosphate group donor. I used Aurora B kinase as a positive control for successful *in vitro* phosphorylation. As shown in Figure 2.2.8c, I detected the activity of Aurora B kinase but not METTL6 purifications. If GFP-METTL6 purification possesses a phosphorylation activity it could be active on core histones, as a general phosphorylation substrate, SAV1, as it is known to be phosphorylated by STK3/4, or METTL6 itself. We did not detect signal on any of these potential substrates. This might be due to the fact that none of these proteins is indeed a correct substrate for the kinase activity of METTL6/SAV1/STK4 complex or that this complex is not similar to the canonical SAV1/STK3/4 complex in terms of activity.

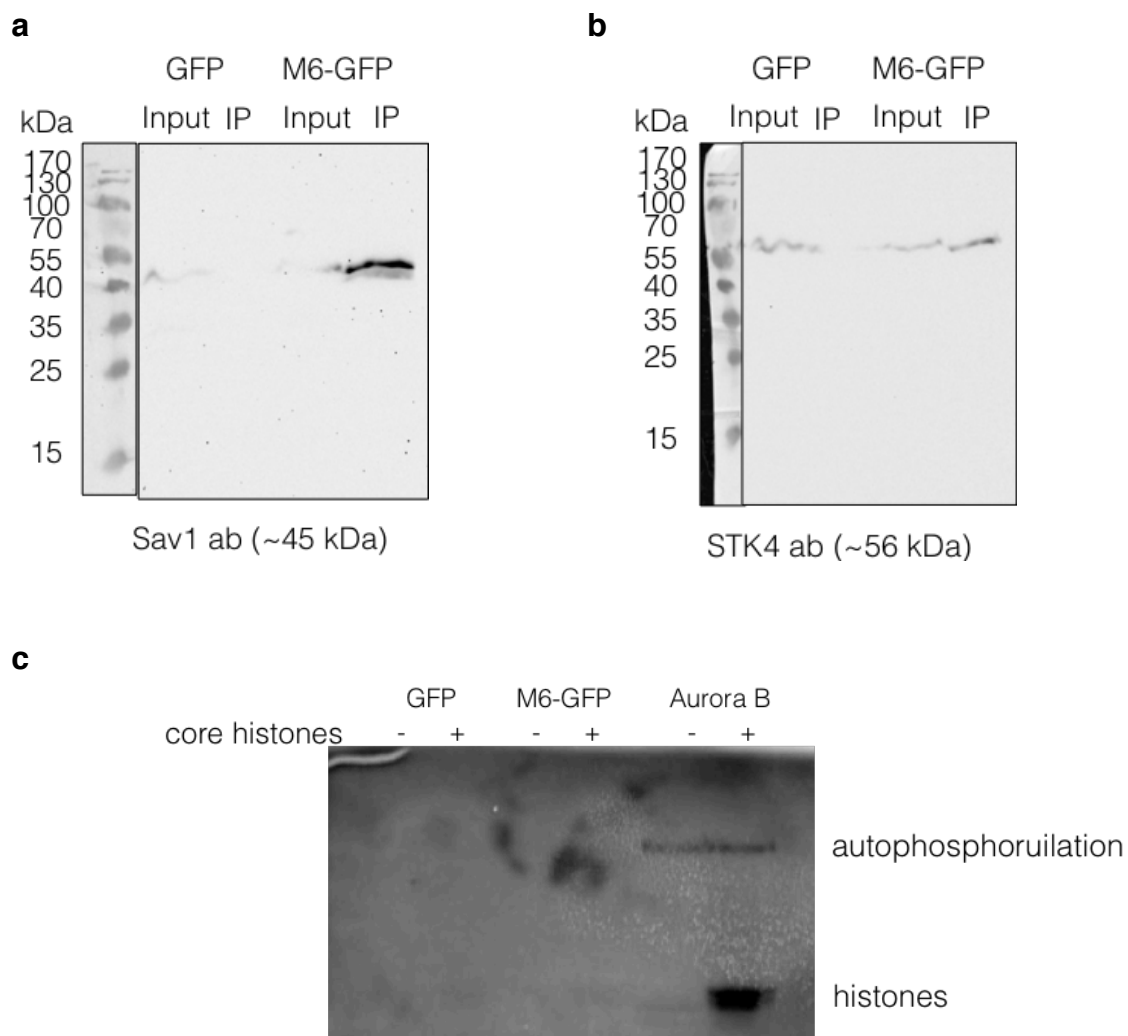


Figure 2.2.8. METTL6 forms a complex with Sav1 and STK3/4 that does not pose phosphatase activity on core histones. (a, b) Validation of interaction between GFP-METTL6 and Sav1 and GFP-METTL6 and STK4 by GFP IP followed by immunoblot with indicated antibodies. (a) Sav1 is detected in GFP-METTL6 IP (a, lane 5) but not GFP-alone IP control (a, lane 3). (b) STK4 is detected in GFP-METTL6 IP (a, lane 5) but not the GFP-alone IP control (a, lane 3). 10 μ l of GFP trap and 2 mg of whole-cell extracts were used. 20 μ g of Inputs material were loaded for comparison. (c) *In vitro* phosphorylation assays demonstrating that GFP-METTL6 purification does not pose phosphatase activity toward core histones. GFP (as a control) and GFP-METTL6 were purified from corresponding DOX-induced HeLa-FRT cell lines and used in an *in vitro* phosphorylation assay on core histones (Sigma) as a generic phosphorylation substrate and P^{32} as a phosphate group donor. Reactions were resolved with denaturing PAGE followed by gel drying and expose for radioactivity detection. Recombinant Aurora B kinase used as a control for successful *in vitro* phosphorylation assays set up.

2.3 Identification of METTL5 as a novel m⁶A RNA methyltransferase

A significant part of this work is published as:

Ignatova VV., Stolz P., Kaiser S, Gustafsson TH., Rico Lastres P., Sanz-Moreno A., Cho YL., Amarie OV., Aguilar-Pimentel A., Klein-Rodewald T., Calzada-Wack J., Becker L., Marschall M., Kraiger M., Garrett L., Seisenberger C., Höltér SM., Borland K., Van De Logt E., Jansen PWTC., Baltissen MP., Valenta M., Vermeulen M., Wurst W., Gailus-Durner V., Fuchs H., Hrabe de Angelis M., Rando OJ., Kellner SM., Bultmann S., and Schneider R. (2020) The rRNA m⁶A methyltransferase METTL5 is involved in pluripotency and developmental programmes (Gene&Dev, 34: 715-729)⁶⁸.

METTL5 is an RNA methyltransferase

In my screen for novel RNA and DNA methyltransferases I identified METTL5 as an RNA methyltransferase (Table 2.1.2). In my *in vitro* assays, GST-METTL5 was able to methylate polyA-enriched RNA too, although I detected less tritium incorporation than in on the same amount of total RNA (Figure 2.3.1a). To exclude that the activity we detected with GST-METTL5 is due to co-purification of a bacterial methyltransferase I generated a HeLa-FRT cell line for inducible expression of GFP-METTL5 (as described in van Nuland et al.⁶⁴ and Ignatova et al.⁴¹ and section 4.2.1, 4.2.4, 4.2.6 of Material and Methods) and repeated the methyltransferase assay with GFP-METTL5 purified from these cells. I detected a strong activity of GFP-METTL5 on total RNA (Figure 2.3.1b). Due to the absence of immunoprecipitation (IP) grade antibodies, I used the same GFP-METTL5 cell line to purify interaction partners of METTL5 from HeLa whole-cell extract using label-free quantitative mass spectrometry. I found that METTL5 interacts specifically (with a log₂ fold change (FC) > 8 compared to the GFP-alone expressing control) with the multifunctional methyltransferase subunit TRM112-like protein (Trmt112) (Figure 2.3.1c, collaboration

with M. Vermeulen lab), a previously described interactor of multiple different methyltransferases^{69,70}. Point mutations of METTL5 in the methyltransferase domain (D81H or D81A) and the N6-adenosine-specific DNA methyltransferase site (N126A) (Figure 2.3.1d and e) abolished the activity of GFP-METTL5, demonstrating that the methyltransferase activity I observed is indeed due to the catalytic activity of METTL5.

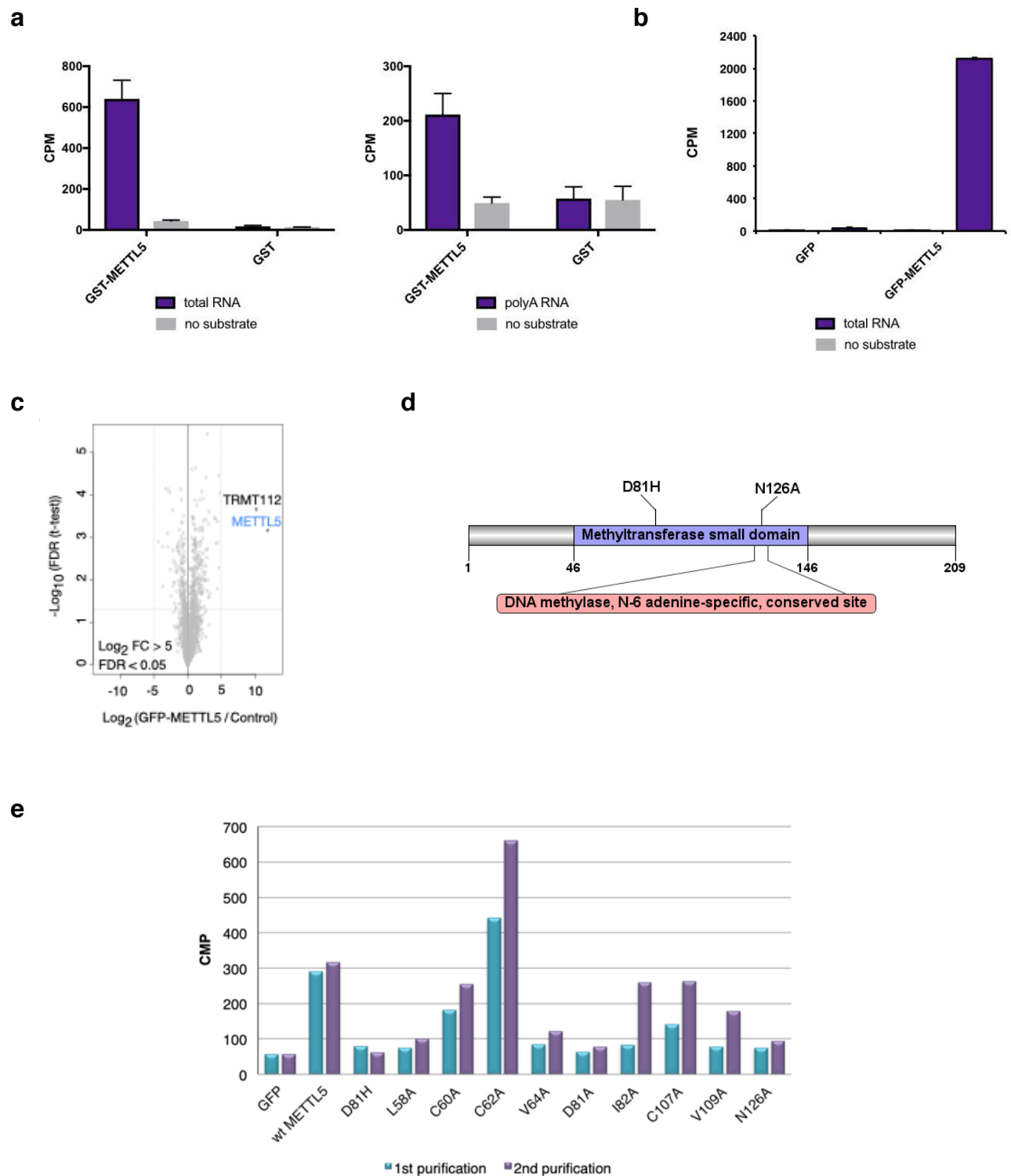


Figure 2.3.1. METTL5 methylates RNA *in vitro*. (a) *In vitro* RNA methyltransferases assay (MTA) with recombinant wildtype GST-METTL5 vs. GST alone as control on total RNA from HeLa cells (left) and polyA fraction of total HeLa RNA (right) with tritium labeled SAM (S-adenosylmethionine) as methyl group donor. RNA was purified and tritium signal quantified by liquid scintillation counting (LSC). Counts per minutes are shown. One representative experiment is shown. Data displayed as an average of 3 technical replicates with a standard deviation plotted. (b) *In vitro* RNA methyltransferases assay (MTA) with GFP-METTL5 purified from HeLa cells vs. GFP alone as a control on total RNA from HeLa cells (left) with tritium labeled SAM (S-adenosylmethionine) as a methyl donor. RNA was purified and tritium signal quantified by liquid scintillation counting (LSC). Counts per minutes are shown. One representative experiment is shown. Data displayed as an average of 3 technical replicates with a standard deviation plotted. (c) TRMT122 interacts with METTL5. The log₂ Fold Change (FC) of GFP-METTL5 to control (GFP alone expressing cell line) in label-free quantification are plotted against the -log₁₀ of the FDR calculated by a permutation-based FDR adapted t-test as described before⁴¹. (d). Domain structure of METTL5. Point mutations used in this study that disrupt catalytic activity are indicated. e. *In vitro* RNA methyltransferases assay (MTA) on total HeLa RNA with recombinant wildtype (wt) GFP-METTL5, GFP-METTL5 mutants with tritium labeled SAM (S-adenosylmethionine) as a methyl donor. RNA was purified and tritium signal quantified by liquid scintillation counting (LSC). Counts per minutes are shown. Data are displayed as 2 biological replicates.⁶⁸

METTL5 catalyses N⁶-methyladenosine formation on 18S rRNA at A₁₈₃₂

Next, I wanted to identify the type of methylation catalysed by METTL5. For this, I grow HAP1 METTL5 KO cells (obtained from Horizon discovery, section 4.1.9 of Materials and Methods) in the media supplemented with D₃-methionine, isolated total RNA and used it as a substrate in the *in vitro* RNA MTAs with recombinant GST-METTL5 and unlabeled SAM as methyl group donor. LC-MS/MS of the *in vitro* reactions revealed m⁶A as the *de novo* methylated nucleoside (collaboration with S. Kellner). We detected no changes in the abundance of 2' O-methyladenosine and 2'-O-methyluridine, but a strong increase in N⁶-methyladenosine abundance (Figure 2.3.2a). These data demonstrate that, *in vitro*, METTL5 is an m⁶A specific RNA methyltransferase.

To confirm the activity of METTL5 in cells and to narrow down the type of methylated RNA, I used *Mettl5* KO mESC lines that were generated by Sebastian Bultmann lab⁶⁸. RNA isolated from these KO cells has indeed lower m⁶A level (data not shown). In a collaboration with the Stefanie Kellner lab, we size-fractionated RNA isolated from three independent *Mettl5* KO clones and wt mESC cells and analysed m⁶A abundance in the different RNA factions. Since it was shown that TRMT112 (interaction partner of METTL5) interacts with WBSCR22, an 18S rRNA methyltransferase involved in pre-rRNA processing and ribosome 40S subunit biogenesis, we specifically wanted to check whether rRNAs can be among the METTL5 substrates. Indeed, we observed a more than 10 fold decrease in the amount of m⁶A per RNA in the fraction containing 18S rRNA as the major component (Figure 2.3.2b), whereas amounts of other methylations such as Am, m⁵C or m^{6,6}A did not change in this fraction. The 18S rRNA has been shown to contain a single m⁶A site at position A₁₈₃₂ (m⁶A₁₈₃₂)⁷¹ with a 99% of the methylation level, located at the base of helix h44, in proximity to the decoding center of the ribosome (Figure 2.3.2c). The drop from ~ 1 molecule of m⁶A per RNA to < 0.1 molecule of m⁶A per RNA suggests that

loss of METTL5 strongly affects m^6A_{1832} . To demonstrate that METTL5 can indeed methylate 18S rRNA I used 18S rRNA gel purified from *Mettl5* KO mES cells as a substrate in *in vitro* RNA MTA with recombinant GST-METTL5 and GFP-METTL5. As shown in Figure 2.3.2d METTL5 has activity on 18S rRNA isolated from *Mettl5* KO cells. This experiment suggests that METTL5 methylates 18S rRNA in wt cells, but that this methylation is absent in *Mettl5* KO and can hence be subsequently added by METTL5 *in vitro*. In summary, my analysis demonstrated that m^6A_{1832} in 18S rRNA is catalyzed by METTL5.

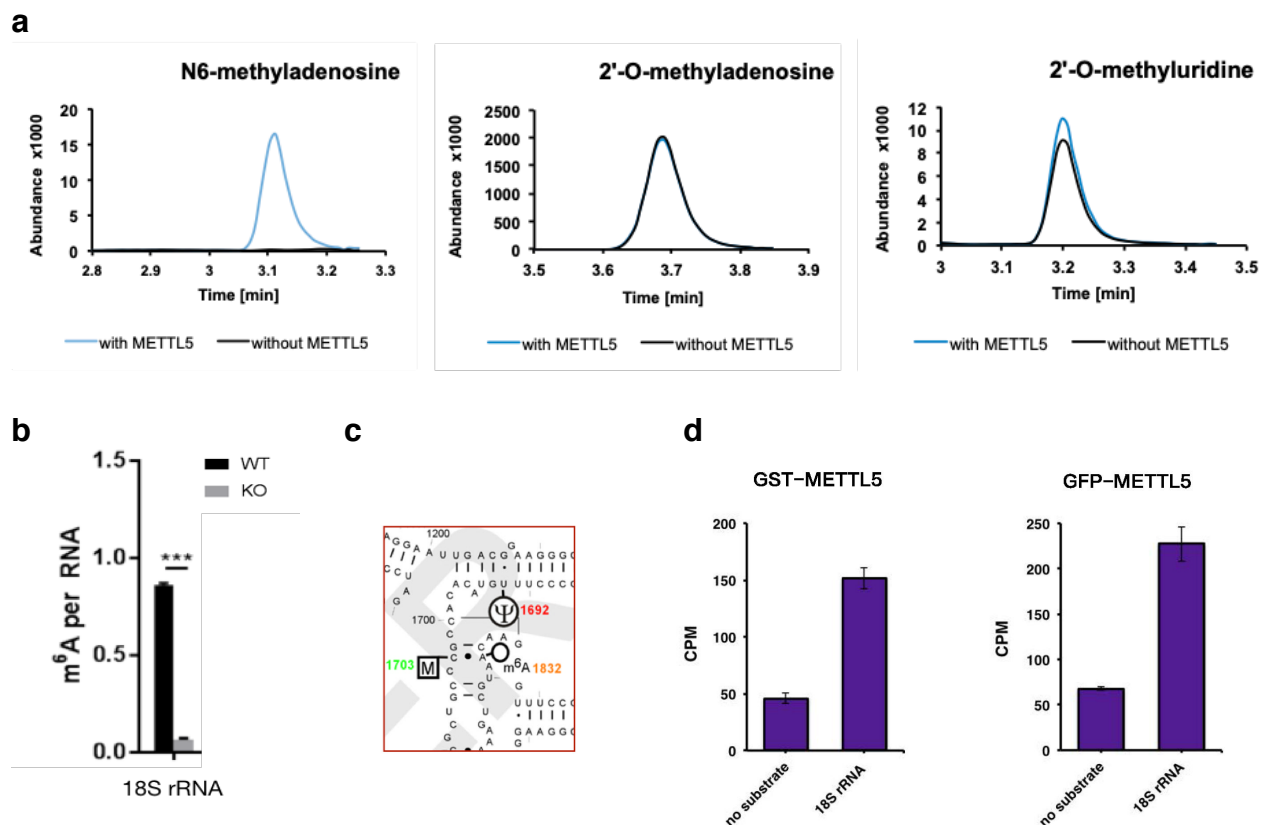


Figure 2.3.2. METTL5 catalyzes m^6A *in vitro* and *in cells*. (a) *In vitro* RNA methyltransferases assay (MTA) followed by NAIL-MS. LC-MS/MS elution profiles of indicated modifications in total RNA. Incubation with SAM and METTL5 (blue) increased the abundance of N6-methyladenosine (m^6A), compared to incubation with SAM alone (black) but not of 2'-O-methyladenosine and 2'-O-methyluridine. (b) Analysis of m^6A

abundance in different fractions revealed 18S rRNA among METTL5 targets. (c) Localization of m⁶A₁₈₃₂ in human 18S rRNA, adopted from Piekna-Przybylska⁷². (d) *In vitro* RNA methyltransferases assay (MTA) with recombinant GST-METTL5 (left) purified from *E.coli* and GFP-METTL5 (right) purified from HeLa cells on 18S rRNA from *Mettl5* KO mESC with tritium labeled SAM as a methyl donor. Tritium signal was quantified by liquid scintillation counting (LSC). One representative experiment is shown. Data are displayed as an average of 3 technical replicates with a standard deviation (SD).⁶⁸

To investigate effects of an absence of METTL5 on mature rRNAs levels I check total RNA from wt and *Mettl5* KO mES cells by Bioanalyzer (Fig.2.3.3). I did not detect alterations in the 28S/18S rRNA ratios. This suggests that loss of m⁶A at 18S rRNA doesn't substantially affect rRNA processing.

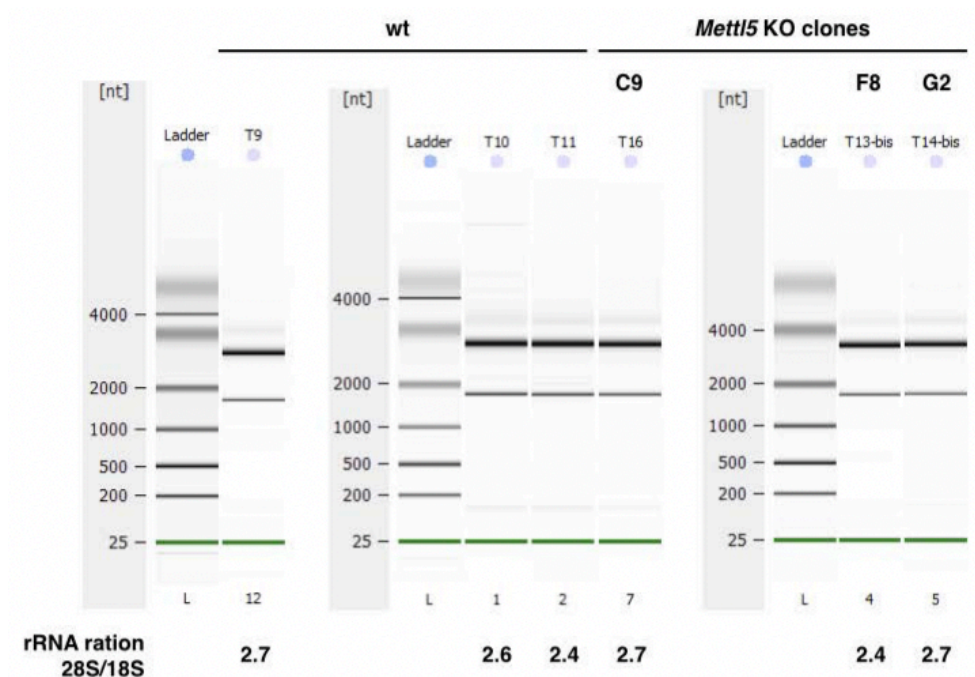
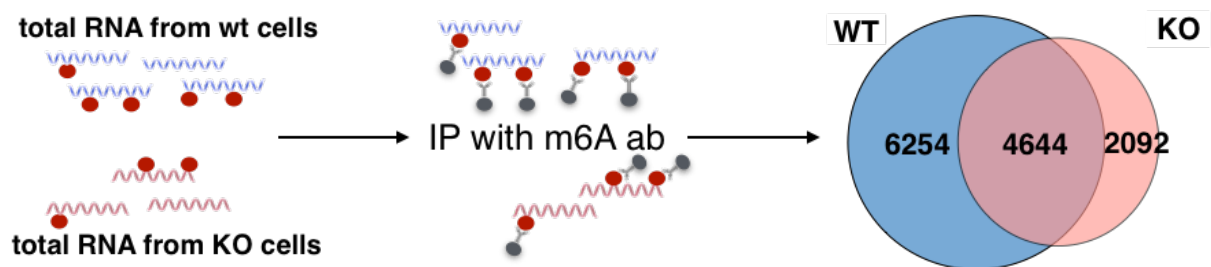


Figure 2.3.3. rRNA maturation is not affected by the loss of 18S rRNA methylation. Electropherograms and quantification of rRNA ratios obtained from Bioanalyzer profiling of total RNA from wt and *Mettl5* KO mESC.

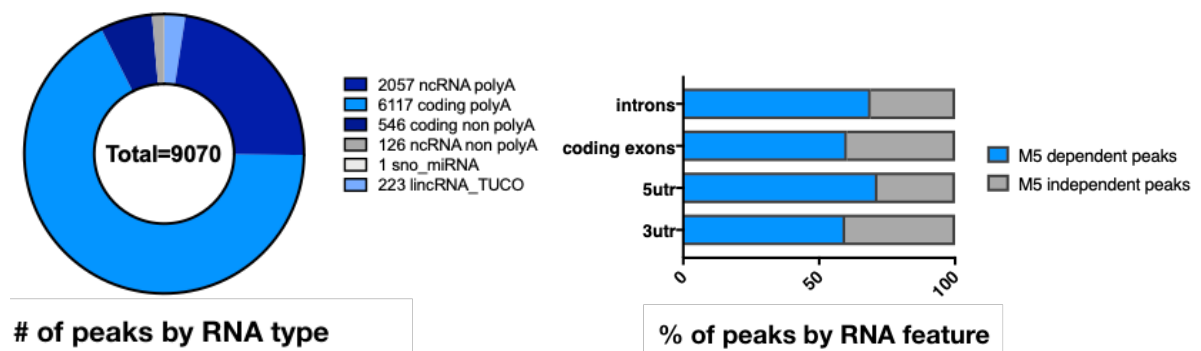
m⁶A-IP reveals METTL5-dependent methylation on mRNA

To search for other potential targets of METTL5 I performed m⁶A-IP followed by sequencing in HAP1 wt and METTL5 KO cells. I used the modified version of m⁶A-IP protocol¹⁸ in that total RNA was immunoprecipitated with m⁶A antibodies followed by rRNA depletion and library preparation (Figure 2.3.4a). I perform m⁶A-IP analysis using pipeline developed by Evgenia Ntini from Annalisa Morsico lab and identified more than 6000 of m⁶A peaks that were absent in METTL5 KO cells indicating m⁶A-dependent methylation of other RNAs than 18S rRNA in human cells (Figure 2.3.4a). I considered wt-only peaks (absent in the KO) and all common peaks with fold change wt vs. ko > 1.5 as METTL5-dependent m⁶A peaks. Analysis of RNA types and features harboring these peaks show that all type of RNAs, but mainly polyA RNA have METTL5 dependent peaks (Figure 2.3.4b and c). Using HOMER motif search, I identified several motifs in that METTL5 dependent peaks preferentially can be found (Figure 2.3.4d).

a



b



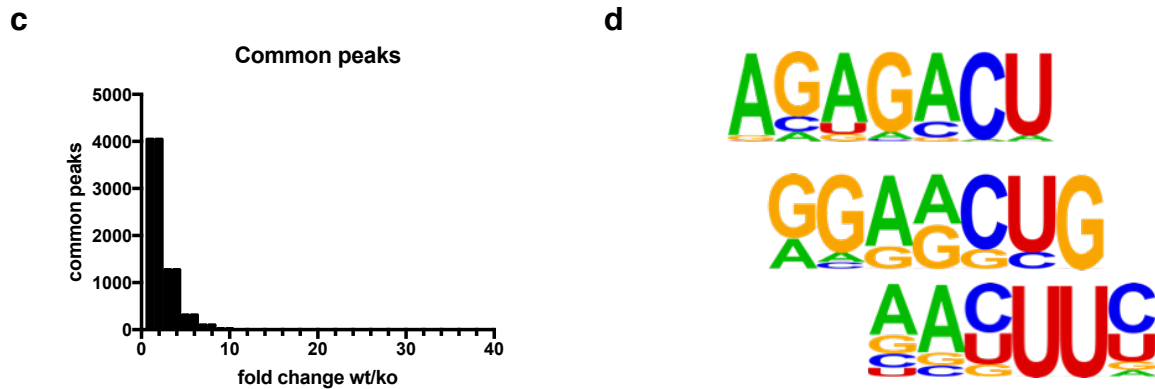


Figure 2.3.4. m⁶A-IP followed by sequencing revealed METTL5-dependent methylation of RNA from human cells. (a) Scheme of the m⁶A-IP experiment with results of peak calling in HAP1 wt and METTL5 KO cells. (b) Fractions of METTL5 dependent peaks split by RNA type (left) and RNA feature (right). (c) Fold change of m⁶A signal in wt to m⁶A signal in METTL5 KO cells for common peaks. (d) METTL5-dependent m⁶A preferentially found within motifs identified by HOMER⁷³.

Next, I wanted to analyse METTL5 dependent methylation in mESC. Since m⁶A-IP in HAP1 cells demonstrated that most of METTL5 dependent methylation occur at polyA RNA, this time I used standard m⁶A-IP protocol with polyA selected RNA as an input for the immunoprecipitation with m⁶A antibodies¹⁸. The m⁶A-IP analysis is still ongoing but the first results revealed a global re-distribution of m⁶A-IP signal within all RNA features (Figure 2.3.5a). To check for potential cross-talk between m⁶A methylation and RNA abundance I performed a comparison of RNA-seq and m⁶A-IP data sets. For this I compared fold change of RNA levels in *Mettl5* KO vs. wt cells for two groups of transcripts: (1) all transcripts that have m⁶A peaks in wt but not in *Mettl5* KO cells and (2) the same number of randomly selected transcript those methylation status doesn't change between wt and KO cells. As shown in Figure 2.3.5 b and c, transcripts that have METTL5-

dependent m⁶A methylation, in general, are down regulated in *Mettl5* KO cells (after losing this methylation). Important to note, the transcripts whose abundance decrease in *Mettl5* KO cells comprise transcripts of different expression levels, thus this result is not an artifact of quantification on low expressed transcripts as visualized by scatter plot (Figure 2.3.5b).

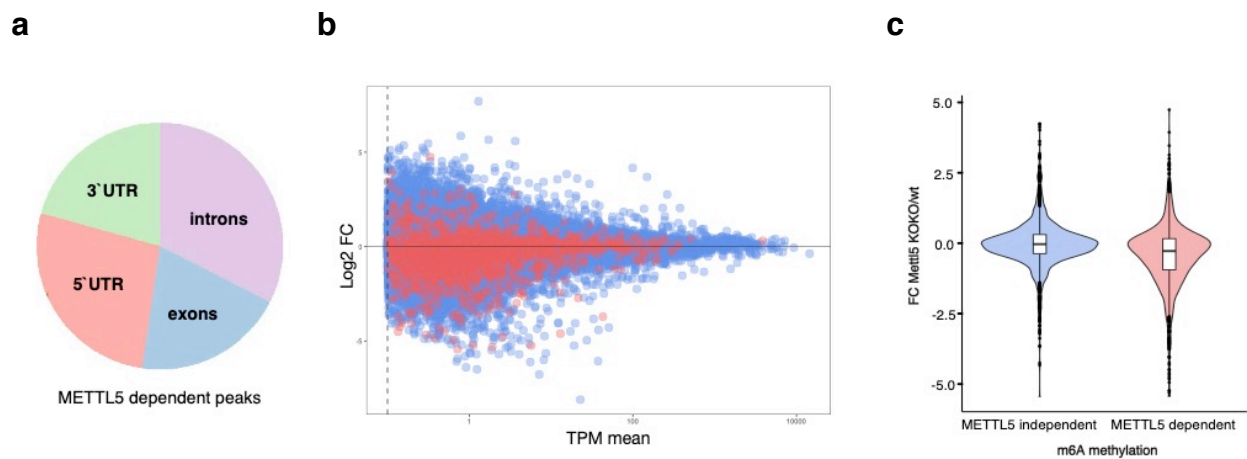


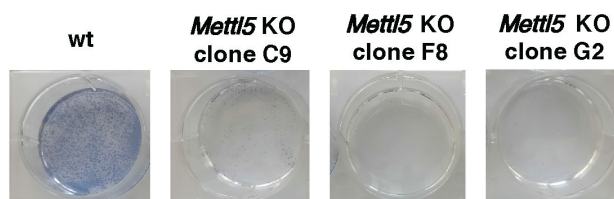
Figure 2.3.5. METTL5-dependent methylation is linked to decreased abundance of transcripts in mESC. (a) Fractions of m⁶A peaks which are gone in *Mettl5* KO mESC split by RNA features. (b) Scatter plot of mRNA log₂ fold change (ko vs. wt) vs abundance (transcripts per million) for mRNA losing m⁶A peaks in *Mettl5* KO mES cells (pink) and the same number of randomly selected mRNA that have no changes in m⁶A methylation in *Mettl5* KO mES cells (blue). (c) Violin plots of log₂ fold change (ko vs. wt) of transcript abundance for mRNAs that lose m⁶A peaks in *Mettl5* KO mES cells (pink) and the same number of randomly selected mRNA that have no changes in m⁶A methylation in *Mettl5* KO mES cells (blue).

METTL5 is essential for mESC pluripotency and correct differentiation

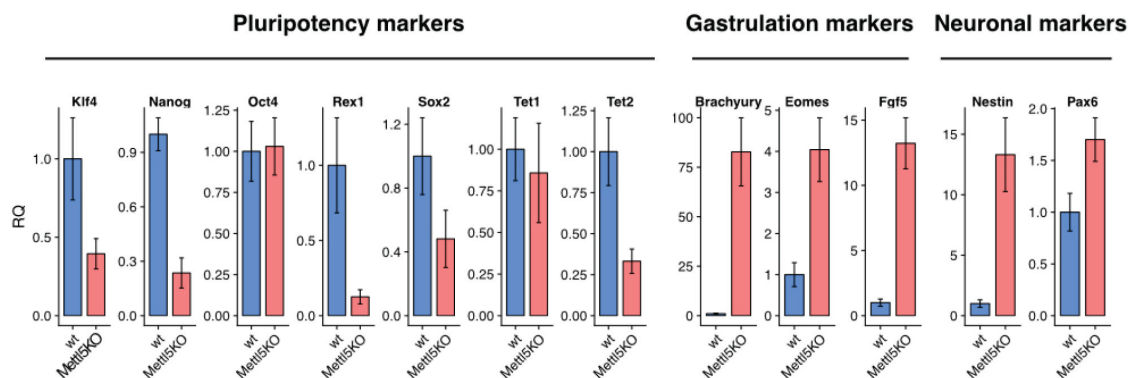
To analyse the effects of loss of METTL5 on pluripotency and differentiation, we performed a further characterization of the mESCs in collaboration with Sebastian Bultmann laboratory. First, we used alkaline phosphatase staining that can differentially stain pluripotent stem cells but not differentiating cells. After 5 days in Serum-LIF medium alkaline phosphatase staining is almost lost in all of the *Mettl5* KO clones analyzed, suggesting a spontaneous tendency to differentiate (Figure 2.3.6a). In line with this, most of the pluripotency markers were downregulated and gastrulation and neuronal markers were upregulated in *Mettl5* KO mES cells (Figure 2.3.6b).

In order to investigate effects METTL5 loss on lineage specific differentiation, we performed a neuronal differentiation of wt and *Mettl5* KO mESCs (Figure 2.3.6c)⁷⁴. Whereas wt mESCs differentiate as expected into neuronal progenitors cells (NPC), as evidenced by staining for the microtubule-associated protein 2 (MAP2) (Figure 2.3.6d), *Mettl5* KO cells fail to differentiate into NPC. Thereby loss of METTL5 in mESCs results in a loss of pluripotency and a failure to correctly differentiate.

a



b



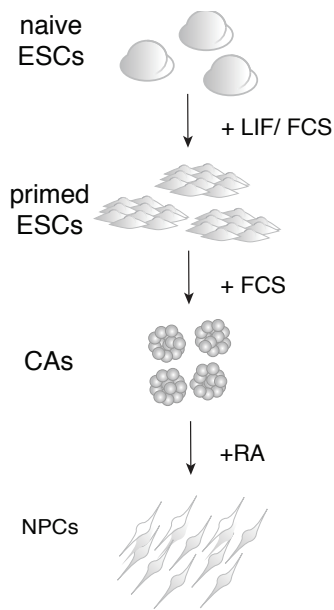
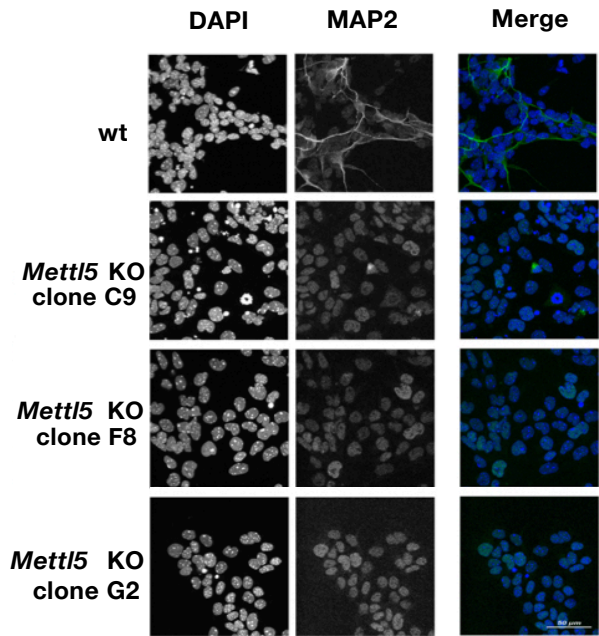
c**d**

Figure 2.3.6. METTL5 KO mESC loose pluripotency and are impaired in their ability to differentiate into neuronal precursors cells. (a) Alkaline phosphatase staining of wt and *Mettl5* KO mES cells (clones C9, F8, G2) four days after seeding. A representative experiment of three independent experiments is shown. Wt mES cells maintain pluripotent state whereas three independent *Mettl5* KO mES cell clones starting to differentiate. (b) qPCR analysis of pluripotency and differentiation markers of wt and *Mettl5* KO mES cells. Average of 3 biological replicates plus standard deviation is shown (c) Neuronal differentiation protocol scheme⁷⁴. (d) Immunofluorescence analysis of wt and *Mettl5* KO mES cells (clones C9, F8, G2) stained with MAP2 antibodies and DAPI.⁶⁸

2.4 Characterization of METTL-interacting proteins

This part of the thesis is published at Ignatova VV, Jansen PWTC, Baltissen MP, Vermeulen M, Schneider R (2019) The interactome of a family of potential methyltransferases in HeLa cells, Scientific Reports. 9: 6584.

Here I wanted to gain insight into the functions of the individual members of the METTL protein family that were part of the MTA screen (Figure 2.4.1). For this, I used an alternative approach and identified the complexes in which the METTL proteins might act. I generated cell lines expressing GFP-tagged METTL proteins and performed systematic immunoprecipitation from HeLa FRT cells followed by label-free quantitative mass spectrometry (collaboration with Michiel Vermeulen lab). We found that many of the METTL proteins appear to function outside of stable complexes whereas others including METTL7B, METTL8 and METTL9 have high-confidence interaction partners. This study is the first systematic and comprehensive overview of the interactome of METTL protein family and can provide a crucial resource for further studies of these potential novel methyltransferases⁴¹.

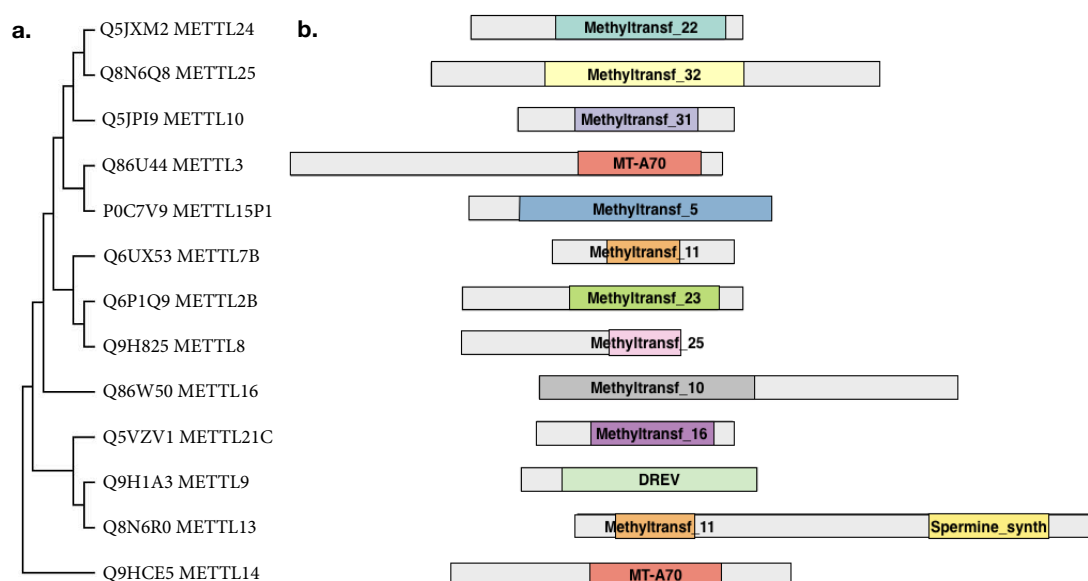


Figure 2.4.1. METTL family members studied. (a) Phylogenetic tree of METTL proteins by the Maximum Parsimony method in MEGA7. UNIPROT numbers are indicated. (b) METTL proteins domain organization annotated according to Pfam (Methyltransf - methyltransferase domain, MT-A70 - N6-adenosine-methyltransferase 70 kDa subunit domain, DREV - DORA reverse strand protein domain, Spermine synth - Spermine/spermidine synthase domain).⁴¹

Establishment of a setup to study METTL interactome

I aimed to systematically identify interaction partners of METTL family members. Due to the absence of specific and immunoprecipitation (IP) grade antibodies for most METTL proteins I generated N-terminal GFP-fusions of 13 METTL proteins under the control of a DOX-inducible CMV (cytomegalovirus) promoter. I used a HeLa-FRT cell line for recombination mediated targeted integration and inducible expression as described in van Nuland et al.⁶⁴ To control for GFP-fusion proteins expression I used Microscopy and WB with GFP antibodies. Additionally, I performed a comparison of localization of GFP-METTL proteins in the cell lines that I generated to data published at Human Protein Atlas (HPA) consortiums based on IF staining (Table 2.4.1).

Protein	According to HPA (antibody staining)	After DOX-induction
GFP-METTL2B	no data	Cytosol
GFP-METTL3	no data	Nucleus
GFP-METTL5	Nucleoli / Cytosol	Nucleus
GFP-METTL6	Vesicles	Whole cell
GFP-METTL7B	Vesicles / Microtubules	Nucleus
GFP-METTL8	Cytosol	Nucleus
GFP-METTL9	Nucleus / Cell Junctions / Cytosol	Cytosol / whole cell
GFP-METTL10	Nucleoplasm / Nuclear bodies	Cytosol

GFP-METTL13	Cytosol	Whole cell
GFP-METTL14	Nucleoplasm	Nucleus
GFP-METTL15	Golgi apparatus / Plasma membrane / Actin filaments	Whole cell
GFP-METTL16	Nucleoplasm / Cytosol	Nucleus
GFP-METTL21C	no data	Unclear
GFP-METTL24	no data	Can't be induced
GFP-METTL25	Plasma membrane / Mitochondria / Cytosol	Unclear

Table 2.4.1. Cellular localization of GFP-METTL family members studied.

METTL interaction proteomics

In collaboration with Vermeulen laboratory, we use first Methyl-CpG-binding domain protein 3 (MBD3) fused to GFP as a control to verify that under the conditions we use we can purify and identify well-defined protein complexes from total cellular HeLa extract by label-free quantitative mass spectrometry (Figure 2.4.2a). As expected, the majority of previously described interaction partners of MBD3 including multiple members of the Nucleosome Remodeling and Deacetylase (NuRD) complex was detected (Figure 2.4.2b)⁷⁵.

We additionally tested this approach on METTL3 and METTL14 that I was also using to optimize *in vitro* MTA screen. The interaction between METTL3 and METL14 was detected in both METTL3 (Figure 2.4.2c) and METTL14 (Figure 2.4.2d) purifications. Having validated that we can detect stable interactions I extended this study towards 11 other members of the METTL family (Figure 2.4.3a-k).

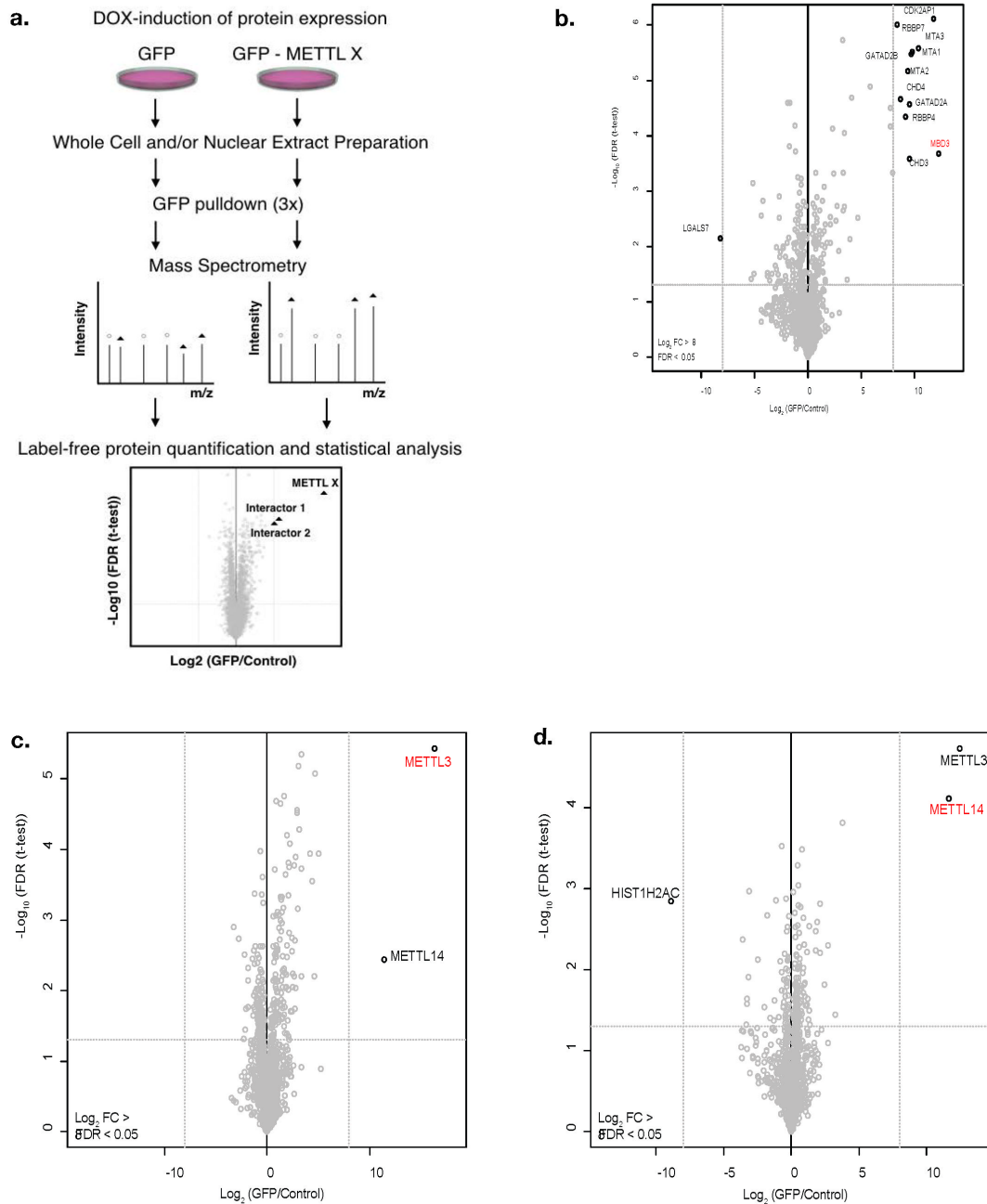


Figure 2.4.2. Experimental workflow. (a) ORFs of METTL proteins were cloned as GFP fusions under the control of a DOX-inducible promoter for targeted single-copy integration into HeLa FRT cells. Whole-cell extracts and/or nuclear extracts were prepared from GFP-METTL or GFP (control) expressing cells. GFP pull-downs were performed in triplicate followed by mass spectrometry analysis. Analysis of raw data was performed in MaxQuant⁷⁶ (version 1.5.1.0) and Andromeda. Data filtering and generation of volcano plots were done essentially as described using a one-way ANOVA test⁷⁷ with log2 fold change (FC) > 8 and false discovery rate (FDR) < 0.05 as thresholds. (b) Volcano plot of

GFP-MBD3 interacting proteins as an example of successful complex identification using this protocol. Significant interactors are indicated. Volcano plots show (c) METTL3 and (d) METTL14 interactors. The \log_2 FC of GFP fusions to control in label-free quantification are plotted against the $-\log_{10}$ of the FDR calculated by a permutation-based FDR adapted t-test. The baits are indicated in red.⁴¹

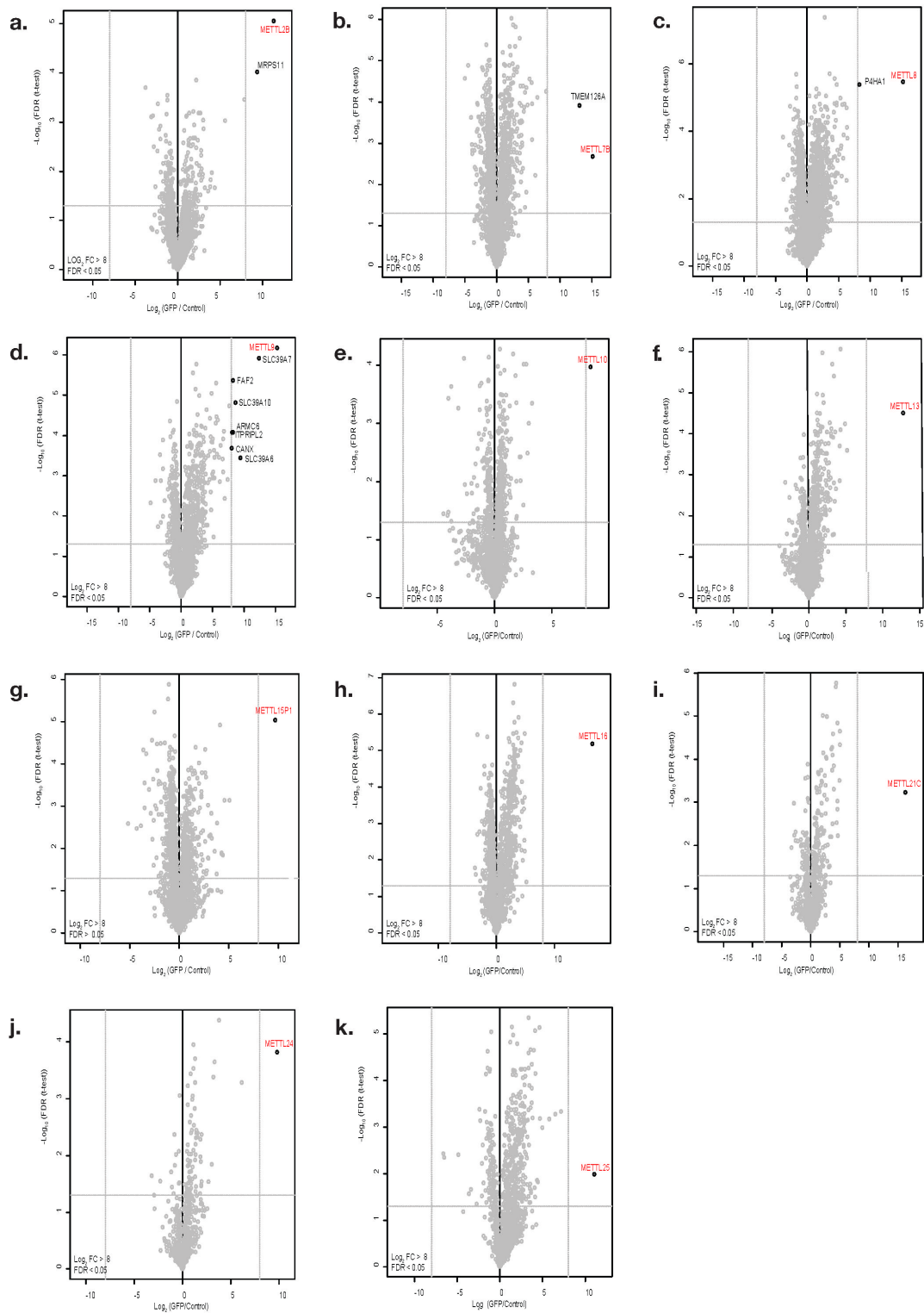


Figure 2.4.3. Interactome of METTL family members. Volcano plots show interaction partners for: (a) METTL2B, (b) METTL7B, (c) METTL8, (d) METTL9, (e) METTL10, (f) METTL13, (g) METTL15P1, (h) METTL16, (i) METTL21C, (j) METTL24, (k) METTL25. Purifications were performed from whole cell extracts. Data displayed as described in the legend of Figure 2.4.2.

For METTL7B (Figure 2.4.3b) we identified the transmembrane protein TMEM126A as a high confidence interactor (with a log2 fold change (FC) > 8 compared to the GFP-alone expressing control). TMEM126A is a Myc proto-oncogene protein (MYC) target and a mitochondrial membrane protein of unknown function. Defects in the gene encoding TMEM126A can cause optic atrophy type 7 (OPA7)^{78,79}. This interaction with a mitochondrial membrane protein could suggest a potential function of METTL7B in, for instance, RNA methylation in mitochondria.⁴¹

Prolyl 4-Hydroxylase Subunit Alpha 1 (P4HA1) is a high confidence interactor for METTL8 (Figure 4.2.3c). P4HA1 has dioxygenase and oxidoreductase activity and catalyzes the post-translational formation of 4-hydroxyproline⁸⁰. Xu et al.¹² recently showed that METTL8 catalyzes m³C in mRNA *in vitro* and in human cells. Identification of P4HA1 as a high confidence interactor for METTL8 suggests that METTL8 could couple RNA modifications with transcriptional regulation.⁴¹

Loosening of a threshold to log2 FC > 5 revealed additional potential interactors for METTL2B, METTL13, METTL15P1, METTL16, METTL21C, METTL24, and METTL25 although often close to the threshold. Surprisingly, METTL10 has no interaction partners even with log2 FC > 5 threshold.⁴¹

I wanted to confirm that with our purification method I indeed enrich for previously described enzymatic activity and not e.g. loose interaction partners essential for this activity due to the presence of the GFP tag at the N-terminus of the potential enzymes or due to the experimental procedure. For this, I performed *in vitro* RNA MTA with purifications of two enzymes (GFP-METTL8 and GFP-METTL16 that were shown to have RNA methyltransferase activity). In this *in vitro* assay both GFP-purifications retained, as expected, methyltransferases activity on total cellular RNA from HeLa cells (Figure 2.4.4).

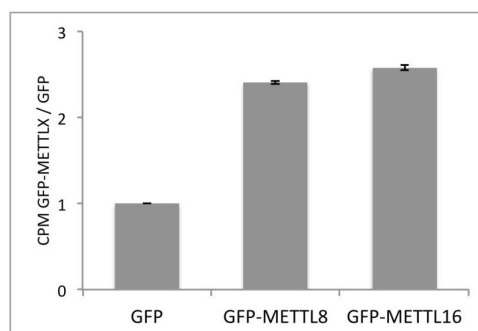


Figure 2.4.4. Confirmation of enzymatic activity of GFP-METTLs. *In vitro* methyltransferase assays demonstrating that our GFP-METTL8 and GFP-METTL16 purifications have the expected RNA methyltransferase activity. GFP (as a control) and GFP-fusion proteins were purified from corresponding DOX-induced HeLa FRT cell lines and used in an *in vitro* methyltransferase assay on total RNA from HeLa cells as a substrate and ³H-SAM as a methyl-donor. After purification of the RNA, counts per minute (CPM) were quantified by liquid scintillation counting. The ratio of CPM measured for reactions with GFP-METTL fusion proteins relative to GFP alone are plotted. Data are shown as mean \pm SD from three replicates.⁴¹

METTL9 interacts with CANX

METTL9 was the only METTL protein for which we identified multiple interaction partners including membrane proteins such as Calnexin precursor (CANX), a potential chaperone, and multiple Solute carrier family 39 (SLC39) proteins (Figure 2.4.3d).

Next, we repeated the purifications for METTL9 using nuclear extract instead of total cellular extract. I chose METTL9 for this experiment as an example since it has multiple interactors and narrowing down the cellular localization of these interactors could bring additional insights into METTL9 functions. Figure 2.4.4 shows additional proteins interacting with METTL9 with a threshold of \log_2 FC > 5 (Figure 2.4.5).

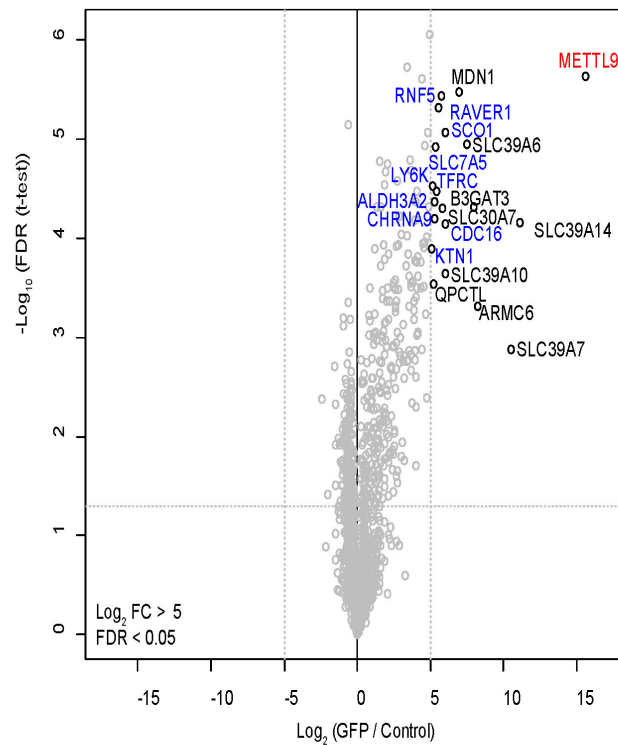


Figure 2.4.5. Nuclear interactome of METTL9. Volcano plot shows METTL9 interaction partners. Purifications were performed from the nuclear extract. Data displayed as described in Figure 2.2.4 but using cutoff \log_2 FC > 5. The interactors, detected only in the nuclear interactome, are indicated in blue.⁴¹

To verify those results, I chose to confirm the interaction between METTL9 and CANX. To do so, I performed GFP-METTL9 immunoprecipitation and detected, as expected, CANX as an interactor by western blotting (Figure 2.4.6a). Also, I detected GFP-METTL9 as a CANX interacting protein in the reverse IP (Figure 2.4.6b). CANX plays an important role in the regulation of endoplasmic reticulum luminal calcium concentration⁸¹ and can act as a protein chaperone that assists protein folding and quality control⁸². Based on this interaction one could speculate that METTL9 is a protein rather than an RNA methyltransferase and could couple nascent protein folding with post-translation modifications.

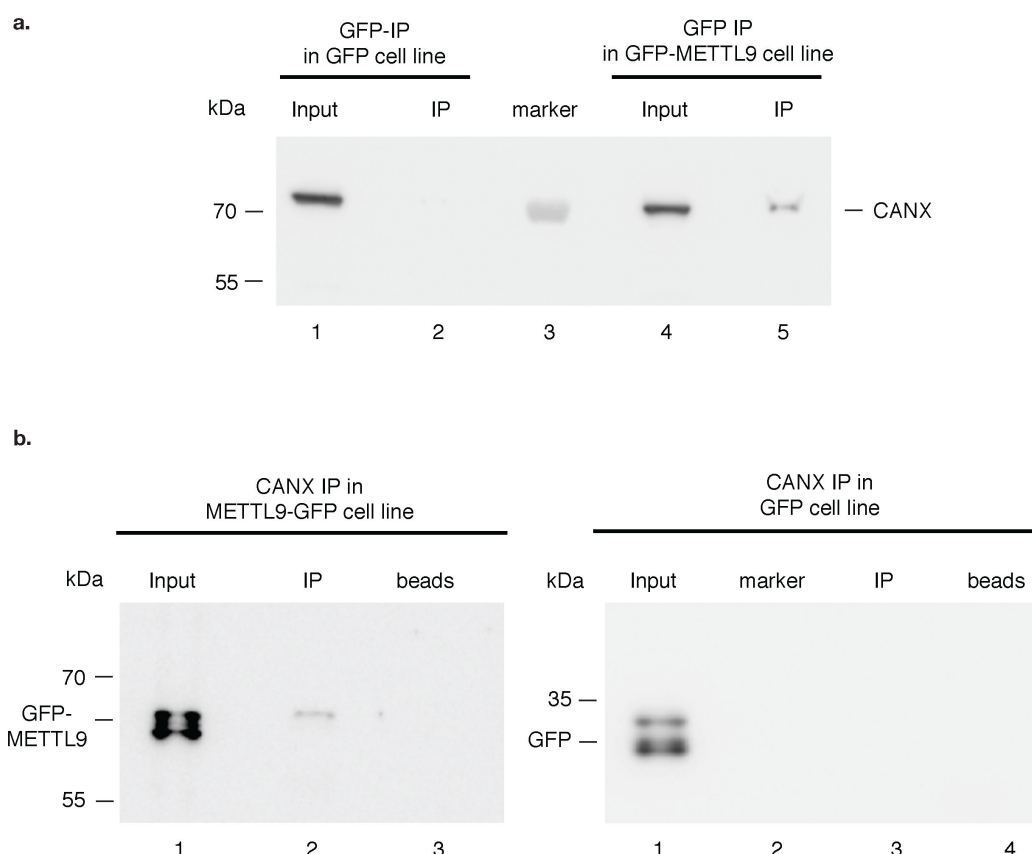


Figure 2.4.6. Confirmation of METTL9 interactors. (a, b) Validation of interaction between METTL9 and CANX by co-IP. (a) CANX is detected in GFP-METTL9 IP (a, lane 5) but not GFP IP (a, lane 2). 10 μ l of GFP trap and 2 mg of whole-cell extract were used. 20 μ g of Input material were loaded for comparison. (b) GFP-METTL9 (left panel, line 2) but not GFP (right panel, line 3) can be detected by immuno-blot with GFP antibody in the CANX IP. 10 μ g of calnexin antibody and 4 mg of whole-cell extract were used. 200 μ g of Input material was loaded for comparison. No antibody (beads alone) used as control.⁴¹

In summary, this first systematic and comprehensive overview of the interactome of METTL protein family can provide a crucial resource for further studies of these potential novel methyltransferases.

3. Discussion

3.1. Systematic identification of novel methyltransferases from METTL protein family

METTL proteins are currently of high interest since this is a protein family considered to encompass many potential methyltransferases. Yet for most of METTL proteins it is unclear whether they are indeed active enzymes, which modification they catalyze and what are their substrates: RNA, DNA or proteins. To gain insight into their catalytic activities, we systematically screened the activity of recombinant METTL proteins in *in vitro* RNA and DNA methyltransferase assays. Besides METTL5 and METTL6, whose enzymatic activities on total RNA were very pronounced and will be discussed later in chapters 3.2 and 3.3, METTL8, METTL13 and METTL16 exhibited clear methyltransferase activities under the conditions used. Initially, we choose all five of them for follow up studies. The only potential hit we missed, known to date, – is METTL2B that recently was shown to deposit m³C into several tRNAs¹². This initial false-negative result might be e.g. due to inactive enzymes we obtained in the first purifications. Later on, we re-purified and checked METTL2B again on total RNA and indeed detected an activity. Thus it seems that the first purification of METTL2B was less active and, having identified more active enzymes during the screen, we didn't consider METTL2B activity clear enough to design follow up studies.

While we were working on an identification of METTL8 substrates, this protein was shown to catalyze m³C in polyA RNA¹². Owing to the difficulties to express and purify METTL8 and to completely deplete rRNA from the polyA RNA fraction for mass spectrometry we decided not to follow up METTL8 and put more effort on other hits from the screen. This year METTL8 was shown to bind *Mapkbp1* mRNA and inhibit its translation albeit the authors didn't unravel the exact molecular mechanism nor check m³C

level in that mRNA⁸³.

METTL13 had methyltransferase activity in the screen, but we had difficulties to purify it clean enough to confidently distinguish METTL13 activity from activities of others, co-purifying with it, proteins. Later, METTL13 was shown to methylate eEF1A at the N terminus and Lys55 resulting in altered translation rate of specific codons⁸⁴. In a follow study METTL13 methylation of eEF1A was shown to be implicated in the development of KRAS-Driven Cancers⁸⁵. If it is an RNA and protein or only a protein methyltransferase remains an open question.

METTL16 had a clear activity on dsRNA and DNA in our hands. In fact, m⁶A methylations of DNA and RNA are chemically very similar since a methyl group is deposited on a nitrogenous base. Thus it is possible that m⁶A methyltransferases, in suboptimal *in vitro* conditions, might methylate both: DNA and RNA. In our *in vitro* conditions METTL3 and METTL14, despite being very well characterized RNA methyltransferases with known sequence specificity, were able to methylate DNA though to a much lower extent than RNA. Having this in mind, we always aimed to validate the activities that we observed *in vitro* using a cell culture model. We were not able to obtain METTL16 KO since it was not viable in HAP1 cells that we used for enzymes validation. While we were overcoming this issue, METTL16 was shown to catalyze m⁶A in several RNA types^{3,53,54}, so we decided to focus on other proteins from the screen.

In summary, we designed and carried out a systematic *in vitro* screen for novel nucleic acid methyltransferases from the METTL protein family. We identified several novel RNA methyltransferases and performed extensive follow-up characterization for two of them as discussed below.

3.2. tRNA m³C methyltransferase METTL6 regulates translation

tRNAs are the most modified type of cellular RNA molecules and their modifications play a major role in their functionality¹. Yet the exact role of each modified residue and corresponding enzymes catalyzing these modifications remain to be discovered. Here, by using a combination of *in vitro* and *in cells* approaches we identified METTL6 as a tRNA methyltransferase that specifically methylates position C32 in distinct tRNA^{Ser} isoacceptors.

This modification is evolutionarily conserved with m³C in tRNA^{Ser} has been identified in *S. cerevisiae* and *S. pombe*. *S. cerevisiae* m³C methyltransferases were identified a while ago as Trm140 and Trm141 that are responsible for m³C formation at position 32 in tRNA^{Thr} and tRNA^{Ser}, respectively^{86,87}. In mammals there are three Trm140 and Trm141 homologues shown to possess m³C methyltransferase activity during the same time as I was working on my thesis: METTL2, -6 and -8¹². In this study METTL6 was mentioned to contribute to tRNA methylation, however, no catalytic activity or biological function was shown. The same study showed that METTL2 can methylate tRNA^{ThrAGU}, tRNA^{ThrUGU} and tRNA^{ArgCCU}¹². In agreement with these data, we did not observe any effect of METTL6 knock out on the methylation of these tRNA isoacceptors. Here we demonstrate for the first time that METTL6 catalyses the formation of m³C in specific tRNAs^{Ser}, but not other tRNAs that carry m³C. Knock out of METTL6 leads to a two-fold decrease in m³C levels of these tRNA^{Ser} isoacceptors, suggesting that the second m³C site in these tRNA isoacceptors is methylated by another enzyme (e.g. METTL2). We did not detect any noticeable effects of METTL6 depletion on m³C levels in polyA RNA, what is in line with previous reports describing METTL8 as potential m³C mRNA methyltransferase¹².

We performed RNA-seq and Ribosome profiling in the wt and *Mettl6* KO mES cells to characterise the effects of METTL6 loss on mRNA levels and translation efficiency. We observed a misregulation of mRNAs and altered translation efficiency of genes related to

proliferation, signaling and growth control, as well as translation and proteostasis. These changes in the translational landscape could potentially be the cause of the observed phenotypic abnormalities such as differentiation defects in the mESCs.

As some RNA methyltransferases work in stable complexes with additional proteins, we wanted to search for METTL6 interacting proteins. We identified Hippo signaling pathway regulators: SAV1 and STK4 (MST1 is an alternative name) as METTL6 interactors in HeLa cells. SAV1 is the main activator of the Hippo pathway that acts via a cascade of the MST-LATS kinase and controls cell proliferation, growth, death, and cellular homeostasis⁶⁵. None of the METTL6 interactors we found has RNA binding or methyltransferase domains indicating that METTL6 does not rely on other proteins for performing its enzymatic function. In support of this, recombinant GST-METTL6 purified from *E.coli* and lacking its interacting partners can specifically methylate C32 position in tRNA^{Ser}. Taking together, our data suggest an intriguing possibility of crosstalk between cellular signaling pathways and translation regulation via modifications on tRNAs.

In summary, we performed a comprehensive characterisation of METTL6 as tRNA^{Ser} m³C methyltransferase that is important for correct translation, affects proliferation of mES cells and forms a complex with components of the Hippo signaling pathway. Meanwhile, our collaborators from Ernesto Guccione lab identified METTL6 as a protein implicated in cancer progression in a pooled shRNA *in vivo* screen and showed that METTL6 loss inhibits liver cancer cell proliferation⁵⁵. In line with these findings, a high expression of METTL6 correlates with reduced survival of hepatocellular carcinoma patients. Also, the role of METTL6 extends beyond liver cancer as METTL6 has been found amplified in different tumors such as highly proliferative luminal tumors and its amplification predicts a significantly worse outcome in patients^{55,88–90}. Given the recent success in identifying selective and potent small molecule inhibitors of methyltransferases⁹¹, METTL6 and other RNA methyltransferases could be promising targets of disease therapies.

3.3. METTL5 is m⁶A RNA methyltransferase that controls pluripotency and differentiation

Here we identified METTL5 as an m⁶A RNA methyltransferase and demonstrated for the first time that loss of METTL5 severely affects ES cell pluripotency and differentiation. Our experiments *in vitro* and *in cells* strongly suggest that METTL5 is an 18S rRNA specific m⁶A methyltransferase. However, we cannot exclude additional targets with structure and/or sequence similarity to the region around A₁₈₃₂ in 18S rRNA since we also observed *in vitro* activity of METTL5 on polyA RNA and identified thousands of METTL5-dependent m⁶A peaks on polyA RNA in our m⁶A-IP, both in human and mouse cells.

Although many rRNA modifications are highly conserved in eukaryotes, m⁶A₁₈₃₂ in 18S rRNA is absent in *S. cerevisiae*. As most research investigating ribosomes structure is done in yeast, this resulted in a modifying enzyme for A₁₈₃₂ has been unknown for a very long time. According to the Human Protein Atlas project⁹², METTL5 can be found in the nucleoli and cytoplasm. We suggest that in nucleoli, a cellular compartment where initial steps of ribosome biogenesis take place, METTL5, in a complex with TRMT112, methylates 18S rRNA. The interaction of METTL5 with TRMT112 has recently been described⁹³. It has been suggested that TRMT112 stabilizes METTL5 and at the same time acts as its co-activator, similarly to TRMT112 co-activator activity in complexes with other methyltransferases^{69,70,94}. In line with these reports, we observed higher activity of GFP-METTL5 purified from mammalian cells compared to GST-METTL5 purified from *E. coli* and thus, lacking its interaction partner TRMT112.

Modifications of rRNA can affect ribosome structure and function, including mRNA decoding, dwelling time, peptidyl transfer, as well as rRNA interactions with tRNA, mRNA and translation factors. rRNA modifications have also been shown to alter translation

rate^{95,96,97,98}. Interestingly, m⁶A₁₈₃₂ is the only described m⁶A site in human 18S rRNA and located with the 3' minor domain of the 18S rRNA, at the base of helix h44, in proximity to the decoding center (Figure 2.3.2c). This region base pairs with C₁₇₀₃, that is in direct contact with mRNA, and might only be accessible and exposed in 40S precursors⁹³, supporting our hypothesis that METTL5-TRMT112 complex methylates 18S rRNA in the nucleoli. This area within the ribosome is extremely conserved in all kingdoms of life. Because of the proximity to the mRNA, the modification of A₁₈₃₂ may be involved in fine-tuning of decoding and translation efficiency.

To analyse changes of m⁶A signal in other RNA types than 18S rRNA in the absence of METTL5, we performed immunoprecipitation with m⁶A antibodies of total RNA and polyA selected RNA from wt and KO cells. These experiments revealed groups of transcripts that loose m⁶A methylation upon METTL5 loss. m⁶A on RNA was shown to affect its biogenesis, stability, and translation⁹. Indeed, we observed a correlation between loss of m⁶A and decrease in mRNA levels in *Mettl5* KO cells. At that moment we cannot distinguish between direct methylation of mRNA by METTL5 *in vivo* and m⁶A changes due to misregulation of other m⁶A writers and erasers. To tackle this question m⁶A-CLIP, that can detect a binding pattern of METTL5 on polyA RNA in cells, would be the next step.

We found that the loss of *Mettl5* negatively affects the self-renewal of mES cells and severely affect their differentiation potential. The later is similar to results of knockdown of proteins involved in ribosome biogenesis and protein syntheses that were shown to cause an accumulation of undifferentiated germ cells³⁶. It was shown by a number of reports that the differentiation process relies on a robust translation system. Low polysomes number characterizes undifferentiated ESCs^{99,100}, probably, due to an inefficient loading of most transcripts with ribosomes. Differentiation requires an increase in protein synthesis with most genes showing at least a 1.5-fold increase in ribosome loading and failure to do so

prevents differentiation³⁶. The increase in translation of differentiated cells coincides with a significant increase in the total RNA (~50%), ribosomal RNA (~20%), and proteins (~30%) amounts³⁷.

Mutations of METTL5 have been reported in human patients with learning impairment, intellectual disorders, motor-weakness, microcephaly and nasal bone deformation as summarized in the table 3.3.1^{101–103}. In collaboration with German Mouse Clinic, we generated *Mettl5* knock out mice to identify *in vivo* consequences of METTL5 loss and provide a mouse model potentially useful to study METTL5-related diseases. Knockouts of two other m⁶A RNA methyltransferases are lethal: *Mettl3* is an early embryonic lethal¹⁰⁴ and *Mettl16* is lethal around implantation stage¹⁰⁵. In contrary to this, we found *Mettl5* KO mice are viable although with a significant sub-viability and clear phenotypes⁶⁸.

Organism	Phenotype	Study
Human	moderate intellectual disability, self-mutilation, short stature, microcephaly, truncal ataxia	Riazuddin S, et al., Mol Psychiatry. 2016
Human	severe intellectual disability, speech delay, attention deficit hyperactivity disorder, aggression, autism, abnormal dentation, large ears, mild hypotonia, growth retardation, motor weakness	Reuter et al., J JAMA Psychiatry. 2017
Human	severe microcephaly, learning impairment, aggression, narrow nasal base, severe intellectual disorders	Hu H, et al., Mol Psychiatry. 2016.
Mice	alveolar bone loss	Sima et al., J Periodont Res 2016

Table 3.3.1. Diseases associated with METTL5 mutations in human and mice.

In mice, alveolar bone loss upon *Mettl5* mutations had been described¹⁰⁶. Our *Mettl5* KO mice recapitulate these phenotypes and can, therefore, serve as a new mouse model to study this disorders⁶⁸. Additionally, we observed a decrease in locomotors activity of *Mettl5* KO mice that could be a sign of altered novelty-induced anxiety, yet may also reflect motor dysfunction. Understanding the full impact of *Mettl5* loss on brain function will require additional investigation. Importantly, we observed the reduced body weight, eye and craniofacial malformations activity in *Mettl5* KO mice. All together these suggest that METTL5 plays an essential role during mouse development and that its loss can result in failure to thrive, as well as in morphological and behavioral abnormalities.

In summary, we identified METTL5 as m⁶A RNA methyltransferase that catalyses m⁶A on 18S rRNA and, potentially, polyA RNA in human and mouse cells. Our work also revealed that METTL5 has an impact on mES cell pluripotency and their differentiation potential. Additional studies will be required to investigate the structural impact of methylation loss at A₁₈₃₂ on ribosomes structure and on a selective translation of specific mRNAs that is essential during stem cells specification and zygotic genome activation¹⁰⁷.

3.4. METTL proteins interactome

In the last part of my Ph.D. project, I aimed to get insights into the functions of METTL family members by systematically purifying and identifying their interaction partners from HeLa cells. To the best of my knowledge, this work is the first comprehensive proteomics interaction study of METTL proteins. Besides METTL6 and METTL5, whose interaction partners we studied separately, only METTL7B, METTL8, and METTL9 have interaction partners and many METTL members, including some that are active methyltransferases

(such as METTL16 and METTL10), seem not to have any stable high confidence interaction partners (with $\log_2 \text{FC} > 8$) and to act without being part of well-defined complexes.

Since for many of the METTL proteins I was focused on in my project no commercial IP validated antibodies were available I had to use a GFP-tagging strategy. As expected, all the bait proteins were detected by mass spectrometry (Figures 2.2.7, 2.3.1, 2.4.2). Nevertheless, it is still a possibility that GFP tag might e.g. affect interactions with specific partners. The advantage of the DOX-inducible expression system I used is that it allows avoiding potential toxic effects or phenotypic changes of cells due to long-term over-expression of proteins that might be active enzymes. Since our lab and Michiel Vermeulen's lab who performed LC-MS/MS experiments had successfully applied similar purification protocols relying on GFP fusions stably integrated in HeLa-FRT cells combined with DOX inducible expression before^{64,108 109–111} we are rather convinced that the low number of stable interaction partner we detected is not simply due to technical limitations of our approach. As an additional validation, the purification of GFP-MBD3 was used as a positive control as well as the confirmation of the previously described interaction between METTL3 and METT14, by purifying both GFP-METTL3 and GFP-METTL14. Note that the third previously reported METTL3/METT14 interacting protein – pre-mRNA-splicing regulator (WTAP) has been described to be less stably associated and therefore we did not detect it under the conditions we used²⁵. Furthermore, throughout my thesis, I showed that the N-terminal GFP tagging did not interfere with methyltransferases activity of the purifications (Figures 2.3.1, 2.4.5) suggesting that no interaction partners essential for METTLs activity are getting lost during our purifications. All together this strongly suggests that the chosen approach works technically and that most METTLs indeed act outside of stable complexes and do not need partners to be active. Interestingly, multiple METTLs have potential substrate binding ability e.g. for RNA^{54,112,113} that could allow them to bind

their substrates and thus act alone. In line with this, the recently published crystal structure of METTL16 bound to its target RNA¹¹⁴ revealed the structural basis for RNA binding and methylation by METTL16 alone and supports our conclusion that many METTL proteins may act outside of stable protein complexes. This would be comparable to many kinases that are important enzymes and often lack strong interactors. However, it is important to mention the possibility of additional transient weaker interactions that were not identified by affinity purifications-mass spectrometry experiments. For this, alternative approaches such as cross-linking mass spectrometry or proximity labeling followed by mass spectrometry such as APEX¹¹⁵ or bioID¹¹⁶ could be applied to capture enzyme-substrate relations. Furthermore, it is possible that potential interactions might not be present in the HeLa cells.⁴¹

Overall, I systematically characterized for the first time the interactome of an important family of putative novel methyltransferases. These data is an important resource and can serve as a starting point for future studies on the functional significance of the interactions that we report. Since there is currently a lack of high quality antibodies for many METTL proteins, the large set of cell lines I created, expressing inducible GFP fusions of METTL proteins, could be a valuable tool for further studies such as identifications of the potential binding sites of these proteins to RNAs or DNAs as well as to screen for potential substrates and modification sites.

4. Materials and Methods

4.1 Materials

If not listed below, common chemicals and reagents were purchased from the following suppliers: BD Lifesciences, Bio-Rad, Cayman Chemicals, Greiner, Merck-Millipore, Roche, Roth, Serva, Sigma-Aldrich, Thermo Fisher Scientific, VWR.

Oligonucleotides were purchased from Sigma; restriction enzymes, dNTPs and ferments (if not listed below) were purchased from New England Biolabs.

4.1.1 Chemicals and reagents

Chemical	Company
1,4-Dithiothreitol (DTT)	Roth
1 kb DNA ladder	Thermo Fisher Scientific
6 x loading dye solution	Thermo Fisher Scientific
A	
Acetic acid	VWR
Acetone	Baker
Agarose GTQ	Roth
Ammonium acetate	Roth
Ammoniochloride	Roth
Ammoniunperoxodisulfat	Roth
Ammoniumsulfat	Roth
Aurora B kinase	Robert Schneider lab
ABsolute Blue QPCR Mix, SYBR Green, with separate ROX vial	Thermo Fisher Scientific
Acrylamide/Bis Solution, 29:1 (40 % w/v), 3.3 % C	SERVA
Adenosine	Sigma-Aldrich
ATP-P32 alpha	Perkin Elmer

B	
BCA	Roth
C	
Calciumacetat x-Hydrat	Roth
Calciumchlorid Dihydrat	Roth
CAPS	Roth
Cäsiumchlorid	Roth
Chloroform	Roth
Chloroquine diphosphate salt	Sigma-Aldrich
Coomassie Brilliant Blue	Roth
Cysteaminehydrochlorid	Fluka
L-Cystein	Roth
D	
DAPI	Sigma-Aldrich
Desoxicholic Na-Salt	Fluka
Dimethylpimelinediimidate	Fluka
Dimehtylsulfoxid	Roth
Dam from E.coli	Sigma-Aldrich
DMEM medium	Gibco
DPBS	Gibco
Doxycycline	Sigma-Aldrich
D3-methionine	Silantis
E-F	
EDTA Ethylendiaminetetraacetic acid	Roth
Ethanol	Baker
Ethanolamine	Sigma-Aldrich
Formaldehyd	Sigma-Aldrich
Formamid	Fluka
Formic acid, 88%	Alfa Aesar
Fetal bovine serum (FBS)	Gibco

G	
G418 Sulfat	Calbiochem
D(+) Glucose	Baker
Glycerol 2-phosphat	Sigma-Aldrich
Glycin	Baker/Roth
Guanidin HCl	Roth
D-Glucose C13	Silantis
H-L	
HEPES	Roth
Hydrochloric acid 37%	Roth
Hygromycin B	Sigma-Aldrich
Imidazol	Sigma-Aldrich
	Merck
Isoamylalkohol	
Potassium	Sigma-Aldrich
Lithiumacetat-Dihydrat	Applichem
L-glutamine 200 mM	Gibco
IPTG min.99%	Sigma-Aldrich
M	
Magnesiumchlorid *6H ₂ O	Baker
Methanol	Lager
MOPS	Roth
N	
Sodium	Sigma-Aldrich
Nonidet P40	Fluka
NP40/Igepal CA-630	Sigma-Aldrich
Neomycin (G148)	Sigma-Aldrich

O	
Orange G	Sigma-Aldrich
P-Q	
Perchlorsäure	Sigma-Aldrich
PIPES	Roth
Ponceau S	Roth
Potassium acetate	Roth
Potassium chloride	Roth
Potassium dihydrogen phosphate	Roth
di-Potassium hydrogen phosphate 3*H2O	Roth
Potassium hydroxide	Baker
Potassium phosphate monobasic	Riedle-de Haen
2-Propanol	Baker
Penicillin/Streptomycin 10k U/ml	Gibco
Phenylmethanesulfonyl fluoride (PMSF)	Sigma-Aldrich
Powdered milk, blotting grade	Sigma-Aldrich
Prestained Protein Ladder Plus	Thermo Fisher Scientific
Protein A Sepharose 4 Fast Flow	Thermo Fisher Scientific
Pierce Prestained Protein MW Marker	Pierce
Pierce™ Unstained Protein MW Marker	Pierce
Q5® High-Fidelity DNA Polymerase	NEB
R	
RPMI medium 1640	Gibco
RPMI medium 1640 w/o methionine	Gibco
RPMI medium 1640 w/o glucose	Gibco
RiboRuler RNA ladder	Thermo Fisher Scientific
S	
D(+) Saccharose	Roth
SAM	NEB
SAM	Perkin Elmer

SDS	Roth
Silbernitrat	Roth
Sodium acetate 3*H2O	Baker
Sodium citrate 2-hydrate	Roth
Sodium chloride	Roth
Sodium di-hydrogen phosphate 2*H2O	Roth
di-Sodium hydrogen phosphate 2*H2O	Roth
Sodium hydroxide	Roth
Sodium orthovanadate	Sigma-Aldrich
Sodium tetraborate 10*H2O	Fluka
Sodium thiosulfate	Sigma-Aldrich
SYBR safe DNA gel stain	Invitrogen
T	
Tris	Applichem
Triton X100	Roth
Tween 20	Roth
Trypan blue	Sigma-Aldrich
Tetramethylethylenediamine (TEMED)	Sigma-Aldrich
TRYPsin-EDTA SOLUTION	BIOREAGENT
Tetracycline	Sigma-Aldrich
TRIzol™ Reagent	Ambion
U-Z	
Urea PAGE system	National Diagnostics
Ultima Gold LSC-cocktail	Perkin Elmer
Wasserstoffperoxid 35%	Roth
Xylencyanol FT	Applichem

4.1.2 Consumables and kits

10 ml pipettes	Greiner
15 ml Falcons	Greiner

25 ml pipettes	Greiner
50 ml Falcons	Falcon
5 ml pipettes	Greiner
Agarose (ultrapure)	Invitrogen
Albumin Fraction V, ≥98 %, powdered, for molecular biology	Sigma-Aldrich
Clarity Western ECL Substrate, 500ml	Bio-Rad
cOmplete™, EDTA-free Protease Inhibitor Cocktail	Roche
Countess™ Cell Counting Chamber Slides	Thermo Fisher Scientific
Cryovials 1.5 ml	Grainer
Dynabeads mRNA DIRECT Kit	Intirogen
Filtertips Tipone 01-10 µl 960St	StarLab
Filtertips Tipone 1-200 µl 960St	StarLab
Filtertips Tipone 1-20 µl 960St	StarLab
Filtertips Tipone 101-1000 µl 960St	StarLab
Gel extraction	Qiagen
GeneRuler DNA Ladder Mix	Thermo Fisher Scientific
HANDSCHUHE-NITRIL PURPLE S PUDERFR 100ST	KimTech
High Sensitivity DNA Kit	Agilent Technologies
Hybond N+ nylon membrane	Amersham
Maxiprep	Sigma-Aldrich
Miniprep	Sigma-Aldrich
Monarch RNA clean up	NEB
NextGen Nitrilhandschuhe, S, 100 Stk./Pkg.	Meditrade
PCR purification	Qiagen
Plastic ware for cell culture	Greiner
Qubit dsDNA BR Assay	Life Technologies
Qubit dsDNA HS Assay	Life Technologies
Qubit Protein Assay Kit	Life Technologies
Qubit RNA HS Assay	Life Technologies
Quick-RNA Miniprep	Zymo Research

RNA 6000 Nano Kit	Agilent Technologies
Safe-Lock Tubes 1,5 ml PCRclean 1000ST	Eppendorf
Safe-Lock Tubes 2,0 ml farblos 1000ST	Eppendorf
Stericup 500ml	Merck

4.1.3 Technical instruments

-80°C freezer	Liebherr
agarose gel electrophoresis	multisub
analytical balance	Sartorius
B7925 Rotator	Agar Scientific Ltd.
BBD 6220	Heraeus
Benchtop Centrifuge Mikro 200R	Hettich
Benchtop Centrifuge Mikro185	Hettich
Benchtop Centrifuge Rotanta 460R - S	Hettich
Big centrifuge 5810R	Eppendorf
Freezer -20	Liebherr
Bioanalyzer 2100	Agilent Technologies
bunsenburner	Campingaz
ChemiDoc Touch	Biorad
Countess II FL Automated Cell Counter	Thermo Fisher Scientific
Dell Power Edge R740 Server	Etomer
Duomax 1030	Heidolph
Eppendorf ThermoMixer™ F1.5	Eppendorf
Eppendorf ThermoMixer™ F1.5	Eppendorf
F205 series rotary shaker	FLC
Gel photo printer P95DE	Mitsubishi
Heracell™ 240i	Thermo Fisher Scientific
Heraeus Fresco 17	Thermo/Heraeus
Heraeus Pico 17	Thermo/Heraeus
HFU T Hera freeze	Thermo Fisher Scientific
Ice machine ZBE 150	Ziegra

Lamda Bio+ with Printer	Perkin Elmer
Laptop for Multiskan go	Toshiba
LED lamp	MH
Leica M165 C Stereomicroscope	Leica
LightCycler 480	Roche
MDF-U55V	Panasonic
Microplate Reader Varioskan LUX	ThermoFisherScientific
microwave	Sharp
Model 583	Bio-Rad
Model BD 56	Binder
MR Hei-Standard	Heidolph
MR Hei-Standard	Heidolph
Multichannel Pipette electric	Eppendorf
Multichannel Pipette electric spacer E1- ClipTip Equalizer 8-channel 10-300 uL	Thermo Fisher Scientific
Multichannel pipette manual, 8 tips, 10-100 ul	Eppendorf
Multiskan go	Fisher
Multistep Pipette	Eppendorf
Multitron Pro	Infors HT
My Cloud Pro Server	Western Digital via NCS GmbH
MyFuge 12 mini centrifuge	Sigma-Aldrich
N2 tank + protection + towers	tec-lab
neoLab Rotator, 90°-27° verstellbar, 5-50 UpM variabel	NeoLab Migge GmbH
ph Meter C5010	Consort
Pipetboy	Hirschmann
Pipetgirl - Pink	Integra
Pipette 10 uL	Gilson
Pipette 1000 uL	Gilson
Pipette 2 uL	Gilson
Pipette 20 uL	Gilson
Pipette 200 uL	Gilson
Polymax 1040	Heidolph

Power Supply (Netzgeraet) E443	Consort
Power Supply EV202	Consort
Power Supply EV231	Consort
Q800R1 Sonicator	Qsonica
Qubit 3.0 Quantitation Starter Kit	Life Technologies
Rotating wheel SB3	Stuart
Rotofix32A	Hettich
SDS-PAGE chamber, OmniPAGE Mini Wide	Cleaver Scientific
Shake 'n' Stack	Hybaid
SimpliAmp Thermal Cycler	Applied Biosystems
Sorvall LYNX 6000	Thermo Fisher Scientific
SpeedVac Quattro miVac System	SP Scientific. Genevac Ltd.
Spinner Control Unit, Biosystem	Thermo Fisher Scientific
stir CB 161	Stuart
T professional basic thermocycler gradient	biometra
tabletop centrifuge	Dutscher
tabletop centrifuge	Dutscher
ThermoMixer comfort	Eppendorf
ThermoMixer compact	Eppendorf
ThermoMixer F1.5	Eppendorf
timer	Conrad
Tornado Vortexer™(Edvotek®)	Heathrow Scientific
Triathler LSC	Hidex
Tube rotator H5 600	VWR
U:Genius3	Syngene
Ultracentrifuge Optima XE-90	Beckmann Coulter
under bench freezer -20	Liebherr
Underbench Centrifuge Rotanta 460RC	Hettich
Upright freezer -20	Liebherr
UV crosslinker 1800	Stratagene
Veriti® 96-Well Thermal Cycler	Applied Biosystems
Visi-Blue UV Transilluminator	UVP
Vortex	Heidolph

Vortex 7-2020	neolab
Vortex VF2	Jank+Kunkel
Water bath TW20	Julabo
Western chamber tank	Bio-Rad

4.1.4 Buffers and solutions

If not specify below, common lab buffers or buffers that are part of the kit from the section 4.1.2 were used.

PBS

137 mM NaCl

2.7 mM KCl

4.3 mM Na₂HPO₄*6H₂O

1.4 mM KH₂PO₄

TAE

40 mM Tris Acetate

1 mM EDTA

adjust pH to pH 8.0

TBE 10x

Tris base 1 M

Boric acid 1 M

EDTA (disodium salt) 0.02 M

TBS

10 mM NaCl

1 mM Tris/HCl pH 7.5

SDS Running Buffer

60.4 g Tris/Base

288 g Glycin

5 ml SDS 20%

add 2 L H₂O

Transfer Buffer

60.4 g Tris/Base

288 g Glycin

5 mL SDS

20% 200 mL ethanol

add 2 L H₂O

0.7% Agarose-TAE-Gel for DNA

2.1 g Agarose

300 mL 1x TAE

boil in microwave

cool to 65°C

LB Agar plates

LB-Agar	# 1083.00	35 g
	(Conda)	
Water	VE-H ₂ O	Up to 1 L
Antibiotics	1 :1000 stock	1X
Ampicillin	100 ug/mL final	400 uL auf 400 mL
Kanamycin	50 ug/mL final	400 uL auf 400 mL

Milk powder solution

4% powdered milk in 1 x TBST

SDS-PAGE separating gel (10%)

4.3 mL PAA 30%

10 mL 2xTris/SDS pH 8.8

5.5 mL H₂O

1167 µL APS

17 µL TEMED

SDS-PAGE stacking gel (4%)

2 mL PAA 30%

15 mL 2xTris/SDS pH 6.8

5.4 mL H₂O

90 µL APS

20 µL TEMED

Western-blocking-reagent

10% (v/v) TBS

0.1% (v/v) Tween 20

4% (w/v) powdered milk

GFP purification buffer

150 mM NaCL

50 mM Tris-HCl pH 8.0

0.5 mM DTT

1X Complete Protease

GST purification buffer

25 mM Tris-HCl pH8

150 mM NaCl

1 mM EDTA

0.5% Triton X-100

0.2 mM PMSF

m⁶A-IP buffer

50 mM Tris, pH 7.4

100 mM NaCl

0.05% NP-40

m⁶A-IP high salt wash buffer

50 mM Tris, pH 7.4

0.5 M NaCl

1 mM EDTA

0.1 % NP-40

0.1 % SDS

MTA buffer

6 mM HEPES-KOH (pH 8)

0.4 mM EDTA,

10 mM DTT

80 mM KCl

1.5 mM MgCl₂

0.2 U/mL RNasin

1.6% glycerol

Kinase buffer 5x

150 mM Tris-Cl (pH 7.5)

100 mM MgCl₂

RIPA buffer

NaCl 150 mM

Nonidet P-40 1%

Sodium deoxycholate (DOC) 0.5%

SDS 0.1%

Tris (pH 7.4) 25 mM

4.1.5 Antibodies

Primary antibodies	Source	Dilution
Anti-GFP	HMGU monoclonal antibody facility	WB 1:50
Anti-Sav1	#3507, Cell Signalling	WB 1:1000
Anti-STK4	ab51134, Abcam	WB 1:5000
anti-Calnexin	ab22595, Abcam	WB 1:1000, IP
Anti-m ⁶ A	SySy	IP
anti-MAP2	TA336617, Acris	IF 1:500

Secondary antibodies	Source	Dilution
goat anti-mouse	P0447, Dako	WB 1:1500
anti-rabbit	111-035-003, Jackson Laboratory	WB 1:100000
donkey anti-chicken conjugated to Alexa 488	711-547-003, Jackson Immuno Research	IF 1:500

4.1.6 Oligo nucleotides

Name	5`-3`	Application
Cloning		
M5-L58A-FW	CGTTGCAGATgcAGGATGTGGTTG	METTL5 mutagenesis
M5-L58A-RV	ACTTTATTTTCAATGTCATCATAAGTG	METTL5 mutagenesis
M5-C60A-FW	AGATCTAGGAgcTGGTTGTGGAGTACTT AG	METTL5 mutagenesis
M5-C60A-RV	GCAACGACTTTATTTTCAATG	METTL5 mutagenesis
M5-C62A-FW	AGGATGTGGTgcTGGAGTACTTAGC	METTL5 mutagenesis
M5-C62A-RV	AGATCTGCAACGACTTTATTTTC	METTL5 mutagenesis
M5-V64A-FW	TGGTTGTGGAgcACTTAGCATC	METTL5 mutagenesis

M5-V64A-RV	CATCCTAGATCTGCAACG	METTL5 mutagenesis
M5-D81A-FW	GTTGGATTGcCATAGATGAAGACG	METTL5 mutagenesis
M5-D81A-RV	ACACAACCCTGCTCCTAA	METTL5 mutagenesis
M5-I82A-FW	TGGATTGACgcAGATGAAGACGCATTG G	METTL5 mutagenesis
M5-I82A-RV	ACACACAACCCTGCTCCT	METTL5 mutagenesis
M5-D108A-FW	GTTCAATGTGcTGTGTGCTTATTATC	METTL5 mutagenesis
M5-D108A-RV	CATGTCAATATTTGTAACTCAAAC	METTL5 mutagenesis
M5-V109A-FW	CAATGTGATGcGTGCTTATTATC	METTL5 mutagenesis
M5-V109A-RV	AACCATGTCAATATTTGTAAAC	METTL5 mutagenesis
M5-N126A-FW	AGTAATTATGgcTCCTCCCTTTGGG	METTL5 mutagenesis
M5-N126A-RV	GTATCGAATGACTTGGAC	METTL5 mutagenesis
Q5SDM_N92A_F	TGGGGTTGGAgcCTGTTTATTCCCAC	METTL6 mutagenesis
Q5SDM_N92A_R	CAGCCAGCTTCAAGCATT	METTL6 mutagenesis
Q5SDM_F111A_F	TGCCTGTGATgcTTCTCCAAGAG	METTL6 mutagenesis
Q5SDM_F111A_R	TAGGCAAAGATATTCGGATC	METTL6 mutagenesis
qPCR primers		source
Gapdh_qPCR_F	CATGGCCTTCCGTGTTCTTA	Sebastian Bultmann
Gapdh_qPCR_R	CTTCACCACCTTCTTGATGTCATC	Sebastian Bultmann
Nanog_qPCR_F	ATTCTGGGAACGCCTCATCAA	Sebastian Bultmann
Nanog_qPCR_R	TTCAGAGGAAGGGCGAGGA	Sebastian Bultmann
Oct4_qPCR_F	TCACCCTGGGCGTTCTCTT	Sebastian Bultmann
Oct4_qPCR_R	GGCCGCAGCTTACACATGTT	Sebastian Bultmann
Rex1_qPCR_F	CTGGGACACGTGGCAAAAGAA	Sebastian Bultmann
Rex1_qPCR_R	GGGACAACACTTGGAGGCAG	Sebastian Bultmann
Klf4_qPCR_F	GCACACCTGCGAACTCACAC	Sebastian Bultmann
Klf4_qPCR_R	CCGTCCCAGTCACAGTGGTAA	Sebastian Bultmann
Sox2_qPCR_F	ACAGATGCAACCGATGCACC	Sebastian Bultmann
Sox2_qPCR_R	TGGAGTTGTACTGCAGGGCG	Sebastian Bultmann
Brachyury_qPCR_F	CTCCAACCTATGCGGACAATTC	Sebastian Bultmann
Brachyury_qPCR_R	ATGACTCACAGGCAGCATGCT	Sebastian Bultmann

Eomes_qPCR_F	ACCGGCACCAAAGTAGATGA	Sebastian Bultmann
Eomes_qPCR_R	GGGGTTGAGTCCGTTTATGTTGAA	Sebastian Bultmann
Fgf5_qPCR_F	GATCTACCCGGATGGCAAAG	Sebastian Bultmann
Fgf5_qPCR_R	TGCTGAAAACCTCCTCGTATTCCT	Sebastian Bultmann
Pax6_qPCR_F	ACACGTACAGTGCTTTGCCA	Sebastian Bultmann
Pax6_qPCR_R	ATGAGGAGGTCTGACTGGGG	Sebastian Bultmann
Nestin_qPCR_F	ACTCTGCTGGAGGCTGAAACT	Sebastian Bultmann
Nestin_qPCR_R	CAAGGAAATGCAGCTTCAGCTT	Sebastian Bultmann
Mettl3_qPCR_F	TTCATCTTGGCTCTATCCGGC	Sebastian Bultmann
Mettl3_qPCR_R	GCACGGGACTATCACTACGG	Sebastian Bultmann
Tet1_qPCR_F	CCAGGAAGAGGCGACTACGTT	Sebastian Bultmann
Tet1_qPCR_R	TTAGTGTTGTGTGAACCTGATTTATTGT	Sebastian Bultmann
Tet2_qPCR_F	ACTTCTCTGCTCATTCCCACAGA	Sebastian Bultmann
Tet2_qPCR_R	TTAGCTCCGACTTCTCGATTGTC	Sebastian Bultmann
<i>In vitro</i> transcribed tRNA		source
tRNA Ser wt	UGG CGU AGU CGG CAG GAU UCG AAC CUG CGC GGG GAA ACC CCA AUG GAU UUC AAG UCC AUC GCC UUA ACC ACU CGG CCA CGA CUA CGA CGG UAC CGG GUA CCG UUU CGU CCU CAC GGA CUC AUC AGG UAG UCG UGU CUC CCU AUA GUG AGU CGU AUU	Stefanie Kellner
tRNA Ser U47dC	UGG CGU AGU CGG CAG GAU UCG AAC CUG CGC GGG GAG ACC CCA AUG GAU UUC AAG UCC AUC GCC UUA ACC ACU CGG CCA CGA CUA CGA CGG UAC CGG GUA CCG UUU CGU CCU CAC GGA CUC AUC AGG UAG UCG UGU CUC CCU AUA GUG AGU CGU AUU	Stefanie Kellner
tRNA Ser C32G	UGG CGU AGU CGG CAG GAU UCG AAC CUG CGC GGG GAG ACC CCA	Stefanie Kellner

	AUG GAU UUC AAC UCC AUC GCC UUA ACC ACU CGG CCA CGA CUA CGA CGG UAC CGG GUA CCG UUU CGU CCU CAC GGA CUC AUC AGG UAG UCG UGU CUC CCU AUA GUG AGU CGU AUU	
--	--	--

4.1.7 Bacteria

strain	source	usage
DH5alpha	Robert Schneider lab	Plasmid cloning, propagation and purification
BL21Gold(DE3)	Robert Schneider lab	Recombinant protein expression
Rosetta Blue	Robert Schneider lab	Recombinant protein expression

4.1.8 Expression plasmids

Title	protein name	source
pGEX-4T1	GST	Robert Schneider lab
pGEX-4T1 METTL2B human	GST-METTL2B	Robert Schneider lab
EX-V0505-B06	GST-METTL3	OriGene
EX-Z2099-B06	GST-METTL5	OriGene
EX-H0241-B06	GST-METTL6	OriGene
EX-Y4506-B06	GST-METTL7B	OriGene
EX-H9312-B06	GST-METTL8	OriGene
pGEX-4T1 METTL9 human	GST-METTL9	Robert Schneider lab
EX-H0245-B06	GST-METTL10	OriGene
EX-S0450-B06	GST-METTL13	OriGene
EX-V1065-B06	GST-METTL14	OriGene

EX-T4017-B06	GST-METTL15	OriGene
EX-A3136-B06	GST-METTL16	OriGene
EX-Y3651-B06	GST-METTL21C	OriGene
EX-Y4502-B06	GST-METTL24	OriGene
EX-I1387-B06	GST-METTL25	OriGene
EX-H0241-B06 N92A	GST-METTL6 N92A	Created during this study
EX-H0241-B06 F111A	GST-METTL6 F111A	Created during this study
pcDNA5/FRT/TO	GFP	Michiel Vermeulen lab
pcDNA5/FRT/TO_METTL2B	GFP-METTL2B	Created during this study
pcDNA5/FRT/TO_METTL3	GFP-METTL3	Created during this study
pcDNA5/FRT/TO_METTL5	GFP-METTL5	Created during this study
pcDNA5/FRT/TO_METTL6	GFP-METTL6	Created during this study
pcDNA5/FRT/TO_METTL7B	GFP-METTL7B	Created during this study
pcDNA5/FRT/TO_METTL8	GFP-METTL8	Created during this study
pcDNA5/FRT/TO_METTL9	GFP-METTL9	Created during this study
pcDNA5/FRT/TO_METTL10	GFP-METTL10	Created during this study
pcDNA5/FRT/TO_METTL13	GFP-METTL13	Created during this study

pcDNA5/FRT/TO_METTL14	GFP-METTL14	Created during this study
pcDNA5/FRT/TO_METTL15	GFP-METTL15	Created during this study
pcDNA5/FRT/TO_METTL16	GFP-METTL16	Created during this study
pcDNA5/FRT/TO_METTL21C	GFP-METTL21C	Created during this study
pcDNA5/FRT/TO_METTL24	GFP-METTL24	Created during this study
pcDNA5/FRT/TO_METTL25	GFP-METTL25	Created during this study
pcDNA5/FRT/TO_METTL5 D81H	GFP-METTL5 D81H	Created during this study
pcDNA5/FRT/TO_METTL5 L58A	GFP-METTL5 L58A	Created during this study
pcDNA5/FRT/TO_METTL5 C60A	GFP-METTL5 C60A	Created during this study
pcDNA5/FRT/TO_METTL5 C62A	GFP-METTL5 C62A	Created during this study
pcDNA5/FRT/TO_METTL5 V64A	GFP-METTL5V64A	Created during this study
pcDNA5/FRT/TO_METTL5 D81A	GFP-METTL5 D81A	Created during this study
pcDNA5/FRT/TO_METTL5 I82A	GFP-METTL5 I82A	Created during this study
pcDNA5/FRT/TO_METTL5 C107A	GFP-METTL5 C107A	Created during this study
pcDNA5/FRT/TO_METTL5 V109A	GFP-METTL5 V109A	Created during this study
pcDNA5/FRT/TO_METTL5 N126A	GFP-METTL5 N126A	Created during this study

4.1.9 Cell lines

Name	source
HeLa FRT	Michiel Vermeulen lab
GFP-METTL2B HeLa FRT	Created during this study
GFP-METTL3 HeLa FRT	Created during this study
GFP-METTL5 HeLa FRT	Created during this study
GFP-METTL6 HeLa FRT	Created during this study
GFP-METTL7B HeLa FRT	Created during this study
GFP-METTL8 HeLa FRT	Created during this study
GFP-METTL9 HeLa FRT	Created during this study
GFP-METTL10 HeLa FRT	Created during this study
GFP-METTL13 HeLa FRT	Created during this study
GFP-METTL14 HeLa FRT	Created during this study
GFP-METTL15 HeLa FRT	Created during this study
GFP-METTL16 HeLa FRT	Created during this study
GFP-METTL21C HeLa FRT	Created during this study
GFP-METTL24 HeLa FRT	Created during this study
GFP-METTL25 HeLa FRT	Created during this study
GFP HeLa FRT	Created during this study
mESC J1	Sebastian Bultmann lab
mESC J1 METTL5 KO (multiple clones)	Sebastian Bultmann lab
mESC J1 METTL6 KO (multiple clones)	Sebastian Bultmann lab
HAP1 wt clone: C631	Horizon Discovery
HAP1 METTL6 KO clones: HZGHC005030c008 HZGHC005031c011 HZGHC005031c010	Horizon Discovery
HAP1 METTL5 KO clones: HZGHC29081 HZGHC005029c005	Horizon Discovery

4.1.10 Software

Adobe Acrobat 9 Pro

Adobe Illustrator 16.0.4

Adobe Photoshop 16.0.4

ApE v1.10.4

BEDtools

Cisco AnyConnect 4.6.03049

Fastqc v0.11.8

HOMER⁷³

Illustrator of Biological Sequences¹¹⁷

Image J 2.0.0-rc-44/1.50e

Keynote 9.0.1

Mega 7

Mendeley Desktop 1.19.4

Microsoft Office for Mac 2011

Prizm 8

R 3.5.3

SAMtools

SnapGene Viewer 2.5

Sublime text 3.1.1

STAR V2.5.3a

4.2 Methods

4.2.1. Molecular biology methods

If not stated otherwise, standard molecular biology laboratory protocols were used¹¹⁸.

Cloning GFP-METTL plasmids

For the generation of pcDNA5/FRT/TO METTL plasmids, the ORFs of METTL proteins were amplified from plasmids obtained from Origene and cloned into pcDNA5/FRT/TO backbone in frame with an N-terminal GFP tag using GATEWAY cloning.

METTL5 and METTL6 catalytic mutants cloning

A plasmid encoding GST-METTL6 was obtained from OriGene. GST-METTL6 N92A and F111A mutants were created by Q5 site-directed mutagenesis following the standard protocol from NEB with GST-METTL6 plasmid as a template. A plasmid encoding GFP-METTL5 was created during this study. GFP-METTL5 mutants were created by Q5 site-directed mutagenesis following the standard protocol from NEB with GFP-METTL5 plasmid as a template. All mutants were verified by Sanger sequencing. Mutagenesis primers are listed in the table 4.1.6.

RT-PCR analysis

500 ng of RNA was reverse-transcribed using cDNA Reverse Transcription Kit RevertAid H Minus (Thermo Fisher Scientific). The quantitative PCR analysis was performed in triplicate for each sample by using 2 ul of the reverse transcription reaction in a Light Cycler 480 (Roche) with Fast SYBR®Master Mix (Roche). Error bars indicate standard deviation of pooled triplicate measurements per sample. qPCR primers are listed in the table 4.1.6.

Agarose gel electrophoresis

DNA samples were mixed with DNA loading buffer and routinely separated on 1% agarose gels in TAE buffer followed by SyberSafe staining according to standard protocol.

Bands were visualized using a UV-light gel documentation system. If needed, bands of interest were excised from agarose gels and purified using a GenElute gel extraction kit (Sigma-Aldrich) following the manufacturer's instructions.

4.2.2. Bacterial cell culture

Competent bacteria cells were transformed by mixing 50 μ L of DH10B either with the whole ligation product (for cloning) or with 50 ng of purified plasmid DNA for recombinant protein expression, followed by incubation for 20 min on ice. Next, a heat shock was performed for 45s at 42°C and the cells were directly put on ice for 2 min. 500 μ L LB medium was added and the cells were incubated at 37°C. After 30-60 min the cells were plated on selective agar plates. The plates were stored at 37°C o/n.

For plasmid purification, single clones were picked and inoculated into liquid LB selection media. Sigma-Aldrich Mini and Maxi prep kits were used for purification plasmids for sequencing and cell culture transfections respectively. Plasmids were stored at -20°C in DNase/RNase free water to ensure compatibility with all downstream applications.

4.2.3. Mammalian cell culture

GFP-METTLs doxycycline-inducible (DOX) cell lines were created by transfecting HeLa-FRT cells with modified pcDNA5/FRT/TO and pOG44 plasmids as described in Ignatova et al⁴¹. HeLa-FRT cells inducibly expressing GFP and GFP-METTL constructs were cultured in high glucose Dulbecco's modified Eagle medium (DMEM) supplemented with 10% fetal bovine serum, 2 mM L-glutamine (Sigma-Aldrich) and 1% penicillin–streptomycin (Life Technologies, Inc.). Cells, at a confluency of 80%, were treated with doxycycline at a final concentration of 1 μ g/ml for 16h to induce expression of the GFP fusion proteins.

ESCs were maintained on 0.2% gelatin-coated dishes in Dulbecco's modified Eagle's medium (Sigma-Aldrich) supplemented with 16% fetal bovine serum (FBS, Sigma-Aldrich),

0.1 mM β -mercaptoethanol (Invitrogen), 2 mM L-glutamine (Sigma-Aldrich), 1 \times MEM Non-essential amino acids (Sigma-Aldrich), 100 U/mL penicillin, 100 μ g/mL streptomycin (Sigma-Aldrich), homemade recombinant LIF tested for efficient self-renewal maintenance with or without 2i (1 μ M PD032591 and 3 μ M CHIR99021 (Axon Medchem, Netherlands)).

HAP1 wt and KO cells were obtained from Horizon Discovery and cultured in high glucose Dulbecco's modified Eagle medium (IMDM) supplemented with 10% fetal bovine serum and 1% penicillin–streptomycin (Life Technologies, Inc.).

Cell proliferation assays

Wt and *Mettl6* KO mESC were seeded two days before measurements at density 500 cells per well in 96-well plates. At each time point, cells were lysed on ice in 10 mM Tris pH 8, 1 mM EDTA, 0.2% Triton X-100. Cell numbers were determined using Quant-iT PicoGreen dsDNA Assay Kit and standard curves as described by the manufacturer.

4.2.4. RNA methods

Standard Trizol protocol and/or ZymoResearch RNA miniprep kit were used for total RNA extraction. polyA RNA was selected with Dynabeads mRNA DIRECT Kit from Intirogen following manufacturer's instructions.

For gel purification of tRNA, RNA of the size range from 20-200 nucleotides was purified from total RNA using the Zymo research column followed by standard protocol. 10 μ g of RNA was loaded per well of 12% UREA gel (prepared according to the standard protocol from National Diagnostics), RNA fragments in the size range 70-80 nucleotides and ~85 nucleotides were excised from the gel, the gel was homogenized and snap-frozen in liquid nitrogen in the presence of 3 volume of 1x TBE. RNA was recovered by 4 subsequent cycles of thawing and snap freezing in liquid nitrogen, followed by Isopropanol precipitation at -80°C o/n in the presence of glycogen.

For Gel purification of 18S rRNA, 10 ug of RNA was loaded per well of 4% UREA gel (prepared according to standard the protocol from National Diagnostics), RNA in the size range ~1800 nucleotides were cut from the gel, the gel was homogenized and snap-frozen in liquid nitrogen in the presence of 3 volume of the running buffer. RNA was recovered by 4 subsequent cycles of thawing and snap freezing in liquid nitrogen, followed by Isopropanol precipitation at -80°C o/n.

RNA amounts and purity were assessed with spectrophotometer Multiscan GO (Thermo Fisher Scientific) and fluorometer Qubit3 (Invitrogen). RNA integrity and purity of individual RNA fractions were checked on an Agilent BioAnalyzer 2100 with the Agilent RNA nano chip kit. All RNA samples were stored in DEPC-water or RNA/DNA free water at -80°C.

4.2.5. Biochemistry methods

Cell extracts preparation

Cell extracts were prepared as described earlier⁴¹. Cells were harvested, extensively washed with PBS and resuspended in 5 volumes of a buffer containing 10 mM Hepes KOH pH 7.9, 1.5 mM MgCl₂, 10 mM KCl followed by incubated for 10 minutes on ice. After centrifugation, cells were suspended in 2 volumes of a buffer containing 10 mM Hepes KOH pH 7.9, 1.5 mM MgCl₂, 10 mM KCl supplemented with 1 × Complete Protease Inhibitors (Roche) and 0.15 % NP40 and dounced with 30-40 strokes with a type B pestle (tight). 10 seconds break was taken per 10x dounces. The suspension was centrifuged at 3200 x g for 15 minutes. The supernatant was collected as the cytoplasmic extract.

Pellet of the crude nuclei was washed with PBS and centrifuged at 3200 g for 5 minutes, resuspended in 2 volumes of a buffer containing 420 mM NaCl, 20 mM Hepes KOH pH 7.9, 20% v/v glycerol, 2 mM MgCl₂, 0.2 mM EDTA supplemented with 1 × Complete Protease Inhibitors (Roche), 0.1% NP40 and 0.5 mM DTT. Tubes with the

suspension were rotated for an hour in the cold room. Both nuclear suspension and the cytoplasmic extract were centrifuged at maximum g for 30 min in a table top centrifuge. Extracts were aliquoted and snap-frozen in liquid N₂ until further use.

Co-immunoprecipitation (co-IP) and Western blot.

Whole-cell extracts were prepared as described above. Total protein concentration was measured with Pierce™ BCA Protein Assay Kit (Thermo Fisher Scientific). 4 mg of whole-cell extract was used per immunoprecipitation (IP). IP with GFP nanobody sepharose beads (Chromotek) was performed as described in 4.2.6. For Calnexin-IP, 10 µg of anti-Calnexin antibody from Abcam per IP was used. Input and IP samples were separated by SDS–PAGE and transferred to a nitrocellulose membrane, followed by immunostaining. The antibodies used for immunostaining in Figure 2.4.5: anti-GFP (1:50; HMGU monoclonal antibody facility) or anti-Calnexin (1:1000; ab22595, Abcam) primary antibodies followed by horseradish peroxidase (HRP)-conjugated secondary antibodies goat anti-mouse (1:1500, P0447, Dako) and anti-rabbit (1:100000, 111-035-003, Jackson Laboratory) correspondingly. The antibodies used for immunostaining in Figure 2.2.8: Anti-Sav1 (1:1000; #3507, Cell Signalling) and Anti-STK4 (1:5000; ab51134, Abcam) primary antibodies followed by horseradish peroxidase (HRP)-conjugated secondary antibody anti-rabbit (1:100000, 111-035-003, Jackson Laboratory).

4.2.6. Protein purification

GFP affinity purifications

For GFP affinity purification of METTL proteins, 4-10 mg of WCE was incubated with 20 µl GFP nanobody sepharose beads (Chromotek) in 5 volumes 150 mM NaCl, 50 mM Tris-HCl pH 8.0, 0.5 mM DTT and 1X Complete Protease Inhibitor cocktail for 1.5 h at 4°C on a rotation wheel. After incubation, beads were washed twice with 1 ml of 300mM NaCl, 50 mM Tris-HCl pH 8.0, 0.5 mM DTT and 1X Complete Protease Inhibitor cocktail and

three times with 150 mM NaCl, 50 mM Tris-HCl pH 8.0, 0.5 mM DTT and 1X Complete Protease Inhibitor. After the last wash, beads were re-suspended in MTA buffer and used within 24 hours. Purity and amount of proteins were assessed with PAGE followed by Coomassie Brilliant Blue staining.

GST fusion purifications

BL21 Gold (DE3) *E.coli* strain was transformed with plasmids for recombinant protein expression followed by induction with 0.5M IPTG at 18°C o/n. *E.coli* were harvested, and cell pellets were lysed in 25 mM Tris-HCl pH8, 150 mM NaCl, 1 mM EDTA, 0.5% Triton X-100, 0.2 mM PMSF with mild sonication. Lysates were centrifuged at 20000g for 30 min at +4°C, supernatant was collected and incubated with Glutathion Sepharose beads for 4 hours at +4°C with rotation, followed by washes with lysis buffer (with NaCl adjusted to 300 mM), competitive elution with 10 mM reduced glutathione in 50 mM Tris-HCl pH 8.0 and dialysis o/n against methyltransferase assay. Purity and amount of proteins were assessed with PAGE followed by Coomassie Brilliant Blue staining.

4.2.7. Microscopy

Immunofluorescence

For immunostaining, mESCs were cultured for one week in Serum LIF and seed in 5×10^6 densities on geltrex (Gibco, A1569601) treated coverslips. All following steps were performed at room temperature. The cells were fixed for 10 min with 4% paraformaldehyde (pH 7.0), washed 3x for 10 min with PBST (PBS, 0.01% Tween20), permeabilized for 5 min in PBS supplemented with 0.5% Triton X-100 and washed 2x for 10 min with PBS. Cells were then incubated in blocking solution (PBST, 4% BSA) for 1 h. Coverslips were incubated with primary and secondary antibody (diluted in blocking solution) in dark humid chambers for 1 h and washed three times for 10 min with PBST. For DNA counterstaining, coverslips were incubated 10 min in PBST containing a final concentration of 2 µg/mL

DAPI (Sigma-Aldrich) and washed three times for 10 min with PBS-T. Coverslips were mounted in antifade medium (Vectashield, Vector Laboratories) and sealed with colorless nail polish.

The following antibodies were used: primary polyclonal chicken anti-MAP2 (1:500, TA336617, Acris), polyclonal goat anti-rabbit conjugated to Alexa 488 (1:500, A-11034, ThermoFisher Scientific), polyclonal donkey anti-chicken conjugated to Alexa 488 (1:500; 711-547-003, Jackson ImmunoResearch).

Immunofluorescence Intensity Analysis

For immunofluorescence, images were collected on a Nikon TiE microscope equipped with a Yokogawa CSU-W1 spinning disk confocal unit (50 μ m pinhole size), an Andor Borealis illumination unit, Andor ALC600 laser beam combiner (405nm/488nm), Andor IXON 888 Ultra EMCCD camera, and a Nikon 100x/1.45 NA oil immersion objective. The microscope was controlled by software from Nikon (NIS Elements, ver. 5.02.00). DAPI or Alexa 488 were excited with 405 nm and 488 nm and lasers. Within each experiment, cells were imaged using the same settings on the microscope to compare signal intensities between cell lines. Fiji software was used to analyse images. The region of interest of the entire nucleus was manually selected or thresholded using the Dapi signal. Fluorescence intensities of these regions of interest were measured in the 488nm channel. The mean fluorescence intensities were extracted for each cell line.

4.2.8. *In vitro* assays

***In vitro* methyltransferase assay (MTA)**

Methyltransferase assays were performed in 6 mM HEPES-KOH (pH 8), 0.4 mM EDTA, 10 mM DTT, 80 mM KCl, 1.5 mM MgCl₂, 0.2 U/mL RNasin, 1.6% glycerol, in the presence of 460 nM [3H]-SAM (Perkin Elmer). 5 μ g of total RNA from HeLa cells per reaction was used as a substrate. Assays were performed at RT o/n, followed by acid

phenol-chloroform extraction and column purification (Zymo Research). Tritium incorporation was analyzed by liquid scintillation counting using Triathler counter (HIDEX) in Ultima Gold LSC-cocktail (Perkin Elmer) and shown as counts per minute (CPM). All data of *in vitro* methyltransferase assays are shown as mean \pm SD (standard deviation) from three replicates. For non-radioactive assays, SAM from NEB was used as a methyl group donor according to the manufacturer's protocol.

***In vitro* kinase assay**

Kinase assays were performed with Aurora B recombinant protein and GFP-purifications on beads according to standard protocols. Reactions were performed in the kinase buffer with core histones as substrate, started by adding the mixture of 1 mM ATP with 5 μ Ci γ [³²P]-ATP (PerkinElmer) and incubated for 30 min at 30 °C. Reactions were stopped by adding 5x Laemmli buffer and boiling for 10 min. Proteins were separated by gel electrophoresis, gels were dried and a signal was detected by autoradiography with a Typhoon imager (GE healthcare).

4.2.9. m⁶A-IP

m⁶A-IP on 30 ug total RNA (from HAP1 cells) and 10 ug polyA selected RNA (from mES cells) were performed as described in Engel et al¹⁰⁴ with minor modifications. For m⁶A-IP on polyA RNA, total RNA from mESC were polyA enriched twice as described above, fragmented to 100nts with NEB RNA fragmentation solution according to manufacturer's protocol and precipitated with m⁶A-IP antibody (SySy). For m⁶A-IP on total RNA, total RNA was fragmented to 100nts, precipitated with 1 ug m⁶A-IP antibody (SySy) following by treatment of Input and IP samples with RiboZero Gold rRNA depletion kit (Illumina). For IP RNA were incubated with 1 ug of m⁶A antibodies (SySy) in 1 ml of m⁶A-IP buffer for 2 hours in the cold room with rotation, following by incubation with Protein A/G beads for 2 hours in the cold room with rotation. After 2 washes with m⁶A-IP buffet, 3

washes with m⁶A-IP high salt wash buffer and 2 washes with m⁶A-IP buffer, immunoprecipitated RNA was eluted from beads with Trizol, followed by column purification according to the manufacturer's protocols. Recovered RNAs were measured by Qubit. No RNA was detected in the "no antibody" control. Libraries from Input and IP RNA were prepared and sequenced by the Helmholtz Zentrum Munich NGS Sequencing facility with 2-4 libraries per line.

4.2.10. Data analysis

For all NGS datasets, sequencing quality control was performed by Fastqc v0.11.8 (Andrews, 2010). For m⁶A-IP analysis, reads were mapped to the hg38 or mm10 genome STAR-aligner¹¹⁹ and uniquely mapped reads were extracted using SAMtools¹²⁰. Correlations between biological replicates were assessed using BEDTools¹²¹ replicates were correlated For the further analysis four best correlating replicates out of five and three best correlation replicates out of four were used for human and mouse cells correspondingly. For calculation of m⁶A signal enrichment over input pipelines from Marsico lab (MPI, Berlin and HMGU Munich) were used^{122,123}. RNA features for analyzing peaks distribution were obtained from UCSC table browser¹²⁴. Sequencing tracks were visualized with the UCSC genome browser¹²⁵. Motif search within different peaks group were performed using HOMER⁷³.

All none NGS Statistical analysis was performed in R or Prism 8.

4.2.11. Data availability

The proteomics data have been deposited to the ProteomeXchange Consortium via the PRIDE¹²⁶ partner repository with the dataset identifier PXD011125.

5. Bibliography

1. Pan, T. Modifications and functional genomics of human transfer RNA. *Cell Res.* **28**, 395–404 (2018).
2. Ma, H. *et al.* N6-Methyladenosine methyltransferase ZCCHC4 mediates ribosomal RNA methylation. *Nat. Chem. Biol.* **15**, 88–94 (2019).
3. Pendleton, K. E. *et al.* The U6 snRNA m6A Methyltransferase METTL16 Regulates SAM Synthetase Intron Retention. *Cell* **169**, 824-835.e14 (2017).
4. Wu, H. & Zhang, Y. Charting oxidized methylcytosines at base resolution. *Nat. Struct. Mol. Biol.* **22**, 656–661 (2015).
5. Jia, G. *et al.* N6-Methyladenosine in nuclear RNA is a major substrate of the obesity-associated FTO. *Nat. Chem. Biol.* **7**, 885–887 (2011).
6. Boccaletto, P. *et al.* MODOMICS: a database of RNA modification pathways. 2017 update. *Nucleic Acids Res.* **46**, D303–D307 (2018).
7. Grosjean, H. *DNA and RNA modification enzymes : structure, mechanism, function, and evolution.* (Landes Bioscience, 2009).
8. Zhao, B. S., Roundtree, I. A. & He, C. Post-transcriptional gene regulation by mRNA modifications. *Nat. Rev. Mol. Cell Biol.* **18**, 31–42 (2017).
9. Shi, H., Wei, J. & He, C. Molecular Cell Review: Where, When, and How: Context-Dependent Functions of RNA Methylation Writers, Readers, and Erasers. *Mol. Cell* **74**, 640–650 (2019).
10. Culp, L. A., Dore, E. & Brown, G. M. Methylated bases in DNA of animal origin. *Arch. Biochem. Biophys.* **136**, 73–79 (1970).
11. Sheid, B., Wilson, S. M. & Morris, H. P. Transfer RNA methylase activity in normal rat liver and some Morris hepatomas. *Cancer Res.* **31**, 774–7 (1971).
12. Xu, L. *et al.* Three distinct 3-methylcytidine (m3C) methyltransferases modify tRNA

- and mRNA in mice and humans. *J. Biol. Chem.* **292**, 14695–14703 (2017).
13. O'Connell, M. RNA modification and the epitranscriptome; the next frontier. *RNA* **21**, 703–4 (2015).
 14. Gkatza, N. A. *et al.* Cytosine-5 RNA methylation links protein synthesis to cell metabolism. *PLoS Biol.* **17**, e3000297 (2019).
 15. de Crécy-Lagard, V. *et al.* Matching tRNA modifications in humans to their known and predicted enzymes. *Nucleic Acids Res.* **47**, 2143–2159 (2019).
 16. Zhang, C., Fu, J. & Zhou, Y. A Review in Research Progress Concerning m6A Methylation and Immunoregulation. *Front. Immunol.* **10**, 922 (2019).
 17. Desrosiers, R., Friderici, K. & Rottman, F. Identification of methylated nucleosides in messenger RNA from Novikoff hepatoma cells. *Proc. Natl. Acad. Sci. U. S. A.* **71**, 3971–5 (1974).
 18. Dominissini, D. *et al.* Topology of the human and mouse m6A RNA methylomes revealed by m6A-seq. *Nature* **485**, 201–206 (2012).
 19. Meyer, K. D. *et al.* Comprehensive analysis of mRNA methylation reveals enrichment in 3' UTRs and near stop codons. *Cell* **149**, 1635–1646 (2012).
 20. Wang, X. *et al.* Structural basis of N6-adenosine methylation by the METTL3-METTL14 complex. *Nature* **534**, 575–578 (2016).
 21. Wang, X. *et al.* N6-methyladenosine-dependent regulation of messenger RNA stability. *Nature* **505**, 117–120 (2013).
 22. Alarcón, C. R., Lee, H., Goodarzi, H., Halberg, N. & Tavazoie, S. F. N⁶-methyladenosine marks primary microRNAs for processing. *Nature* **519**, 482–485 (2015).
 23. Patil, D. P. *et al.* m(6)A RNA methylation promotes XIST-mediated transcriptional repression. *Nature* **537**, 369–373 (2016).
 24. Roundtree, I. A., Evans, M. E., Pan, T. & He, C. Dynamic RNA Modifications in

- Gene Expression Regulation. *Cell* **169**, 1187–1200 (2017).
25. Liu, J. *et al.* A METTL3-METTL14 complex mediates mammalian nuclear RNA N6-adenosine methylation. *Nat. Chem. Biol.* **10**, 93–95 (2014).
 26. Pendleton, K. E. *et al.* The U6 snRNA m6A methyltransferase METTL16 regulates SAM synthetase intron retention. *Cell* **169**, 824–835 (2018).
 27. Liu, J. *et al.* A METTL3-METTL14 complex mediates mammalian nuclear RNA N6-adenosine methylation. *Nat. Chem. Biol.* **10**, 93–95 (2014).
 28. Ma, H. *et al.* N6-Methyladenosine methyltransferase ZCCHC4 mediates ribosomal RNA methylation. *Nat. Chem. Biol.* **15**, 88–94 (2019).
 29. Liu, N. *et al.* N(6)-methyladenosine-dependent RNA structural switches regulate RNA-protein interactions. *Nature* **518**, 560–4 (2015).
 30. Yang, Y., Hsu, P. J., Chen, Y.-S. & Yang, Y.-G. Dynamic transcriptomic m6A decoration: writers, erasers, readers and functions in RNA metabolism. *Cell Res.* **28**, 616–624 (2018).
 31. Batista, P. J. *et al.* m(6)A RNA modification controls cell fate transition in mammalian embryonic stem cells. *Cell Stem Cell* **15**, 707–19 (2014).
 32. Wang, Y. *et al.* N6-methyladenosine RNA modification regulates embryonic neural stem cell self-renewal through histone modifications. *Nat. Neurosci.* **21**, 195–206 (2018).
 33. Bohnsack, K. E. & Bohnsack, M. T. Uncovering the assembly pathway of human ribosomes and its emerging links to disease. *EMBO J.* **38**, e100278 (2019).
 34. Lewis, J. D. & Tollervey, D. Like attracts like: getting RNA processing together in the nucleus. *Science* **288**, 1385–9 (2000).
 35. Sanchez, C. G. *et al.* Regulation of Ribosome Biogenesis and Protein Synthesis Controls Germline Stem Cell Differentiation. *Cell Stem Cell* **18**, 276–90 (2016).
 36. Sampath, P. *et al.* A hierarchical network controls protein translation during murine

- embryonic stem cell self-renewal and differentiation. *Cell Stem Cell* **2**, 448–60 (2008).
37. Chang, W. Y. & Stanford, W. L. Translational control: a new dimension in embryonic stem cell network analysis. *Cell Stem Cell* **2**, 410–2 (2008).
 38. Zheng, G. *et al.* ALKBH5 Is a Mammalian RNA Demethylase that Impacts RNA Metabolism and Mouse Fertility. *Mol. Cell* **49**, 18–29 (2013).
 39. Wei, J. *et al.* Differential m⁶A, m⁶A^m, and m¹A Demethylation Mediated by FTO in the Cell Nucleus and Cytoplasm. *Mol Cell* **71**, 973–985 (2018).
 40. Martin, J. L. & McMillan, F. M. SAM (dependent) I AM: the S-adenosylmethionine-dependent methyltransferase fold. *Curr. Opin. Struct. Biol.* **12**, 783–793 (2002).
 41. Ignatova, V. V., Jansen, P. W. T. C., Baltissen, M. P., Vermeulen, M. & Schneider, R. The interactome of a family of potential methyltransferases in HeLa cells. *Sci. Rep.* **9**, 6584 (2019).
 42. Sood, A. J., Viner, C. & Hoffman, M. M. DNAmoD: the DNA modification database. *J. Cheminform.* **11**, 30 (2019).
 43. Rana, A. K. & Ankri, S. Reviving the RNA world: An insight into the appearance of RNA methyltransferases. *Front. Genet.* **7**, 1–9 (2016).
 44. Lyko, F. The DNA methyltransferase family: A versatile toolkit for epigenetic regulation. *Nat. Rev. Genet.* **19**, 81–92 (2018).
 45. Okano, M., Xie, S. & Li, E. Cloning and characterization of a family of novel mammalian DNA (cytosine-5) methyltransferases. *Nat. Genet.* **19**, 219–220 (1998).
 46. Goll, M. G. *et al.* Methylation of tRNA Asp by the DNA Methyltransferase Homolog Dnmt2. *Science* **311**, 395–398 (2006).
 47. Alexandrov, A., Martzen, M. R. & Phizicky, E. M. Two proteins that form a complex are required for 7-methylguanosine modification of yeast tRNA. *RNA* **8**, 1253–66 (2002).

48. Shimazu, T., Barjau, J., Sohtome, Y., Sodeoka, M. & Shinkai, Y. Selenium-based S-adenosylmethionine analog reveals the mammalian seven-beta-strand methyltransferase METTL10 to be an EF1A1 lysine methyltransferase. *PLoS One* **9**, e105394 (2014).
49. Christine E. Schaner Tooley, Janusz J. Petkowski, Tara L. Muratore-Schroeder, Jeremy L. Balsbaugh, Jeffrey Shabanowitz, Michal Sabat, Wladek Minor, D. F. H. and I. G. M. NRMT is an α -N-methyltransferase that methylates RCC1 and Retinoblastoma Protein. *Nature* **466**, 1125–1128 (2010).
50. Heyn, H. & Esteller, M. An adenine code for DNA: A second life for N6-methyladenine. *Cell* **161**, 710–713 (2015).
51. Liu, J. *et al.* A METTL3-METTL14 complex mediates mammalian nuclear RNA N6-adenosine methylation. *Nat Chem Biol* **10**, 93–95 (2014).
52. Mitchell, A. L. *et al.* InterPro in 2019: improving coverage, classification and access to protein sequence annotations. *Nucleic Acids Res.* **47**, D351–D360 (2019).
53. Warda, A. S. *et al.* Human METTL16 is a N^6 -methyladenosine (m^6A) methyltransferase that targets pre-mRNAs and various non-coding RNAs. *EMBO Rep.* e201744940 (2017).
54. Warda, A. S. *et al.* Human METTL16 is a N^6 -methyladenosine (m^6A) methyltransferase that targets pre-mRNAs and various non-coding RNAs. *EMBO Rep.* **18**, e201744940 (2017).
55. Valentina V. Ignatova, Steffen Kaiser, Jessica Sook Yui HO, Xinyang Bing, Paul Stolz, Ying Xim Tan, Chee Leng Lee, Florence Pik Hoon Gay, Palma Rico Lastres, Raffaele Gerlini, Birgit Rathkolb, Antonio Aguilar-Pimentel, Adrián Sanz-Moreno, Tanja Klein-Rod, R. S. METTL6 is a tRNA m3C methyltransferase that regulates pluripotency and tumor cell growth. *Sci. Adv.* (*under Revis.*
56. Reichle, V. F. *et al.* Surpassing limits of static RNA modification analysis with

- dynamic NAIL-MS. *Methods* **156**, 91–101 (2019).
57. Clark, W. C., Evans, M. E., Dominissini, D., Zheng, G. & Pan, T. tRNA base methylation identification and quantification via high-throughput sequencing. *RNA* **22**, 1771–1784 (2016).
 58. Zheng, G. *et al.* Efficient and quantitative high-throughput tRNA sequencing. *Nat. Methods* **12**, 835–837 (2015).
 59. Yaguchi, K. *et al.* Uncoordinated centrosome cycle underlies the instability of non-diploid somatic cells in mammals. *J. Cell Biol.* **217**, 2463–2483 (2018).
 60. Ingolia, N. T., Ghaemmaghami, S., Newman, J. R. S. & Weissman, J. S. Genome-wide analysis in vivo of translation with nucleotide resolution using ribosome profiling. *Science* **324**, 218–23 (2009).
 61. Chou, H. J., Donnard, E., Gustafsson, H. T., Garber, M. & Rando, O. J. Transcriptome-wide Analysis of Roles for tRNA Modifications in Translational Regulation. *Mol. Cell* **68**, 978-992.e4 (2017).
 62. Nedialkova, D. D. & Leidel, S. A. Optimization of Codon Translation Rates via tRNA Modifications Maintains Proteome Integrity. *Cell* **161**, 1606–18 (2015).
 63. Zinshteyn, B., Rojas-Duran, M. F. & Gilbert, W. V. Translation initiation factor eIF4G1 preferentially binds yeast transcript leaders containing conserved oligouridine motifs. *RNA* **23**, 1365 (2017).
 64. van Nuland, R. *et al.* Quantitative Dissection and Stoichiometry Determination of the Human SET1/MLL Histone Methyltransferase Complexes. *Mol. Cell. Biol.* **33**, 2067–2077 (2013).
 65. Bae, S. J. *et al.* SAV1 promotes Hippo kinase activation through antagonizing the PP2A phosphatase STRIPAK. *Elife* **6**, (2017).
 66. Couzens, A. L. *et al.* Protein Interaction Network of the Mammalian Hippo Pathway Reveals Mechanisms of Kinase-Phosphatase Interactions. *Sci. Signal.* **6**, rs15–

rs15 (2013).

67. Callus, B. A., Verhagen, A. M. & Vaux, D. L. Association of mammalian sterile twenty kinases, Mst1 and Mst2, with hSalvador via C-terminal coiled-coil domains, leads to its stabilization and phosphorylation. *FEBS J.* **273**, 4264–4276 (2006).
68. Ignatova, V. V. *et al.* The rRNA m6A methyltransferase METTL5 is involved in pluripotency and developmental programs. *Genes Dev.* **34**, 715–729 (2020).
69. Öunap, K., Leetsi, L., Matsoo, M. & Kurg, R. The Stability of Ribosome Biogenesis Factor WBSR22 Is Regulated by Interaction with TRMT112 via Ubiquitin-Proteasome Pathway. *PLoS One* **10**, e0133841 (2015).
70. Fu, D. *et al.* Human AlkB homolog ABH8 Is a tRNA methyltransferase required for wobble uridine modification and DNA damage survival. *Mol. Cell. Biol.* **30**, 2449–59 (2010).
71. Taoka, M. *et al.* Landscape of the complete RNA chemical modifications in the human 80S ribosome. *Nucleic Acids Res.* **46**, 9289–9298 (2018).
72. Piekna-Przybylska, D., Decatur, W. A. & Fournier, M. J. The 3D rRNA modification maps database: with interactive tools for ribosome analysis. *Nucleic Acids Res.* **36**, D178 (2008).
73. Heinz, S. *et al.* Simple combinations of lineage-determining transcription factors prime cis-regulatory elements required for macrophage and B cell identities. *Mol. Cell* **38**, 576–89 (2010).
74. Bibel, M., Richter, J., Lacroix, E. & Barde, Y.-A. Generation of a defined and uniform population of CNS progenitors and neurons from mouse embryonic stem cells. *Nat. Protoc.* **2**, 1034–1043 (2007).
75. Zhang, Y. *et al.* Analysis of the NuRD subunits reveals a histone deacetylase core complex and a connection with DNA methylation. *Genes Dev.* **13**, 1924–1935 (1999).

76. Cox, J. & Mann, M. MaxQuant enables high peptide identification rates, individualized p.p.b.-range mass accuracies and proteome-wide protein quantification. *Nat. Biotechnol.* **26**, 1367–1372 (2008).
77. Smits, A. H., Jansen, P. W. T. C., Poser, I., Hyman, A. A. & Vermeulen, M. Stoichiometry of chromatin-associated protein complexes revealed by label-free quantitative mass spectrometry-based proteomics. *Nucleic Acids Res.* **41**, e28 (2013).
78. Hanein, S. *et al.* TMEM126A, Encoding a Mitochondrial Protein, Is Mutated in Autosomal-Recessive Nonsyndromic Optic Atrophy. *Am. J. Hum. Genet.* **84**, 493–498 (2009).
79. Hanein, S. *et al.* TMEM126A is a mitochondrial located mRNA (MLR) protein of the mitochondrial inner membrane. *Biochim. Biophys. Acta - Gen. Subj.* **1830**, 3719–3733 (2013).
80. Hu, W. *et al.* Identification of P4HA1 as a prognostic biomarker for high-grade gliomas. *Pathol. - Res. Pract.* **213**, 1365–1369 (2017).
81. Bravo, R. *et al.* Endoplasmic Reticulum and the Unfolded Protein Response: Dynamics and Metabolic Integration. *Int. Rev. Cell Mol. Biol.* **301**, 215–290 (2013).
82. Filipeanu, C. M. Temperature-Sensitive Intracellular Traffic of $\alpha 2C$ -Adrenergic Receptor. *Prog. Mol. Biol. Transl. Sci.* **132**, 245–265 (2015).
83. Gu, H. *et al.* The STAT3 Target Mettl8 Regulates Mouse ESC Differentiation via Inhibiting the JNK Pathway. *Stem Cell Reports* **10**, 1807–1820 (2018).
84. Jakobsson, M. E. *et al.* The dual methyltransferase METTL13 targets N terminus and Lys55 of eEF1A and modulates codon-specific translation rates. *Nat. Commun.* **9**, 3411 (2018).
85. Shuo, L. *et al.* METTL13 Methylation of eEF1A Increases Translational Output to Promote Tumorigenesis. *Cell* **176**, P491-504.E21 (2019).

86. Noma, A. *et al.* Actin-binding protein ABP140 is a methyltransferase for 3-methylcytidine at position 32 of tRNAs in *Saccharomyces cerevisiae*. *RNA* **17**, 1111–9 (2011).
87. D'Silva, S., Haider, S. J. & Phizicky, E. M. A domain of the actin binding protein Abp140 is the yeast methyltransferase responsible for 3-methylcytidine modification in the tRNA anti-codon loop. *RNA* **17**, 1100–10 (2011).
88. Gatza, M. L., Silva, G. O., Parker, J. S., Fan, C. & Perou, C. M. An integrated genomics approach identifies drivers of proliferation in luminal subtype human breast cancer. *Nat. Genet.* **46**, 1051 (2014).
89. Wirapati, P. *et al.* Meta-analysis of gene expression profiles in breast cancer: toward a unified understanding of breast cancer subtyping and prognosis signatures. *Breast Cancer Res.* **10**, R65 (2008).
90. Tan, X.-L. *et al.* Genetic variation predicting cisplatin cytotoxicity associated with overall survival in lung cancer patients receiving platinum-based chemotherapy. *Clin. Cancer Res.* **17**, 5801–11 (2011).
91. Kaniskan, H. Ü., Martini, M. L. & Jin, J. Inhibitors of Protein Methyltransferases and Demethylases. *Chem. Rev.* **118**, 989–1068 (2018).
92. Thul, P. J. *et al.* A subcellular map of the human proteome. *Science (80-.)*. **356**, 820 (2017).
93. van Tran, N. *et al.* The human 18S rRNA m6A methyltransferase METTL5 is stabilized by TRMT112. *Nucleic Acids Res.* (2019).
94. Figaro, S. *et al.* Trm112 is required for Bud23-mediated methylation of the 18S rRNA at position G1575. *Mol. Cell. Biol.* **32**, 2254–67 (2012).
95. Decatur, W. A. & Fournier, M. J. rRNA modifications and ribosome function. *Trends Biochem. Sci.* **27**, 344–351 (2002).
96. Kimura, S. & Suzuki, T. Fine-tuning of the ribosomal decoding center by conserved

- methyl-modifications in the Escherichia coli 16S rRNA. *Nucleic Acids Res.* **38**, 1341–52 (2010).
97. Polikanov, Y. S., Melnikov, S. V, Söll, D. & Steitz, T. A. Structural insights into the role of rRNA modifications in protein synthesis and ribosome assembly. *Nat. Struct. Mol. Biol.* **22**, 342–344 (2015).
 98. Liang, X., Liu, Q. & Fournier, M. J. rRNA Modifications in an Intersubunit Bridge of the Ribosome Strongly Affect Both Ribosome Biogenesis and Activity. *Mol. Cell* **28**, 965–977 (2007).
 99. Ingolia, N. T., Lareau, L. F. & Weissman, J. S. Ribosome profiling of mouse embryonic stem cells reveals the complexity and dynamics of mammalian proteomes. *Cell* **147**, 789–802 (2011).
 100. Shigunov, P., Dallagiovanna, B. & Holetz, F. Stem Cells and the Translational Control of Differentiation: Following the Ribosome Footprints. *J. Mol. Genet. Med.* **2014 82 8**, 1–5 (2014).
 101. Riazuddin, S. *et al.* Exome sequencing of Pakistani consanguineous families identifies 30 novel candidate genes for recessive intellectual disability. *Mol. Psychiatry* **22**, 1604–1614 (2017).
 102. Reuter, M. S. *et al.* Diagnostic Yield and Novel Candidate Genes by Exome Sequencing in 152 Consanguineous Families With Neurodevelopmental Disorders. *JAMA Psychiatry* **74**, 293 (2017).
 103. Hu, H. *et al.* X-exome sequencing of 405 unresolved families identifies seven novel intellectual disability genes. *Mol. Psychiatry* **21**, 133–48 (2016).
 104. Engel, M. *et al.* The Role of m6A/m-RNA Methylation in Stress Response Regulation. *Neuron* **99**, 389-403.e9 (2018).
 105. Mateusz Mendel, A. *et al.* Methylation of Structured RNA by the m 6 A Writer METTL16 Is Essential for Mouse Embryonic Development Article Methylation of

- Structured RNA by the m⁶A Writer METTL16 Is Essential for Mouse Embryonic Development Internal modification of RNAs with N⁶. *Mol. Cell* **71**, 986–1000 (2018).
106. Sima, C. *et al.* Identification of quantitative trait loci influencing inflammation-mediated alveolar bone loss: insights into polygenic inheritance of host-biofilm disequilibria in periodontitis. *J. Periodontal Res.* **51**, 237–249 (2016).
 107. Tahmasebi, S., Amiri, M. & Sonenberg, N. Translational Control in Stem Cells. *Front. Genet.* **9**, 709 (2019).
 108. Hein, M. Y. *et al.* A Human Interactome in Three Quantitative Dimensions Organized by Stoichiometries and Abundances. *Cell* **163**, 712–723 (2015).
 109. Spruijt, C. G. *et al.* ZMYND8 Co-localizes with NuRD on Target Genes and Regulates Poly(ADP-Ribose)-Dependent Recruitment of GATAD2A/NuRD to Sites of DNA Damage. *Cell Rep.* **17**, 783–798 (2016).
 110. Kloet, S. L. *et al.* NuRD-interacting protein ZFP296 regulates genome-wide NuRD localization and differentiation of mouse embryonic stem cells. *Nat. Commun.* **9**, 4588 (2018).
 111. Kloet, S. L. *et al.* The dynamic interactome and genomic targets of Polycomb complexes during stem-cell differentiation. *Nat. Struct. Mol. Biol.* **23**, 682–690 (2016).
 112. Henrike, M., Marcin, K., Norbert, H. & Markus, L. Transcriptome-wide Identification of RNA-binding Protein Binding Sites Using Photoactivatable-Ribonucleoside-Enhanced Crosslinking Immunoprecipitation (PAR-CLIP). *Curr. Protoc. Mol. Biol.* **118**, 27.6.1-27.6.19 (2017).
 113. Brannan, K. W. *et al.* SONAR discovers RNA binding proteins from analysis of large-scale protein-protein interactomes. *Mol Cell.* **64**, 282–293 (2016).
 114. Doxtader, K. A. *et al.* Structural Basis for Regulation of METTL16, an S-

- Adenosylmethionine Homeostasis Factor. *Mol. Cell* **71**, 1001-1011.e4 (2018).
115. Hung, V. *et al.* Spatially resolved proteomic mapping in living cells with the engineered peroxidase APEX2. *Nat. Protoc.* **11**, 456–475 (2016).
116. Roux, K. J., Kim, D. I. & Burke, B. BioID: A Screen for Protein-Protein Interactions. in *Current Protocols in Protein Science* **74**, 19.23.1-19.23.14 (John Wiley & Sons, Inc., 2013).
117. Liu, W. *et al.* IBS: an illustrator for the presentation and visualization of biological sequences. *Bioinformatics* **31**, 3359–61 (2015).
118. *Molecular Cloning: A Laboratory Manual, 4th edition.* (2012).
119. Dobin, A. *et al.* STAR: ultrafast universal RNA-seq aligner. *Bioinformatics* **29**, 15–21 (2013).
120. Li, H. *et al.* The Sequence Alignment/Map format and SAMtools. *Bioinformatics* **25**, 2078–9 (2009).
121. Quinlan, A. R. & Hall, I. M. BEDTools: a flexible suite of utilities for comparing genomic features. *Bioinformatics* **26**, 841–842 (2010).
122. Ignatova, V. V. The rRNA m6A methyltransferase METTL5 regulates pluripotency and differentiation.
123. Louloui, A., Ntini, E., Conrad, T. & Ørom, U. A. V. Transient N-6-Methyladenosine Transcriptome Sequencing Reveals a Regulatory Role of m6A in Splicing Efficiency. *Cell Rep.* **23**, 3429–3437 (2018).
124. Karolchik, D. *et al.* The UCSC Table Browser data retrieval tool. *Nucleic Acids Res.* **32**, D493-6 (2004).
125. Kent, W. J. *et al.* The human genome browser at UCSC. *Genome Res.* **12**, 996–1006 (2002).
126. Vizcaíno, J. A. *et al.* 2016 update of the PRIDE database and its related tools. *Nucleic Acids Res.* **44**, D447-56 (2016).

6. Appendix

Abbreviations

AP – alkaline phosphatase

CPM – counts per minute

GFP - green

GST - Glutathione Sepharose

IP - immunoprecipitation

LS/MS-MS - Liquid chromatography-tandem mass spectrometry

LSC - liquid scintillation counting

mESC – mice embryonic stem cells

MS - mass spectrometry

MT – methyltransferase

MTA - methyltransferase assay

NAIL - Nucleic acid isotope labeling

NE – nuclear extract

NGS – next generation sequencing

o/n – overnight

PAAG – polyacrylamide gel

PAGE – polyacrylamide gel electrophoresis

WCE – whole cell extract

Collaborators

All RNA mass spectrometry, RNA size-exclusion chromatography for mass spectrometry, tRNA isoacceptors analysis (Figures 2.2.2, 2.2.3, 2.2.4b,c, 2.3.2a,b) were performed by Dr. Steffen Kaiser, Dr. Kayla Borland, Erik Van De Logt (Stefanie M. Kellner laboratory, Chemical Faculty, Ludwig-Maximilians Universität München, Munich, Germany).

Generation of mESC with *Mettl5* and *Mettl6* KO, AP staining, qPCR check of pluripotency markers and neuronal differentiation (Figures 2.2.6a, 2.3.6) were performed by Paul Stoltz (Sebastian Bultmann laboratory, Department of Biology II, Human Biology and BioImaging, Ludwig-Maximilians Universität München, Munich, Germany).

All protein mass spectrometry and data analysis (Figures 2.2.7, 2.3.1c, 2.4.2, 2.4.3, 2.4.5) were performed by Pascal W.T.C Jansen and Marijke P Baltissen (Michiel Vermeulen laboratory, Department of Molecular Biology, Faculty of Science, Radboud Institute for Molecular Life Sciences, Oncode Institute, Radboud University Nijmegen, Nijmegen, The Netherlands).

Ribosome profiling and data analysis (Figure 2.2.5) were performed by Dr. Xinyang Bin (Oliver J. Rando laboratory, University of Massachusetts Medical School, Worcester, USA).

For m⁶A-IP data analysis that was included in this thesis, I used scripts and pipelines provided by Dr. Evgenia Ntini (Annalisa Marsico laboratory, Max Planck Institute for Molecular Genetics, Berlin, Germany and Helmholtz Zentrum München, Munich, Germany).

Sequencing of m⁶A-IP libraries was performed by HMGU sequencing facility.

Acknowledgements

Completing this doctoral thesis would not be possible alone, therefore I would like to express my gratitude to all the following people and organisations.

First of all I would like to thank my Ph.D. adviser Robert Schneider for giving me an opportunity to work on this exciting, high-risk project with high level of freedom and for all support during my work in his lab; the past and present members of Schneider lab and IFE for inspiring discussions, sharing they expertise, occasionally taking care of my cells in the days I was not around and fun TGIF discussion; all my interns and lab members who were working with me during my Ph.D. and contributed to development of my project.

During my Ph.D. I was lucky enough to have many outstanding collaborators that are listed above. I want to thank all of them for their contributions, critical discussion and sharing with me their expertise.

I want to thank the members of my Thesis Advisory Committee Prof. Dr. Marc Buehler (FMI, Basel, Switzerland), Prof. Dr. Dirk Eick, Dr. Didier Devys (University of Strasbourg, IGBMC, Strasbourg, France) and Dr. Gerhard Mittler (MPI, Freiburg, Germany) for their valuable feedback on the development of my project.

Additionally, I would like to thank Alone Chan laboratory and Mareen Engel for teaching me m⁶A-IP, Dr. Saulius Lukauskas for introduction to HMGU cluster and helping with managing all software I need for that, Dr. Rin Ho Kim for his advice about my Ph.D. and future job applications, Dr. Andrey Tvardovskiy for his advices in biochemistry, Mass Spectrometry and data visualisation.

I would like to thank IGBMC Ph.D. program, HELENA Ph.D. program and IRTG 1064 for an opportunity to join them, very useful Ph.D. courses and funding for conferences.

I am very thankful to all my family and my friends for their support during that, sometimes stressful, time.

Last but not least, I want to thank Chester Bennington, Rob Bourdon, Brad Delson, Mike Shinoda, Dave Farrell, Joe Hahn. Their music was a soundtrack to the lowest downs and the highest ups during my time as a Ph.D. student.